Journal of Double Star Observations

VOLUME 15 NUMBER 2 April 1, 2019

Inside this issue:

Astrometry of STF 1510 Elizabeth Phillips, Morgan Harrington, Monica Rodriguez, Jiseelle Jimenez, Mandy Lee, Paulina Mondragon Lopez, Leslie Ramirez, Laura Santos, Jon-Paul Ewing, Rachel Freed, and Russell Genet	210
CCD Astrometric Measurements of WDS 12001+7039 Hannah Blythe, Bella Morales, Tatianna Steiner, Marco Sanchez, Pat Boyce, and Grady Boyce	213
An Astrometric Measurement ofWDS 16476-4708 AB and AC Kelcey Davis, Sophia Vanslyke, Pat Boyce, Grady Boyce, and Ashlyn Little	217
Astrometric Measurement and Analysis of Celestial Motion for Double Star WDS 10494+5517 Theophilus Human, Seeraj Somla, Angel Ha, Jae Calanog, Grady Boyce, and Pat Boyce	221
Measurements of Star System 00345-0433 STF 39AB,C Amanda Tran, Audrey Lee, Samuel O'Neill, Abigail Wu, and Allen Priest	225
CCD and GAIA Observations Indicate That WDS 02222+2437 Is Not Gravitationally Bound Hamza Samha, Jonathan Ginouves, Taime Clark, Savana LeBaron, Jasmine Tapia, Micah Jackson, and Cameron Pace	228
Measurement of Star System 00304-0947 CHE 27 Amanda Tran, Audrey Lee, Samuel O'Neill, Abigail Wu, and Allen Priest	232
Astrometric Measurements of WDS 04136-2532 Vivek Vijayakumar, Curran Poulsen, Alex Falatoun, Pat Boyce, and Grady Boyce	235
Measurement of Star System 02442+4914 STF 296AB Amanda Tran, Audrey Lee, Samuel O'Neill, Abigail Wu, and Allen Priest	239
Cross-Match of WDS KOI objects with GAIA DR2 Wilfried R.A. Knapp and John Nanson	242
Astrometry Observations of Six Uncertain Double Stars Cooper Howlett, Erin Pickering, Joshua Breman, Malia Barker	248
Astrometric Measurements of WDS 13169+1701 Binary Star System in Coma Berenices Shannon Pangalos-Scott, Danielle Holden, Melody Fyre, Zach Medici, Jaeho Lee, Micaiah Doughty, Rebecca Chamberlain, Rachel Freed, and Russ Genet	255
Astrometric Measurements of Double Stars HJ 4194 and HJ 4195 Vincent Aguilar, Emmanuel Mercado, Hugh Le, Tianlin Zhao, Jae Calanog, Grady Boyce, and Pat Boyce	260
Measurements of Neglected Double Stars: December 2018 Report Joseph M. Carro	266

Inside this issue:

Duplicity Discovery of HIP 33753 from Asteroidal Occultation by (479)Caprera Toshio Hirose, Miyoshi Ida, Hideto Yamamura, Shigeo Uchiyama, Akie Hashimoto, Reijin Aikawa, Kazumi Terakubo, Mikiya Sato, and Kunihiro Shima	268
Speckle Interferometry with theOCA Kuhn 22" Telescope - II Rick Wasson	273
Measurements of 121 New Visual Binary Stars Suggested by the Gaia Data Release 2 J. Sérot	287
Measurements of the Position Angles and Separations of the Double Stars WDS 16579+4722 AB and AC components Nathan Sharon, Renae Bishop, Cole Rodgers, Sophia Baer, Rachel Freed, Cheryl Genet, and Russell Genet	297

Astrometry of STF 1510

Elizabeth Phillips[1], Morgan Harrington[1], Monica Rodriguez[1], Jiseelle Jimenez[1], Mandy Lee[1], Paulina Mondragon Lopez[1], Leslie Ramirez[1], Laura Santos[1], Jon-Paul Ewing[1], Rachel Freed[2,5], and Russell Genet[3,4,5]

1. Paso Robles High School, CA
2. Sonoma State University, CA
3. Cuesta College, San Luis Obispo, CA
4. Cal Poly State University - San Luis Obispo, CA
5. Institute for Astronomical Research (InStAR), AZ

Abstract: Our team made an astrometric measurement of the double star STF 1510 and found the separation to be 5.52 arc seconds and the position angle to be 327.95 degrees. Our analysis of historic observations as well as our own did not support the contention that STF 1510 is a binary, nor did it eliminate the possibility that it could be a very long-period binary.

Introduction

A group of students from Paso Robles High School formed an astrometry seminar research team (Figure 1). The main goals of the team's research were observations and the analysis of the binary star STF 1510, to help further the information on the orbit of the stars, as well as gain experience measuring binary stars. Through observations and analysis, despite the longevity of this specific orbit, additional data was contributed to hopefully lead to more discoveries about this double star. This was done to help either disprove or support the published elliptical orbit. In order to do this, observations of the double star system and the measurement of its position angle (in degrees) and the separation (in arcseconds) were needed. This binary star was chosen due to its extremely long elliptical period, along with the possibility of past measurements straying from the orbital path into a linear path and being considered an optical binary star.

The first published research on (STF 1510= WDS 11080 + 5249A/B= HD 96527= HIP 54407= BD+53 1466= SAO 27918= TYC 3824-17-1= UCAC4 715-050214) was in 1830, and the most recent one was in 2017. The binary was initially discovered by Frederick William Herschel in 1830, however, Friedrich Georg Wilhelm von Struve is attributed as the discoverer of the binary by making multiple published observations with a larger telescope in 1832. STF 1510 has been

Figure 1. Team members - Laura Santos, Monica Rodriguez, Jiseelle Jimenez, Morgan Harrington, Mandy Lee, Paulina Mondragon Lopez, Leslie Ramirez, Elizabeth Phillips, and Instructor Jon-Paul Ewing

studied for almost 200 years, yet all of the past observations indicate that the orbital period is tremendously long with the data points concentrated only in a certain area of the orbit.

The Hipparcos data point, represented by the red "H", is the satellite telescope used to observe the double star in the early 1990s. The WDS orbit in Figure 2 was calculated recently (Kiselev, et al 2012). The previous measurements made on this orbit are shown by the pink and green points along the orbital path of this star in the graph above. The pink shows the measurement

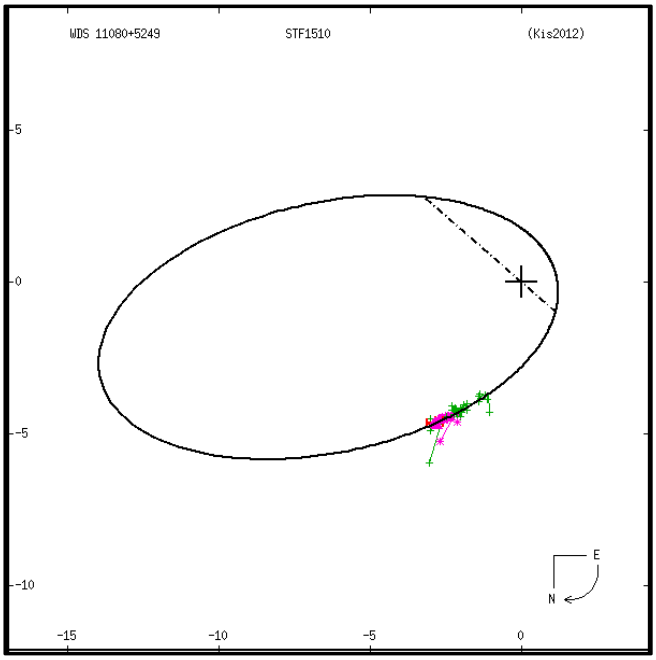

Figure 2. STF 1510 Orbit

made from photographs, while the green shows the measurements made through the use of an eyepiece micrometer.

Equipment and Procedures

Las Cumbres Observatory (LCO) kindly provided observing time to obtain the digital images. Images of STF 1510 were taken on a 0.4 meter telescope at Tenerife, Spain, at three different exposures. There were 10 images taken at exposures of 5 seconds, 1 second, and 0.5 seconds each, producing 30 images total. It was concluded that the images taken at the longest exposure time (5.23s) produced clearer images that could be analyzed more accurately. Figure 3 shows an example image.

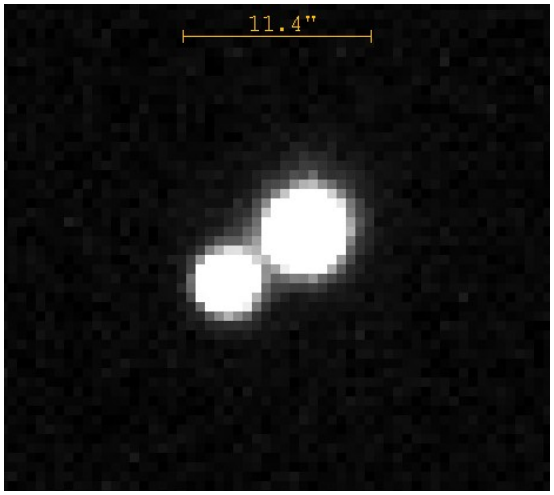

Figure 3: Image of our binary in AstroImageJ software

The 10 images were analyzed using the program AstroImageJ (Collins, et al. 2017), which gave us the primary and secondary stars' centroids' right ascension (RA) and declination (DEC). We then used a formula created by Robert Buchheim (2008) to calculate the average position angle and separation from the RA and DEC.

Results

The observations were taken on 2018.526. The position angle was calculated to be 327.95 degrees and separation as 5.52 arc seconds. These results are summarized in Tables 1 and 2.

Discussion

When trying to find the position angle and separation between the two stars in AstroImageJ, the program did not automatically output these values as expected. Therefore, we used the formula previously mentioned in the Equipment and Procedures section.

Overall, the data recorded of both the separation

Table 1: Calculated separation and position angle of 10 images

Image Number	Trial 1		Trial 2	
	Separation (as)	Position Angle (deg)	Separation (As)	Position Angle (deg)
1	5.5	328.42	5.56	329.31
2	5.55	328.27	5.55	328.05
3	5.54	327.87	5.48	329.18
4	5.51	327.91	5.52	328.05
5	5.57	327.39	5.59	328.11
6	5.57	327.39	5.49	327.32
7	5.34	326.72	5.32	327.32
8	5.52	328.53	5.54	328
9	5.59	327.42	5.57	327.87
10	5.59	327.98	5.59	327.77
Trial Average	5.53	327.79	5.52	328.1
Standard Deviation	0.07	0.56	0.08	0.67
Standard Error of Mean	0.02	0.18	0.03	0.21

Table 2: Averaged solutions using AstroImageJ

	Separation (Arcseconds)	Position Angle (degrees)
Average	5.52	327.95
Standard Deviation	0.08	0.62
Error	0.02	0.14

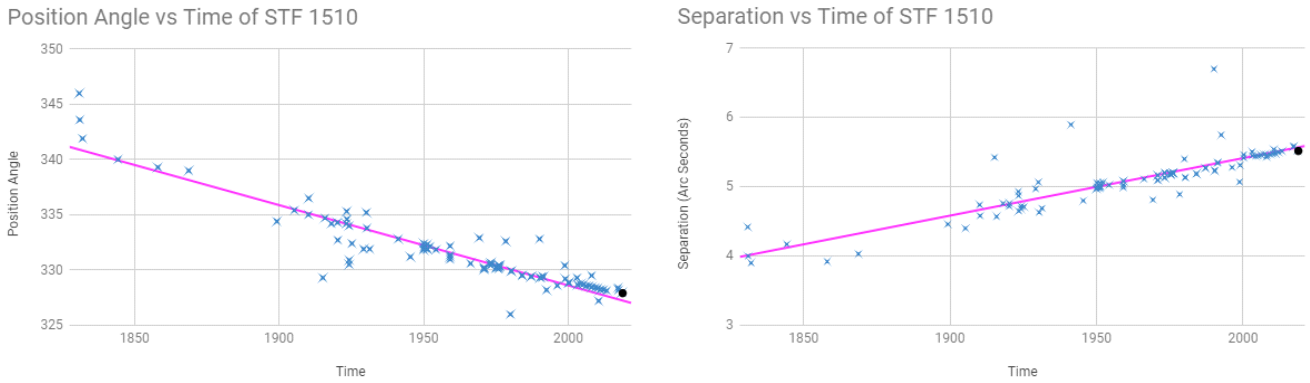

Figure 4. Position angle and separation versus time using historical data on STF 1510. A linear trend line is shown for reference.

and position angle (Figure 4) are pertinent to the previously published data which led to the current orbital path shown above.

Conclusion

The objective of this research was to gather data about the orbit of this binary star by measuring the position angle and separation along with gaining experience of measuring binary stars. The results are consistent with previous observations.

Acknowledgments

We thank Reed Estrada and Rick Wasson for reviewing the paper. Las Cumbres Observatory provided digital images of the binary star, which were later analyzed. Karen Collins developed AstroImageJ, which was used to analyze the images. Brian Mason, from the US Naval Observatory, provided historical observations of this binary star, which allowed us to create historic observational graphs.

References

Buchheim, R., 2008, "CCD Double-Star Measurements at Altimira Observatory in 2007", *Journal of Double Star Observations*, **4** (1), 27-31.

Collins, K., Kielkopf, J., Stassun, K, and Hessman, F., 2017, "AstroImageJ: Image processing and photometric extraction for ultra-precise astronomical light curves", *The Astronomical Journal*, **153**, No. 2.

Kiselev, A.A., Kiyaeva, O.V., Romanenko, L.G. & Gorynya, N.A., 2012, *Astronomicheskii Zhurnal (ARep),* **56**,524.

CCD Astrometric Measurements of WDS 12001+7039

Hannah Blythe[1], Bella Morales[1], Tatianna Steiner[1], Marco Sanchez[1], Pat Boyce[2], and Grady Boyce[2]

1. High Tech High, San Diego, California
2. Boyce Research Initiatives and Education Foundation (BRIEF)

Abstract: The primary focus of this research was to acquire measurements for WDS 12001+7039 AB, AC, and AE system pairs through images acquired through the Las Cumbres Observatory telescope network (LCO), using a 0.4-meter Meade telescope. From the images we calculated the mean position angle and separation of the AB pair to be 328.77° ± 0.03° standard error and 14.39" ± 0.01" standard error respectively, the AC pair to be 158.77° ± 0.01° standard error and 30.61" ± 0.01" standard error respectively, and the AE pair to be 317.13° ± 0.06° standard error and 25.21" ± 0.03" standard error .

Introduction

Double Star WDS 12001+7039 is a quintuple star system, Figure 1, with multiple pairs having a record of historical measurements. This double star system was selected for research due to the AE pair only having a few historical observations; the first in 1885, and the last in 2003. As images were acquired for the entire system, pairs AB and AC were also measured in addition to AE. Measurements we not acquired for the D star (although there was historical data collected on the Cd measurement), because we found that the D star location was blown out in our measurements by the A star (by comparing locations in current measurements to the historic measurements).

The double star pair, 12001+7039 STH 2 AE has only 3 measurements in the last 133 years. A review of these historical measurements, provided by the United States Naval Observatory, show the position angle (theta) between the A and E components constantly at an average of 317.5°, however the separation (rho) between the two stars increased by 4 arc seconds from 21.05" to 24.81" during the same period.

Equipment and Methods

The images for 12001+7039 were taken in Tenerife, Spain, through the Las Cumbres Observatory (LCO) system. Having access to 6 of the LCO telescopes around the world, this double star system was visible to three telescopes during the period requested: Tenerife, Spain, Maui, USA, and Texas, USA. The

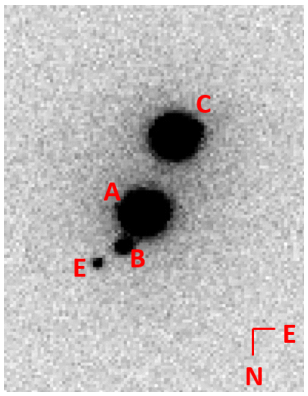

Figure 1. WDS 12001+7039

LCO scheduling system used the telescope in Spain due to weather and availability. A total of 20 images were taken through a Sloan Digital Sky Survey (SDSS) filter for the r band: Five with a three second exposure, five with a five second exposure, five with an eight second exposure, and five with a ten second exposure.

Once the images were acquired by LCO, each image was processed through the Our Solar Siblings Pipeline (OSS). The OSS Pipeline (Fitzgerald 2018) processes images in multiple phases that clean, label, and calibrate all images to prepare the photos for later measurements.

After the OSS pipeline processing, images were opened in the software suite Mira Pro for astrometric measuring using the Distance & Angle tool to accurately locate the stellar center of all stars for each measure-

CCD Astrometric Measurements of WDS 12001+7039

ment. Each separation and angle measure were recorded and organized in an Excel spreadsheet for calculation of the mean, standard deviation, and the deviation of the mean for the entire image set for each individual pair.

Results

The results for the Mean, Standard Deviation, and Standard Error of the Mean are reported for pairs AB, AC, and AE in Tables 1, 2, and 3 respectively.

Discussion

AB

There are 17 measurements in the historical record for the AB pair, plotted in Figure 2 using an Excel plotting tool by Richard Harshaw. The first measurements for these stars were taken in 1881 with a theta of 327.9° and rho of 13.82". The last measurement was in 2015 with the theta of 328.8° and rho of 14.56". The mean of the measurements taken in 2018 were a theta of 328.77° and rho of 14.39". During the last 137 years, theta has stayed the same while rho has decreased by

Table 1. Measurement mean and statistical errors for AB.

	Theta	Rho
Mean	328.77°	14.39"
Standard Deviation	0.15°	0.05"
Standard Error of Mean	0.033°	0.012"

Table 2. Measurement mean and statistical errors for AC.

	Theta	Rho
Mean	158.77°	30.61"
Standard Deviation	0.05°	0.04"
Standard Error of Mean	0.011°	0.008"

Table 3. Measurement mean and statistical errors for AE.

	Theta	Rho
Mean	317.13°	25.21"
Standard Deviation	0.26°	0.14"
Standard Error of Mean	0.057°	0.032"

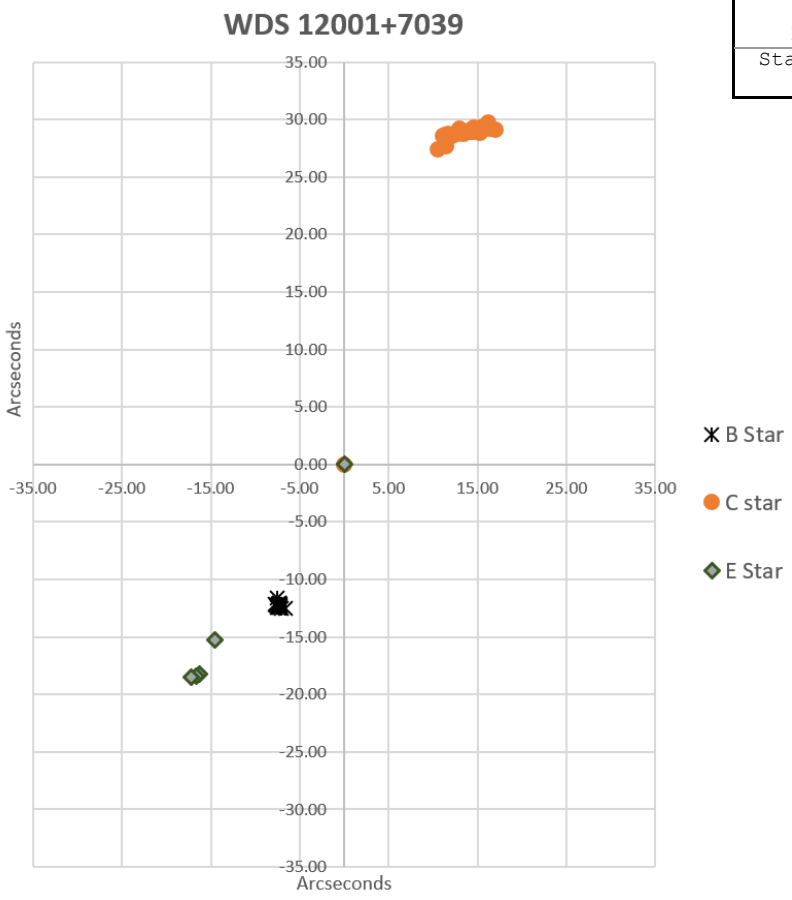

Figure 2. WDS 12001+7039 Measurement history from the WDS catalog.

CCD Astrometric Measurements of WDS 12001+7039

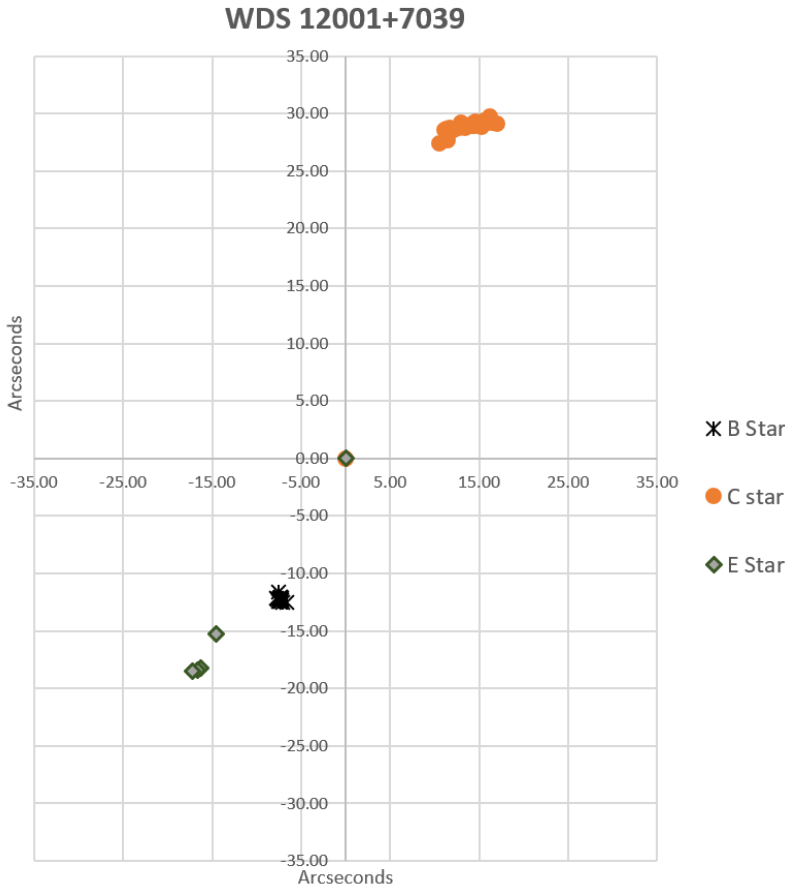

Figure 2. WDS 12001+7039 Measurement history from the WDS catalog.

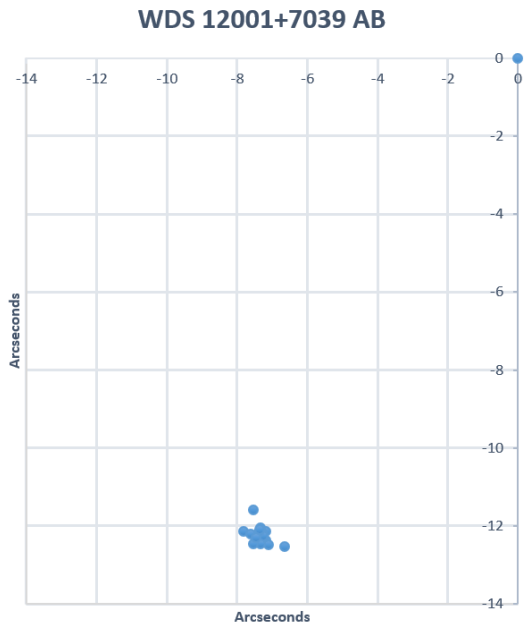

0.16". Comparing all the historic data to the most current measurement, it's observed that there has been little to no movement in this star pair.

AC

There are 39 historical measurements for the AC pair. The first measurements for these stars were taken in 1868. At the time the theta was 149.6° and the rho was 33.72". The last measurement was in 2015 with the theta 158.4° and the rho 30.74". The mean of our measurements in 2018 were a theta of 158.77° and rho of 30.61". By looking at the 39 historical measurements, Figure 3, there is an obvious linear movement, in which the current measurements fall into as well. Using the Excel *Add Trendline* function, Figure 4, there is a close linear fit for all measurements.

AE

As stated above, the first measurements for this pair was taken in 1885 indicating a theta of 316.5° and the rho of 21.05". The last measurement was in 2003 with the theta of 317.9° and the rho of 24.81". The mean of the measurements taken in this project were a theta of 317.13° and rho of 25.21". There is an apparent curve in the visual data, however, this lies within a margin of error and therefore it is not currently possible to determine whether a linear or curved fit best represents the data.

Conclusion

Through the images that were observed and measured, additional measurements were added to this rare quintuplet double star system including the AE pair which has few historical measurements. For the AB measurement the theta stayed at 328.8°, and the rho has decreased by 0.16", now being 14.4", and little to no movement has occurred. The AC theta has increased by 0.4° now being 158.8°, and the rho has decreased by 0.11", now being 30.6", adding to the linear observation. Lastly for the main measurement, AE, the theta had decreased by 0.8°, and the rho increased by 0.39", now being 25.2".

Acknowledgments

We would like to give a special thanks to Pat and Grady Boyce and BRIEF for supporting and helping us throughout the entire process of this paper. We would also like to thank Kelani Love for being interested, and helping others pursues their interest in this project. Thanks to Brian Delgado for passing on the opportunity through Blue Dot Education, and providing academic support. Thanks to Matthew Patrick for supporting us throughout the duration of the paper, because he helped us a lot. Thanks to Richard Harshaw for the spreadsheet tool that he provided to plot the historical and current data. Lastly thank you to all of our parents for providing the support and resources necessary for this paper.

References

Fitzgerald, M.T. (2018, accepted), "The Our Solar Siblings Pipeline: Tackling the data issues of the scaling problem for robotic telescope based astronomy education projects". Robotic Telescopes, Student Research and Education Proceedings.

United States Naval Oceanography Portal. "The Washington Double Star Catalog". 2018. Web. http://ad.usno.navy.mil/wds/Webtextfiles/wdsnewframe3.html. May 31, 2018.

Sordiglioni, Gianluca. "Stella Doppie". Double Star Database, 2018. Web. http://www.stelledoppie.it/index2.php?iddoppia=52449. May 31, 2018.

SIMBAD Astronomical Database. Unistra/CNRS. 2018. Web. http://simbad.u-strasbg.fr/simbad/sim-basic?Ident=12+00+06.01+%2B70+39+33.7&submit=SIMBAD%20search. May 31, 2018.

An Astrometric Measurement of WDS 16476-4708 AB and AC

Kelcey Davis[1], Sophia Vanslyke[2], Pat Boyce[4], Grady Boyce[4], and Ashlyn Little[3]

1. San Diego City College, San Diego, CA
2. Sage Creek High School, Carlsbad, CA
3. Otay Ranch High School, Chula Vista, CA
4. Boyce Research Initiatives and Education Foundation (BRIEF)

Abstract: Over three months, images were taken and processed to observe WDS 16476-4708 AB and AC. This research was conducted to contribute to the historical narrative and attempt to classify the two components as either visual doubles or a gravitationally bound pairs. Using telescopes from the Las Cumbres Observatory network, images were taken using varying filters and exposure times. The data for the AB component showed a mean separation of 4.14" and a mean position angle of 161.5º. The AC component was measured with a mean separation of 28.6" and a mean position angle of 251.4º. After analyzing the data, it was determined that, although furhter measurements would provide a stronger conclusion, it is too soon to determine the system's gravitational nature.

Introduction

WDS 16476-4708 AB and AC, Figure 1, were chosen due to a few aspects of the star system that peaked the group's interest: a gap in historical measurement and a unique opportunity to contribute to the historical narrative of the star system. Although no movement had been previously observed, the long period since the last measurement meant that observations of the system may provide useful data. A total of six observations were recorded for the AB component of the system between 1902 and 1999. Of these observations, a total change in separation of 0.3" and a change in the position angle of 2° were reported. The AC component of the star was measured a total of three times between 1987 and 1989 with a total change in separation of 0.2" and a change in position angle of 2°. All stars in the system are blue-white in spectral type.

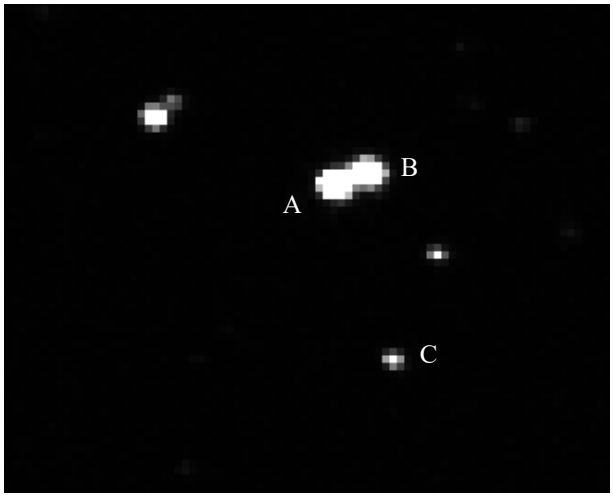

Figure 1. WDS 16476-4708 AB and AC pairs measured with a red filter, April 7, 2018, Julian Date 2458216.

Materials and Methods

The observer portal through the Las Cumbres Observatory (LCO) was used to image the AB and AC components of this system. On April 7, 2018, a Julian date of 2458216, 56 images were collected using the 0.4-meter telescopes with SBIG CCD camera based in Sutherland, South Africa and Siding Spring, Australia. The telescope operated with 2x2 binning fiving with an effective resolution of 1.14" per pixel. The model number of the telescope used was 0M-SCICAM-SBIG. Roughly three quarters of the ordered images returned successfully while the remaining were unsuccessful due to the scheduled window closing. The filters used were the PanSTARRS- W and Z filters, the SLOAN r-band, and luminance. The SLOAN r-band filter was used to even out the brightness of the stars due to the difference in magnitude of 3.4 between the A and C stars. Additionally, the PanSTARRS- Z was used to brighten the C star and make it more visible. PanSTARRS- W was used to highlight the C component of the system.

An Astrometric Measurement of WDS 16476-4708 AB and AC

Image processing was through the Our Solar Siblings (OSS) pipeline (Fitzgerald 2018) to ensure image quality through a process of cleaning and processing, photometry, calibration, and aligning each image with World Coordinate Systems (WCS) positions. The software program, Mira Pro, was used to analyze the images received and take distance and angle measurements. Each measurement was made independently by two team members to reduce the possibility of measurement error. Once each member recorded a value for the separation and angle between the stars, the data was compared to ensure accuracy. Some of the images were only useful in determining the position of the AC component and not the AB component. For these images, only the AC component was considered and used for statistical calculations.

Results

A total of eight measurements for the separation and angle of the AB component were taken, as shown in Table 1. The separation and position angle for the AC component was measured a total of twenty-three times, shown in Table 2. The mean, standard deviation, and standard deviation of the mean for the AB and AC pairs are outlined in Table 3. All the images were taken on April 7th, 2018, or Julian Date 2458216, at Siding Spring Observatory in NSW, Australia.

Discussion

For the AB component of the star system, there were a total of six measurements between 1902 and 1999, Figure 2. As represented by the graph of the historical data, using an Excel tool developed by Richard Harshaw, these measurements present a linear pattern. Table 4 shows the year and data from each measurement.

For the AC component of the star system, a total of three measurements were taken between 1987.36 and 1999.38. The historical data, Figure 3, shows a relatively linear distribution apart from the 1987.36 measurement. This datum is not enough to conlude anything concrete about the movement of the system. Further measurements are necessary to provide an accurate analysis of the system.s gravitational nature.

Upon analysis of the measurements for the AB component of the star, it became clear that the combination of few usable images and a large standard deviation meant that the data needed to be further investigated. The mean for these initial measurements gave a separation of 4.14" and a position angle of 161.51°. The images were originally measured with a three-pixel centroid, so all the images were re-analyzed using a two-pixel centroid. This produced measurements that were all roughly an arc second more than the previous

Table 1. Individual measurements for AB pair taken April 7th, 2018, JD24582216.

Image exposure time	Filter	AB angle	AB separation
3.281 s	SDSS- r (red)	162.49°	3.79"
1.282 s	luminance (clear)	162.19°	3.97"
1.283 s	SDSS- r (red)	160.96°	4.59"
3.282 s	SDSS- r (red)	161.31°	3.95"
6.284 s	PanSTARRS- W	160.57°	4.75"
6.292 s	PanSTARRS- W	160.83°	4.70"
8.28 s	PanSTARRS- Z	161.67°	3.69"
14.291 s	PanSTARRS- Z	162.06°	3.69"
Mean	-	161.51°	4.14"

Table 2. Individual measurements for AC pair taken April 7, 2018., JD 2458216.

Image exposure time	Filter	AC angle	AC separation
3.281 s	SDSS- r (red)	251.26°	28.60"
1.282 s	luminance (clear)	251.33°	28.65"
1.284 s	luminance (clear)	253.16°	28.88"
4.281 s	luminance (clear)	251.36°	28.53"
4.282 s	luminance (clear)	252.22°	28.42"
9.281 s	luminance (clear)	251.12°	28.45"
9.291 s	luminance (clear)	251.75°	28.57"
1.283 s	SDSS- r (red)	250.69°	29.07"
3.282 s	SDSS- r (red)	251.96°	28.58"
6.293 s	SDSS- r (red)	251.12°	28.60"
6.296 s	SDSS- r (red)	250.71°	28.59"
1.285 s	PanSTARRS- W	251.29°	28.39"
1.293 s	PanSTARRS- W	251.90°	28.54"
3.284 s	PanSTARRS- W	251.79°	28.70"
3.291 s	PanSTARRS- W	250.90°	28.76"
6.284 s	PanSTARRS- W	250.80°	28.55"
6.292 s	PanSTARRS- W	250.87°	28.43"
8.28 s	PanSTARRS- Z	251.86°	28.48"
8.281 s	PanSTARRS- Z	250.72°	28.59"
14.285 s	PanSTARRS- Z	251.65°	28.59"
14.291 s	PanSTARRS- Z	251.70°	28.70"
20.29 s	PanSTARRS- Z	250.78°	28.50"
20.288 s	PanSTARRS- Z	252.12°	28.65"
Avg. Stack 60.0 s	luminance (clear)	251.39°	28.54"
Mean	-	251.44°	28.60"

An Astrometric Measurement of WDS 16476-4708 AB and AC

Table 3. Results – Mean, Standard Deviation, and Deviation of the Mean for the AB and AC Pairs. See "Discussion" for explanation of AB measurements.

Results	Epoch	AB		AC	
	2018.27	Theta	Rho	Theta	Rho
Mean		161.5°	4.13"	251.4°	28.6"
Standard Deviation		0.6°	0.5"	0.6°	0.2"
Standard Deviation of the Mean		0.2°	0.2"	0.1°	0.0"

Table 4. Historical measurements of WDS 16476-4708 AB

Epoch	Position Angle	Separation
1902.54	163.0°	4.755"
1903.92	161.1°	5.0"
1904.57	161.2°	5.131"
1904.65	159.6°	5.429"
1987.355	159.78°	5.41"
1998.54	159.8°	5.419"
1999.38	160.6°	5.10"
2018.27	*161.5°*	*4.14"*

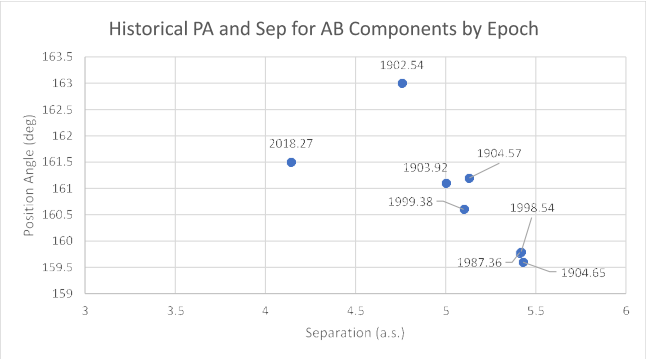

Figure 2. Historical Plot of WDS 16476-4708 AB

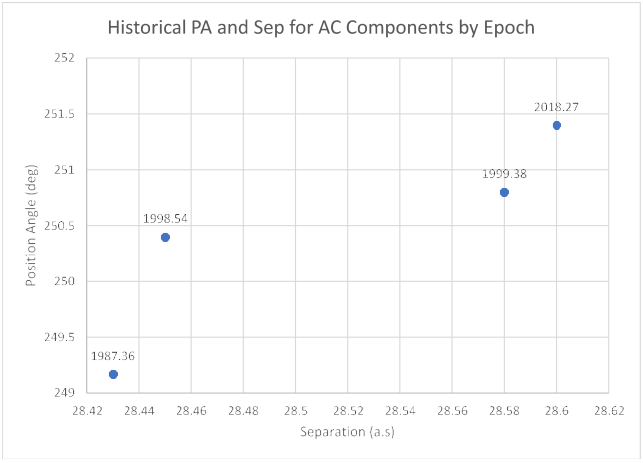

Figure 3 Historical Plot of WDS 16476-4708 AC.

Table 5. Historical measurements for WDS 16476-4708 AC

Epoch	Position Angle	Separation
1987.355	249.17°	28.43"
1998.54	250.40°	28.45"
1999.38	250.80°	28.58"
2018.27	251.40°	28.60"

measurements. Next, data from the Gaia satellite was compared to the measurements to determine a more accurate answer. The Gaia satellite data reported a separation of 4.858" and a position angle of 161.0°, close to what we had reported. It was decided that the Gaia satellite measurement was likely the most accurate and, since our data was so close, we reported our initial measurement. Since none of these problems were present in the measurements of the AC component, it is likely that the small distance between the two stars made it difficult to measure on the available equipment.

Conclusion

Measurements were successfully taken for WDS 16476-4708 AB and AC. The AB component showed a slow but steady increase in separation until this year's measurement, which decreased by roughly an arcsecond. The position angle also steadily decreased but increased in both the 1999 measurement and our measurement. The AC component of the system has seen an increase in separation although it was much smaller than the change observed in the AB component. The position angle for AC has also steadily increased. It is difficult to conclude anything about the gravitational nature of the system with such little data, but future measurements would help identify the possibility of an orbital path.

Acknowledgements

This research was conducted with the help of Boyce Research Initiatives and Education Foundation (BRIEF). We would like to thank them for supporting our research and allowing us to explore astronomy through their generous donations of time and resources. We would also like to thank Dave Rowe for providing additional data for the star system. In addition, we would like to directly thank Hilde van den Bergh for her unlimited support and help throughout the process of this research project. This research would not have been possible without the historical information provided by the United States Naval Observatory. We would also like to thank the Las Cumbres Observatory for the use of their telescopes. We would also like to thank Craig Cavanaugh of San Diego Mesa College for encouraging his students to pursue applications of science outside the classroom.

References

Boyce, G. and Boyce, P. Boyce, Research Initiatives and Education Foundation (BRIEF)

Fitzgerald, M.T. (2018, accepted), "The Our Solar Siblings Pipeline: Tackling the data issues of the scaling problem for robotic telescope-based astronomy education projects.", Robotic Telescopes, Student Research and Education Proceedings

Las Cumbres Observatory, March 20 to April 20, (56 images collected)

"USNO", USNO data for WDS 16476-4708AB and WDS 16476-4708AC, Web. Feb 24, 2018

Astrometric Measurement and Analysis of Celestial Motion for Double Star WDS 10494+5517

Theophilus Human[1], Seeraj Somla[1], Angel Ha[1], Jae Calanog[1], Grady Boyce[2], Pat Boyce[2]

1. San Diego Miramar College
2. Boyce Research Initiatives and Education Foundation (BRIEF)

Abstract: Our team observed and analyzed the double star system WDS 10494+5517 (HJ 2545) through the Las Cumbres Observatory (LCO) telescope network. We used the astrometric software SAOImage DS9 to measure new data for changes in mean position angle and mean separation distance. Our calculations revealed a new value of 25.9" ± 0.3" for the mean separation distance (rho) and a value of 114.2° ± 0.8° for mean separation angle (theta). Based on a consistent proper motion trend, very little retrograde motion or arcing, and a Harshaw value of 0.988, it is likely that HJ 2545 is an optical double.

Introduction

The objective of this research is to observe and analyze double star systems to determine whether the stars are physically bound or just visually associated. If a star is physically bound, the mass can be calculated for the stars in the set through determination of an orbit. Optical double stars are defined to be two stars that, due to forced perspective from the Earth, seem to be within close proximity of each other, yet do not have a gravitational connection. Other doubles are physically or gravitationally bound; these stars are referred to as binary stars. Throughout this paper, the term double star will be used as the gravitational nature of HJ 2545 is uncertain.

A common method for classifying double stars is to compare the position and orientation of the two stars against previous observations. By taking historical data and the double star's current position angle (theta / θ), and separation distance (rho / ρ), an observer can visualize relative motion of the pair.

Our team observed WDS 10494 + 5517 (hereafter referred to as HJ 2545), Figure 1. Initial observations were performed by English astronomer and polymath Sir John William Herschel (1831). Herschel documented many double stars, including HJ 2545, continuing the groundwork laid by his father William Herschel.

This system was selected due to a number of factors. Since our measurement window was in the spring, the Right Ascension (RA) must fall between 08-16 hours. Other criterion included the difference in magnitude between the primary and the secondary stars. Having magnitudes that are close means that similar exposure times can be used for both stars. The magnitude difference for HJ 2545 was 2.77 (Sordiglioni, 2018), which was low enough for good image quality. In addition, we chose apparent magnitudes with values less than 12 to make data collection easier.

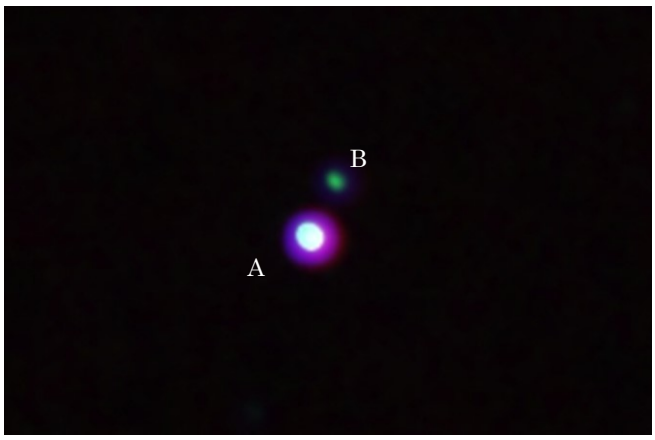

Figure 1. False color image of HJ2545 generated on DS9.

After filtering the list of candidate stars down using this process, HJ 2545 was selected based on a number of additional criteria including: at least ten historical measurements, a change in ρ greater than 5" or a

Table 1. Position angle and separation distance measurements for HJ 2545 10494+5517. Position angle is measured in degrees and separation distance in arcseconds.

Epoch	Position Angle	Separation Distance
1831.11	116.3	15
1902.27	111.11	18.96
1910.22	113.2	20.52
1914.25	113	20.345
1917.28	114.2	21.188
1926.20	114.1	20.403
1991.44	113.8	24.608
1999.88	114.7	25.04
2003.143	113.9	25.097
2007.303	114.4	25.01
2010.183	114.8	25.42
2010.5	115	25.42

change in θ greater than 25°, a long observation period, the most recent observation greater than 5+ years, an uncertain double star nature (physical or optical), and no publication history. HJ 2545 is visible in the Northern Hemisphere in the constellation Ursa Major which was interesting for our group since we can view this pair using a set of binoculars from home.

A summary of the historical measurements is outlined in Table 1 (Mason, 2018), demonstrating the separation distance has changed substantially since first observation. Table 1 also shows an annual rho increase of approximately 58 milliarcseconds per year from first to most recent measurement.

Equipment, Observations, and Data Analysis

Equipment

Data was collected by the Las Cumbres Observatory (LCO) telescope network, a global system of telescopes. The LCO telescopes provided were 0.4-meter modified Meade with SBIG STL-6303 CCD camera, which uses 2 x 2 binning to provide a resolution of 1.14 "/pixel. The telescopes have a field of view of 29.2 x 19.5 arcminutes. Available filters include Sloan u', g', r', i', z', Johnson-Cousins B, V, and Pan-STARRS w. The first data set was collected from the Teide Observatory (telescope code kb88) in Tenerife, Spain. The second data set was collected by the McDonald Observatory (telescope code kb80) in Texas, USA.

Observations

Two sets of images were taken with exposure times ranging from one to five seconds based on filter type, which resulted in non-saturated pictures. The first set of data included eleven images. Due to poor image quality from unfocused telescopes, we analyzed nine of the eleven images: three images taken with the luminance filter, two with the green, three with the red, and one with the infrared filter. The second data set included eight images. Due to poor image quality, only five images were analyzed from this set: two images in the luminance filter, one in the green, and two in the red filter.

Analysis Procedures

Two sets of images were provided to the research team with initial processing already performed. The data was reduced using the Our Solar Siblings Pipeline (Fitzgerald, 2018). This process attached WCS coordinates, removed 'hot' pixels, image artifacts, and flat fielded the images. The image quality was subsequently assessed through visual observation.

Using image analysis software SAOImage DS9 (DS9), the team measured separation distance (ρ) and separation angle (θ) for fourteen data points. Each data point was independently measured by two team members, and the results were averaged. Measurements were taken by placing circles around each star enabling the auto centroid feature to find the star's center. The auto centroid feature works by using pixel values as a weighting tool taking the weighted average of all pixel values within a specific user defined radius and measuring the center point from this average. Multiple iterations of best fit were calculated by the program, and the best option was provided as the actual separation distance and angle. The ruler feature provided the separation angle and distance in degrees and arcseconds respectively.

We averaged the collected data to produce our mean values for reporting purposes. For the first data set (Epoch 2018.22), the average position angle was measured to be 114.1° ± 0.8° and a separation distance of 25.9" ± 0.3". For the second set (Epoch 2018.26), the average position angle was measured to be 114.3° ± 0.7° and a separation distance of 25.8" ± 0.3". Both observations were within a few weeks and are within one standard deviation showing statistical consistency. Due to the close time proximity and the fact that both measures were within a standard deviation, we took the average of all points together to provide a single reported value of 25.9" ± 0.3" for separation distance and 114.2° ± 0.8° for separation angle. The epoch of the second set was used for reporting purposes. This can be observed in Table 2.

Discussion

Comparing the set of newly acquired points with the historical data provided by the WDS catalog showed results consistent with an optical double system. The separation distance, Figure 2, continued to increase linearly with a linear model correlation of 0.986; this suggests that during the historical observation window, that a linear model is a near perfect fit. It

Astrometric Measurement and Analysis of Celestial Motion for Double Star WDS 10494+5517

Table 2. Position angle (θ) and separation distance (ρ) measurements for HJ 2545.

Epoch	# of Images	Mean Separation Angle (θ, deg)	Std. Dev.	Mean Separation Distance(ρ a.s.)	Std Dev.
2018.6	14	114.2	0.8	25.9	0.3
2010.5	Last Measurement	115	0	25.42	0

is also possible that this is within statistical tolerances, however since these are unknown for previous measurements, it cannot be stated certainly. The 1917 data point is the most out of line with the linear increase model. More would have to be known about the conditions of measurement to state if this was due to sampling errors or whether this is indicative of something else.

Observing the separation angle, Figure 3 shows only minor variation. It appears that as the stars separate linearly, and despite a slight oscillation around 114° this does not resemble an arc. The coefficient of determination of the separation angle vs. time is 0.01, which indicates that the linear regression line does not fit the data for angular measurements. Converting raw measurements into a Cartesian plane, Figure 4, shows a more apparent linear path of separation with all values appearing in quadrant I and moving up and right from the primary star. The regression analysis shows a model correlation of 0.921 which suggests that a linear separation model is a good fit for the data. Since this pair of stars is either linearly separating, or has an extremely long period, less frequent astrometry is necessary for continued monitoring of this double star system. A good time to take an additional point would be the 200th anniversary of discovery (2031). Our model would predict that the separation distance should be approximately 26.7".

Additional analyses were performed to determine the characteristics of the primary and secondary stars. First, the minimum possible straight-line distance was calculated using parallax data on the primary star from SIMBAD. This parallax number was 11.6621 with an error of 0.0514. This number was converted to light years, giving a minimum possible distance from Earth to the A star of 278.31 light years. Since the minimum straight line distance would occur if the stars were perpendicular relative to radial distance from Earth, the distance could be calculated using the minimum distance of A*tan(ρ) where ρ is converted to radians and A is the primary star minimum radial distance. This minimum possible straight-line value between the two stars was 0.03 light years. With the assumption that they are physically associated, parallax data would yield approximately equal radial distances for the primary and the secondary star.

The second analysis performed was a vector comparison of proper motions to determine a Harshaw value. The proper motions for the primary and secondary star were acquired from SIMBAD and the vector difference was divided by the vector sum. It has been shown (Harshaw, 2014) that stars with a value close to 0 tend to be physical pairs where stars with a value close to 1 are more likely to be optical doubles. Our values were approximately 0.988 which suggests that it is likely that this pair is an optical pair.

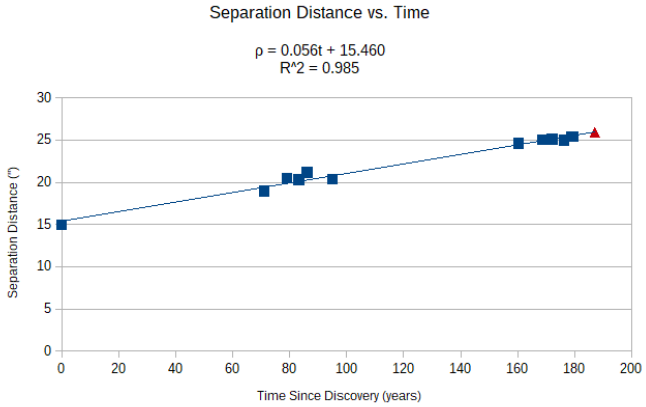

Figure 2. Graph of separation distance in arcsecond and epoch for HJ 2545, including historical data and new measurements. The red triangle is the new measurement. The separation distance has increased over time.

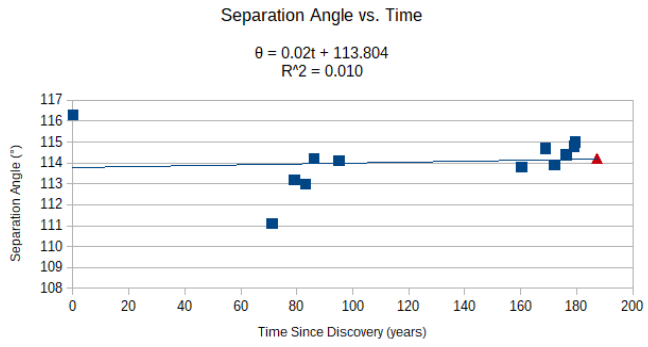

Figure 3. Graph of position angle in degrees and epoch for HJ 2545, including historical data and new measurements. The red triangle is the new data point. The separation angle measurements are relatively the same, which suggests that the star system is an optical pair.

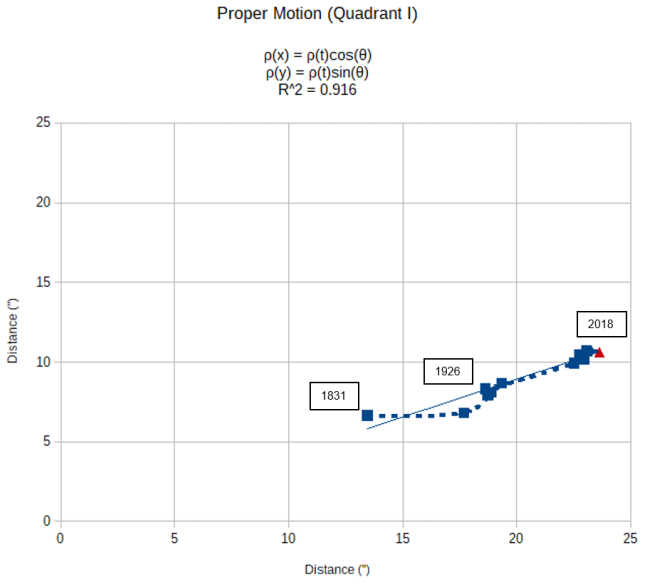

Figure 4. Plot of HJ 2545 movement relative to the primary, placed at the origin. The red triangle is the new data point. The data suggests that the star pairs are separating linearly over time.

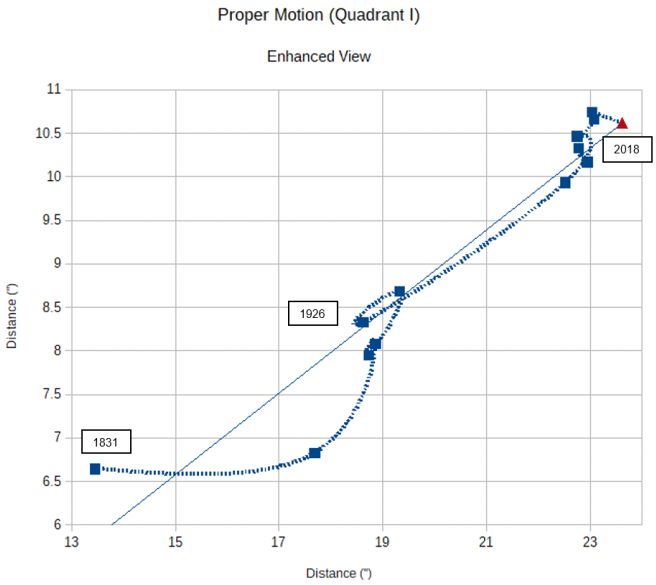

Figure 5. An enhanced plot of HJ 2545 movement relative to the primary, placed at (0,0) which is not pictured in enhanced view. The red triangle is the new data point. This plot shows the subtle amounts of retrograde motion in the data, but still shows the stars separating linearly over time.

Conclusion

The data analysis suggests that the primary and secondary stars of the HJ 2545 double star system are linearly separating. The new data obtained during the course of this research supported the trend of linear separation. Further parallax data should be taken on the B component star to verify minimum possible straight-line distance between primary and secondary components. Due to a strong regression analysis value from a linear model, a non-elliptical change in theta, and a Harshaw value close to one, it is likely that HJ 2545 is comprised of an optical primary and secondary star pair.

Acknowledgements

The students thank the Boyce Research Initiatives and Education Foundation (BRIEF), Jae Calanog, Pat Boyce and Grady Boyce for their mentorship and training material. This work makes use of the observations from the LCOGT network. This research has made use of the SIMBAD database operated at CDS, Strasbourg, France.

References

"Sir John Herschel, 1st Baronet." Encyclopædia Britannica, Encyclopædia Britannica, inc., 28 Feb. 2018, www.britannica.com/biography/John-Herschel.

Boyce, G. and Boyce, P. Boyce, Research Initiatives and Education Foundation (BRIEF), http://www.boyce-astro.org/home.html.

Fitzgerald, M.T., 2018, "The Our Solar Siblings Pipeline: Tackling the data issues of thescaling problem for robotic telescope based astronomy education projects.", *Robotic Telescopes, Student Research and Education Proceedings* (accepted).

Las Cumbres Observatory Network https://lco.global/observatory/sites/.

Mason, Brian, 2018, Washington Double Star Catalog. Astronomy Department, United States Naval Observatory, http://ad.usno.navy.mil/proj/WDS/.

Sordiglioni, Gianluca, 2018, Stella Doppie Double Star Catalog, http://www.stelledoppie.it/index2.php?menu=29&iddoppia=48579.

Sorensen, P., Azzaro, M., Méndez, J., 2002, Isaac Newton Group of Telescopes, http://catserver.ing.iac.es/staralt/.

Harshaw, R., 2014, "Another Statistical Tool for Evaluating Binary Stars", Journal of Double Star Observations, 10, 32.

Wenger, et al., 2000, "The SIMBAD astronomical database", *A&AS*, **143**, 9.

Measurements of Star System 00345-0433 STF 39AB,C

Amanda Tran, Audrey Lee, Samuel O'Neill, Abigail Wu, and Allen Priest
The Cambridge School, San Diego, CA

Abstract: Position angle (theta) and separation (rho) measurements were obtained from multiple images of the star system WDS 00345-0433 STF 39AB,C using a 17" telescope in the iTelescope network. From our 2018 measurements, STF 39 AB,C has a position angle of 45.39° and separation of 20.08" arcseconds. Measurements of STF 39 suggests that it is not a double star system because the data available does not seem to portray any trend of the sort that one would expect in an orbit.

Introduction

Double Star system WDS 00345-0433 STF 39AB,C was imaged with a telescope equipped with a CCD camera to measure the position angle (theta) in degrees and separation (rho) in arcseconds. Measurements were compared to historical data provided by Washington Double Star Catalogue (WDS).

To select double star system candidates for research, a variety of catalogues were used to find stars that fit specific criteria. The star systems had to be a minimum of six arc seconds apart, and the difference in brightness had to be no more than six orders of magnitude. The Washington Double Star Catalog, the Sixth Catalog of Orbits of Visual Binary Stars, and Stelle Doppie were all utilized to find pairs which met the criteria previously stated.

Background

STF 39 was discovered and first measured in 1782 by Friedrich Georg Wilhelm von Struve. The AB,C system does not have a proposed orbit in the WDS and its nature as a double star system is said to be physical on Stelle Doppie (Stelle Doppie Web). STF 39 does have a proposed orbit in the WDS, Figure 1, yet this is for the A and B components and not the AB,C pair.

Equipment

Images were photographed using Telescope T-21 in Mayhill, New Mexico. T-21, a deep field telescope, is a 17" platform with a FLI-PL6303E CCD camera and has a resolution of 0.96 arc-secs/pixel and an aperture of 431 mm. It operates within the iTelescope network and

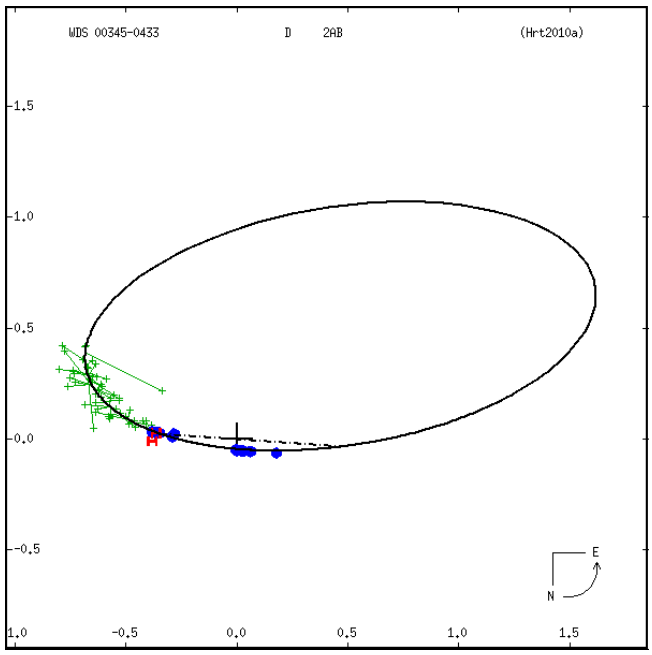

Figure 1. Proposed orbit provided by the USNO.

was selected due to its position in/visibility of the Northern hemisphere. Dark, Flat, and Bias calibration images were provided by the iTelescope network for all images taken with T-21.

Procedures and Methods

Imaging the Stars

Images were ordered from T-21 on the iTelescope

network, with exposure lengths and light filters specified by us, see Figures 2 and 3. Once complete, the requested images were then delivered to the Boyce Astro Research Computer (BARC) Server on a remote desktop for further processing.

Processing and Measuring the Stars

Once all the images had been taken and transferred to the BARC server, they were exported to MaxImDL to be calibrated and plate solved. The process of plate solving was conducted in order to properly orient the image in the sky with the correct Right Ascension and Declination. The PinPoint Astrometry program (included in MaximDL) was used to complete the plate-solving process by comparing stars in our images against the United States Navy UCAC-4 catalog.

The plate solved images were then imported into MiraPro to measure the position angle in degrees and the distance in arcseconds between the two stars. This was accomplished using its distance and angle function, which is able to locate the centroid of each stellar candidate. The measurements and data gathered from MiraPro were copied into Excel for statistical analyses: mean, standard deviation, standard error, and standard error percentage. Once all the data was collected from our processed images, historical data was ordered from the US Naval Observatory.

Results

The Position Angle (Theta) and Separation Distance (Rho) for each of the seven images acquired with iTelescope are outlined in Table 1. The Mean, Standard Deviation, and Standard Error are also calculated for these images.

Table 1. Image measurements and statistics for all seven images acquired in measuring WDS 00345-0433.

Image	Theta	Rho
1	45.1391	19.5583
2	46.1015	19.9555
3	44.6578	20.3332
4	44.9184	20.6401
5	44.4594	20.1468
6	45.4765	19.4361
7	46.9362	20.5064
Mean	**45.39**	**20.08**
Std. Deviation	**0.81**	**0.43**
Std. Error	**0.33**	**0.17**

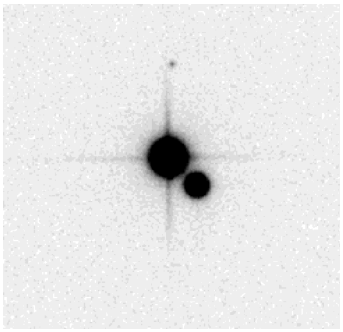

Figure 2. Red filter, 60 sec exposure.

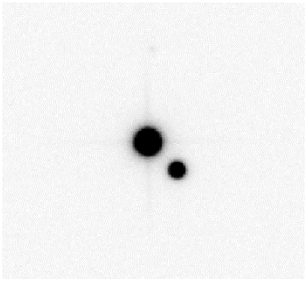

Figure 3. Red filter, 30 sec exposure

Discussion

STF 39 AB,C was studied because Stelle Doppie indicated this pair as a physical double. After analysis of our data, we found that while the two stars have very low proper and relative motion (Stelle Doppie considers star systems with proper motion lower than three, as physical), they appear to be a possible Common Proper Motion (CPM) pair.

The historical data provided 38 historical data points, displaying relatively similar theta and rho measurements. Figure 4, using an Excel plotting tool developed by Richard Harshaw, displays all historical points. In 1892, the historical record shows three observations were made, all with conflicting data points; at first its positional angle decreased by 0.7 degrees, then increased by 1.4 degrees - all in the span of one year. From its first observation in 1782 through its most recent observation in 2018, the double star system's angle and separation keep increasing and decreasing in such a pattern that it does not seem that it is moving elliptically. Instead, the data would suggest that they are moving in roughly the same direction -- linearly.

Conclusion

After analysis of our images, we concluded that the pair displays properties of a Common Proper Motion pair. Throughout our research, we also discovered that Stelle Doppie automatically deems a double star system

physical if and only if its proper motion is less than three, which is characteristic of this pair.

Acknowledgements

We would like to thank the United States Naval Observatory for providing access to historical measurement data through the Washington Double Star Catalog. In addition, we thank Pat and Grady Boyce of the Boyce Research Initiatives and Education Foundation (B.R.I.E.F) for providing access to the educational materials and for providing the funding which allowed us to use the iTelescope robotic telescope system along with other software tools. We are grateful to Mr. Priest, our advisor, mentor, and teacher, for helping us to pursue all aspects of this amazing learning experience.

References

Hartkopf, W.I., Mason, B.D, 2006, "Sixth Catalog of Orbits of Visual Binary Stars", US Naval Observatory, Washington. http://www.usno.navy.mil/ USNO/astrometry/optical-IR-prod/wds/orb6

Stelle Doppie Web Double Star Database: https://www.stelledoppie.it/index2.php

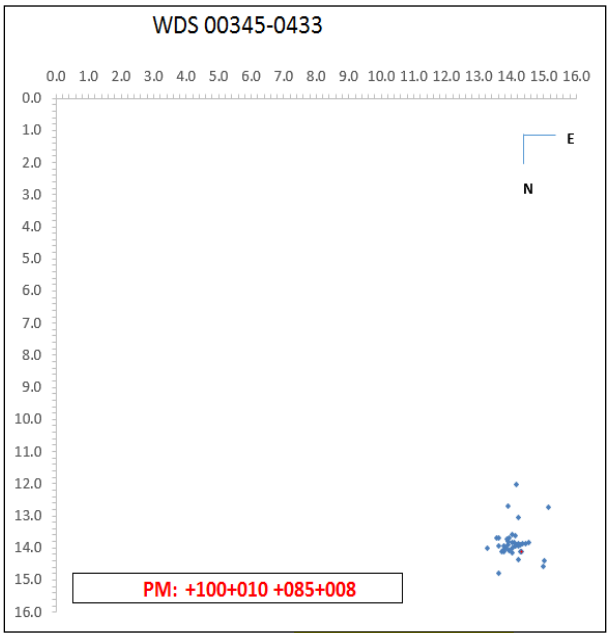

Figure 4. An X-Y plot of the position of the secondary star over time relative to the position of the primary star (in arcseconds) at (0,0)

CCD and GAIA Observations Indicate That WDS 02222+2437 Is Not Gravitationally Bound

Hamza Samha, Jonathan Ginouves, Taime Clark, Savana LeBaron, Jasmine Tapia, Micah Jackson, and Cameron Pace

Southern Utah University
Cedar City, Utah

Abstract: The Double Star system WDS 02222+2437 was observed using the Great Basin Observatory (GBO) telescope. The images were separated and position angle measured using AstroImageJ. Compared to past observations, it was found that the separation in arcseconds decreased marginally while the position angle of the two stars decreased significantly. Our measurements along with proper motion and parallax data from the Gaia database, demonstrate that the two stars are an optical double, not a binary system.

Introduction

A double star is defined as any two stars which appear close to one another when viewed through a telescope. Without a sufficient number of observations, it is impossible to determine whether the double star is an optical double (a pair of stars that only appear to be close together) or a binary system (two stars gravitationally bound to one another). Binary stars are useful because the masses of the stars can be determined by observing the orbital motions of the system, and the mass can be used to determine the evolutionary path of the star. Spectral analysis can also be used to estimate stellar mass, but is not as accurate as determining the mass from the stars' orbit.

For the first time, SUU Success Academy, an early college high school hosted by Southern Utah University (SUU) assembled a student research team for the astronomy research seminar. We used the robotic telescope at Great Basin Observatory (GBO), as seen in Figures 1 and 2, to carry out our observations (Anselmo, 2018). The system observed by our team was WDS 0222+2437 (see Figure 3), and was selected from the Washington Double Star catalog (WDS). This system was selected because it was observable from the telescope's latitude, and the difference between the magnitudes of the primary and secondary star was not excessive. In addition, the primary and secondary components were well resolved by the telescope. In order to maximize the value of our observations, we ensured that the system we selected had not been observed in at least 10 years. The primary star has a magnitude of 12.46 and the secondary star has a magnitude 14.3.

Figure 1. The telescope control software uses the weather station (visible on top of the control room) to determine whether or not it is safe to open the dome. The dome and control room were both painted to match the desert landscape and not detract from the appearance of the park.

Methods

The methods used were based on those in *Small Telescope Astronomical Research Handbook* (Genet 2016). The telescope used, a PlaneWave 0.7m CDK 700, is located at the Great Basin Observatory at Great Basin National Park, Nevada. The GBO is equipped

CCD and GAIA Observations Indicate That WDS 02222+2437 Is Not Gravitationally Bound

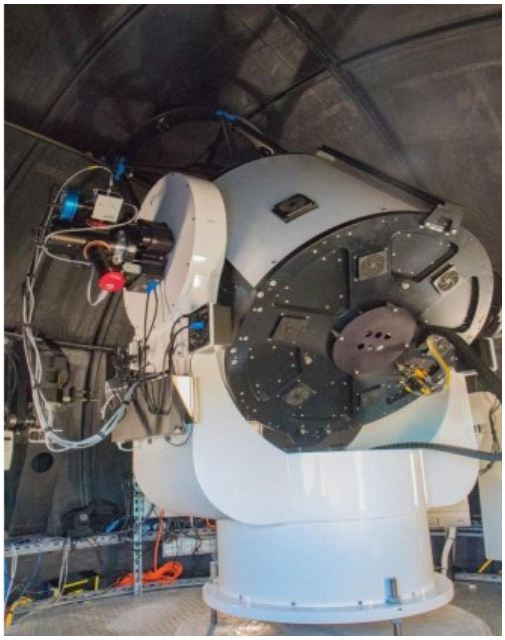

Figure 2: This is the PlaneWave 0.7 m CDK 700 telescope. The spectroscope and planetary camera are mounted at the left Nasmyth port, while the imager and filter wheel are housed at the right Nasmyth port.

with an SBIG STX-16803 CCD camera, and is paired with the telescope which results in a plate scale of 0.4 arcsec per pixel. The telescope has a focal ratio of f/6.5, and the attached camera provides a field view of 27X27 arcminutes (Anselmo, 2018). The telescope is equipped with 16 filters, LRGB, Ha, OIII, SII, BVRI, griz, and a diffraction grating; all of our images were taken using the V filter. We restricted the exposure time to 3 minutes, for a greater amount of time could result in overexposure, which would render the images unuseable. The CCD was in the linear response domain. The images were taken on February 9th, 2018. Once the pictures were taken, we used the AstroImageJ (Collins et al. 2017) program to apply dark, flat, and bias calibrations to each of the images. After the images had been calibrated, the images were plate solved using Astronomy.net. After being plate solved, AstroImageJ was once again used to make the measurements of separation (ρ) and position angle (θ), using centroid apertures to ensure we were measuring from the centers of the stars.

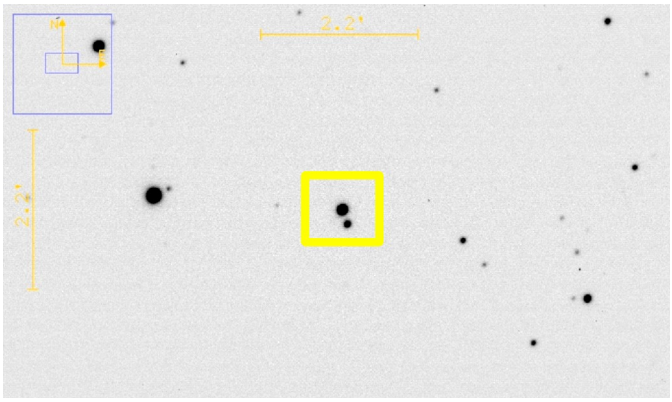

Figure 3: Finder chart for WDS 02222+2437. In this image, north is up, east is right, and the plate scale is 0.4 arcsec/pixel.

Results

Our measurements for the system are given in Table 1, as well as the mean, standard deviation, and standard error. We have measured the average separation (ρ) to be 12.35" ± 0.002" and the average position angle (θ) as 160.16° ± 0.014°.

Discussion

There are 4 data entries for WDS 0222+2437 in the Washington Double Star Catalog. The first measurement was taken in 1899, followed by another almost a century later in 1997 (Tessier, 1933). Measurements were also recorded in 2000 and 2001, and finally in 2018, when our data was collected, as seen in Table 2 (2MASS, 2003; Hartkopf, 2013; Mason, 2018). Over this span of 120 years, the separation between the two stars, measured in arcseconds, decreased from 15" to 12.3". The position angle between the two stars decreased from 167.3° to 161° between 1899 and 1997, and has gradually decreased since, dropping from 161° to our measurement of 160.16°.

The trend of our observation and past observations is shown in Figure 4. The figure displays the historical

Table 1: Measurement data obtained from our twenty-five images. Average separation (ρ), average position angle (θ), and standard deviation and error are shown.

WDS No.	ID	Date	Observations		ρ [Arcsec]	θ [Degrees]
02222+2437	POU 180	2018.11	25	Mean	12.35"	160.16°
				Std. Dev.	0.011"	0.068°
				Std. Error	0.002"	0.014°

Table 2. Historic measurement data for POU 180, courtesy of Brian Mason (Mason, 2018). The data has shown that the separation has changed by about 3", while the position angle has changed by about 7°, both over a 100 year period.

Epoch	ρ [Arcsec]	θ [Degrees]
1899.93	15	167.3
1997.85	12.8	161
2000.985	12.711	161.3
2001.577	12.726	160.9
2018.11	12.35	160.16

trends of Component B (blue circles) and our measurement (red triangle) in relation to Component A (yellow circle). The time gap in the observational measurements does not clear resolve the path of the star over the past 119 years; however, the data does indicate the B component is traveling roughly in a straight line. This seems to indicate that the stars are not gravitationally bound.

To further examine the relationship between these stars, we searched the Gaia database (Gaia Collaboration et al. 2016, 2018) for this system and found parallax and proper motion measurements for both components. These measurements are shown in Table 3. The measurements for Component A are shown in the first row while the measurements for Component B are shown in the second row. This table shows that the two components are actually quite far apart (~2,000 ly). Additionally, the proper motions are quite different, which further illustrates that these stars are an optical double, and not gravitationally bound.

Conclusion

This undergraduate research project performed at Southern Utah University indicated that WDS 0222+2437 is an optical double, not a gravitationally bound star. Based on the proper motion of WDS 0222+2437 it is predicted that the stars will move apart with the passage of time. All of this was concluded based on the measurements which are in concordance with the WDS catalog.

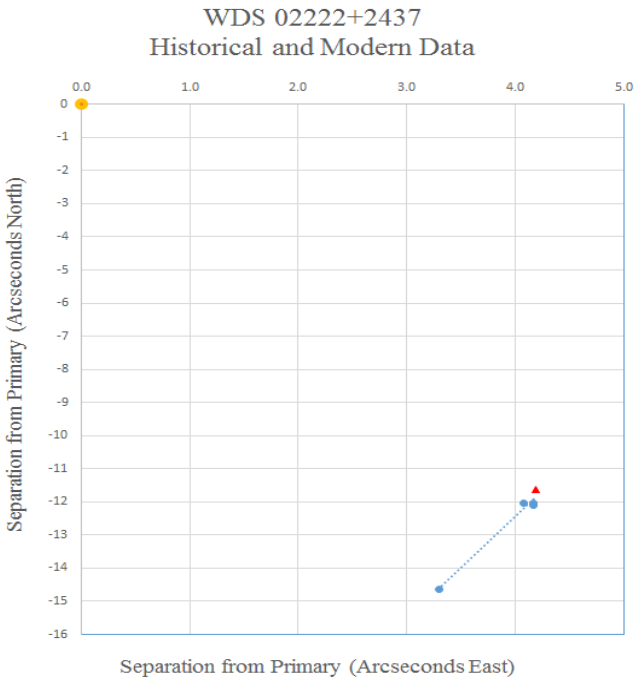

Figure 4: This figure displays the historical measurements of Component B (blue circles), our measurement (red triangle), along with a trend line showing the movement of the star over time. Component A is located at the origin (yellow circle). The first measurement, which is shown at the bottom left of the trend line, was taken in 1899. Our data is in agreement with the historical measurements.

Acknowledgements

We would like to acknowledge the partner institutions of the Great Basin Observatory, the Southern Utah University SUCCESS Academy, and the SUU Department of Physical Science. We also express thanks to Kevin Andrews for the pictures of the GBO. Our research was made possible through the use of the Stellarium and AstroimageJ programs. This research has made use of the Washington Double Star Catalog maintained at the U.S. Naval Observatory. We wish to give special thanks to Brian Mason for providing us with the historical data needed for our research.

This work has made use of data from the European Space Agency (ESA) mission Gaia (https://www.cosmos.esa.int/gaia), processed by the Gaia Data

Table 3: Data obtained from ESA's Gaia astronomy satellite (Gaia Collaboration et al. 2018), which describes the movement and location of POU 180. This given data was used to help determine if these are gravitationally bound, specifically the parallax.

Components	Right Ascension [degree]	Declination [degree]	Parallax [milliarcsec]	Proper Motion RA [milliarcsec /year]	Proper Motion DE [milliarcsec /year]
A	35.55461778	24.6232385	0.711802998	3.676259036	1.784559247
B	35.55334081	24.62648409	1.364860433	2.228916274	-20.53233837

Processing and Analysis Consortium (DPAC, https://www.cosmos.esa.int/web/gaia/dpac/consortium). Funding for the DPAC has been provided by national institutions, in particular the institutions participating in the Gaia Multilateral Agreement.

References

Cat. des etoiles doubles de la zone +24deg de la carte photog. Du ciel, 1933 (Obs. de Paris, H. Tessier)

Collins, K. A, Kielkopf, J. F., Stassun, K. G., & Hessman, F. V., 2017, The Astronomical Journal 153 (2), 77.

2MASS Point Src cat., 2003 all-sky release (http://pegasus.phast.umass.edu/)

Mason, Brian, 2018, The Washington Double Star Catalog, Astronomy Department, U.S. Naval Observatory.

Hartkopf, W.I, Mason, B.D., Finch, C.T, Zacharias, N., Wycoff, G.L., & Hsu, D. 2013AJ. Astronomical Journal 146,76H. (http://adsabs.harvard.edu/abs/2013AJ....146...76H)

Anselmo, D., Nelson, A., Kelvin, A. et al., 2018, "CCD Measurements of AB and AC Components of WDS 20420+2452", *JDSO*, **14** (3), 492 - 495.

Genet, R., Johnson, J., Buchheim, R., & Harshaw, R., 2016, *Small Telescope Astronomical Research Handbook*, Collins Foundation Press, Santa Margarita, California.

Gaia Collaboration: T. Prusti, J. H. J. de Bruijne, A. G. A. Brown, A. Vallenari, C. Babusiaux, C. A. L. Bailer-Jones, U. Bastian, M. Biermann, D. W. Evans, et al., 2016b, The Gaia mission. A&A 595, pp. A1.

Gaia Collaboration: Gaia Data Release 2. Summary of the contents and survey properties. A.G.A Brown, A. Vallenari, T. Prusti, J.H.J. de Bruijne, Babusiaux, C.A.L. Bailer-Jones et al. Accepted 2018.

Measurement of Star System 00304-0947 CHE 27

Amanda Tran, Audrey Lee, Samuel O'Neill, Abigail Wu, and Allen Priest
The Cambridge School, San Diego, California

Abstract: Position angle (theta) and separation (rho) measurements were obtained from multiple images of the star system WDS 00304-0947 CHE 27 using a Celestron C11 SCT. From our 2017 measurements, CHE 27 has a position angle of 223.54° and separation of 20.86" arcseconds. Data recorded for CHE 27, when plotted, proved to be consistent with the trend displayed in the known historical data.

Introduction

Double Star system WDS 00304-0947 CHE 27 was imaged with telescopes equipped with CCD cameras to measure the position angle (theta) in degrees and the separation (rho) in arcseconds. Measurements were compared to data provided by the Washington Double Star Catalogue (WDS).

To select double star system candidates for research, a variety of catalogues were used to find stars that fit specific criteria: the star systems had to be a minimum of six arc seconds apart, and the difference in brightness had to be no more than six orders of magnitude. The Washington Double Star Catalog, the Sixth Catalog of Orbits of Visual Binary Stars, and Stelle Doppie were all utilized to find pairs which met the criteria previously stated.

Background

The star system CHE 27 has not been confirmed as a double star system by the United States Naval Observatory. However, the B component exhibits a fair amount of movement relative to the A component, and thus we chose to image this star with the goal of adding a data point to help in determination of the association, gravitational or not, of this pair.

According to the historical data provided by the US Naval Observatory, CHE 27 does not have a proposed orbit in the Sixth Catalog of Orbits of Visual Binary Stars. The system was discovered by Stanislas Chevalier in 1900. Notes from the Washington Double Star Catalogue indicate that a measurement taken shortly after in 1901 agreed with the measurements by Chevalier. The notes predict the ability to confidently classify this system. There have been nine previous measurements recorded in the Washington Double Star Catalog, the last being in 2010, Figure 1. Our hopes were that providing a new data point would allow us to add additional analysis to the nature of this system.

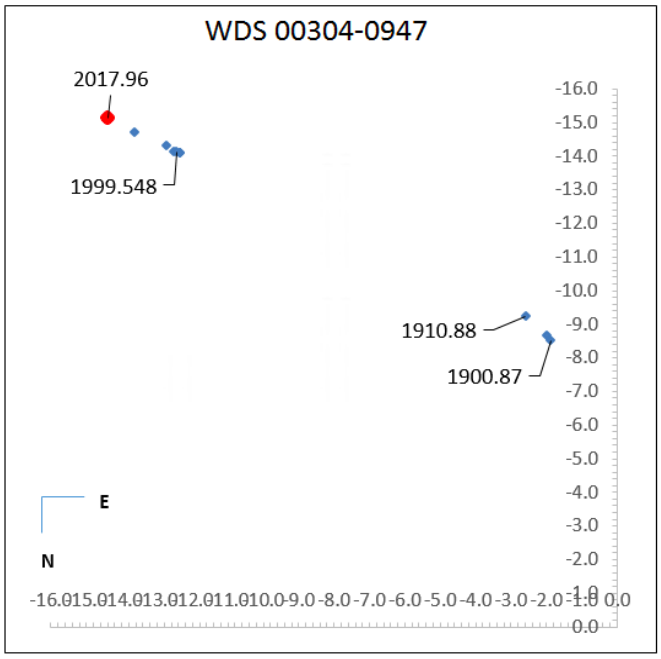

Figure 1. Historical measurements of WDS 00304-0947 plotted using an Excel tool developed by Richard Harshaw.

Equipment

Images of CHE 27 were taken with a Celestron C11 SCT, which did not require any online coordination as this telescope was not part of any remote/robotic tele-

Measurement of Star System 00304-0947 CHE 27

scope network but provided by our instructor in Terra Del Sol (California Northern Hemisphere). It has a 70x magnification, with a resolution of 0.42 arcseconds per pixel, and an aperture of 279.4mm.

Procedures and Methods

Imaging the Stars

Images from the Celestron C11 SCT were taken in Tierra del Sol by our mentor, Mr. Allen Priest. Red and luminance filters were used when taking these images. Once the images were taken, they were delivered to the Boyce Astro Research Computer (BARC) Server on a remote desktop for processing.

Processing and Measuring the Stars

Once all the images had been acquired and transferred to the BARC server, they were exported to MaxImDL to be calibrated and plate solved. The process of plate solving was conducted in order to properly orient the image in the sky with the correct Right Ascension and Declination. The PinPoint Astrometry program (included in MaximDL) was used to complete the plate-solving process by comparing stars in our images against the United States Navy UCAC-4 catalog.

The plate solved images were then imported into MiraPro to measure the position angle in degrees and the distance in arcseconds between the two stars. This was accomplished using its distance and angle function, which is able to locate the centroid of each stellar candidate. The measurements and data gathered from MiraPro were copied into Excel for statistical analyses: mean, standard deviation, standard error, and standard error percentage. Once all the data was collected from our processed images, historical data was ordered from the US Naval Observatory.

Results

Seven images were used in the measurement of CHE 27, Figure 2. After acquiring these images, we were able to collect separation and angle data using the processes described above. Additionally, the mean, standard deviation, and standard error were also calculated, Table 1. The stars in this system have a mean current position angle (theta) of 223.54° and a separation distance (rho) of 20.86" arcseconds. Figure 1 indicates the position of these mean measurements relative to the historical measurements for this star pair.

Discussion

The historical data, Table 2, provided by the United States Naval Observatory, coupled with our 2017 measurement, show a linear trend for CHE 27. There was an increase in both the angle separation and distance when contrasted to the last measurement taken of this system

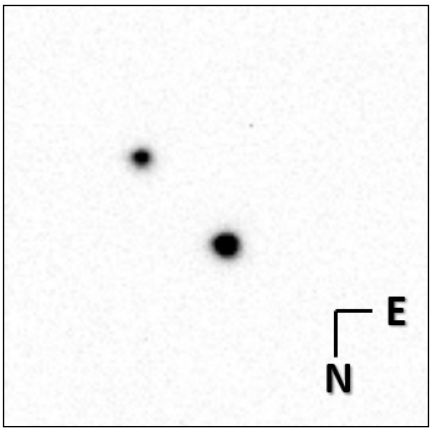

Figure 2. CHE 27 as imaged in 2017.

Table 1. Theta and Rho Measurement

Image	Theta (deg)	Rho (a.s.)
1	223.528	20.8963
2	223.44	20.8941
3	223.558	20.9016
4	223.635	20.8431
5	223.575	20.8565
6	223.622	20.8451
7	223.408	20.7915
Mean	**223.538**	**20.863**
Std. Dev.	**0.086**	**0.040**
Std. Error	**0.033**	**0.015**

Table 2. Historical Measurements

Date Observed	Theta (deg)	Rho (a.s.)
1900.87	192.5	8.72
1901.67	193	8.89
1910.88	195.7	9.6
1988.72	221.5	18.9
1998.816	221.22	18.76
1998.82	221.2	18.76
1999.548	221.4	18.83
2000	221.7	19.17
2010.5	222.8	20.06
2017.96	223.538	20.863

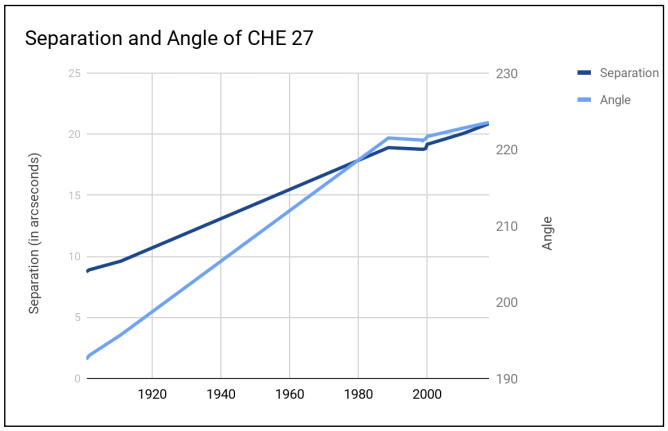

Figure 3. Angle and separation measurements of WDS 00304-0947 represented on a double axis graph.

in 2010. From the results recorded in the above section, we were able to calculate an increase of about 0.73° in angle and separation 0.8025" arcseconds in distance. A graph was created to show the change in theta and rho from observations since 1900, the first observation ever made on CHE 27, Figure 3.

Conclusion

Due to the increase in theta and rho from our recent measurements, our observations have supported the linear trend of this system as seen in previous measurements. There was a lack of observations from 1910 to 1988, which could've caused some uncertainty in the overall trend of this system's nature at that time, but since 1988, there has been consistency with this double star's measurements. Our recent measurements seem to confirm that this linear trend is consistent.

Acknowledgements

We would like to thank the United States Naval Observatory for providing access to historical measurement data through the Washington Double Star Catalog. In addition, we thank Pat and Grady Boyce of the Boyce Research Initiatives and Education Foundation (B.R.I.E.F) for providing access to the educational materials and for providing the funding which allowed us to use the iTelescope robotic telescope system along with other software tools. We are grateful to Mr. Allan Priest, our advisor, mentor, and teacher, for helping us to pursue all aspects of this amazing learning experience.

References

Hartkopf, W.I., Mason, B.D, 2006, "Sixth Catalog of Orbits of Visual Binary Stars", US Naval Observatory, Washington. http://www.usno.navy.mil/ USNO/astrometry/optical-IR-prod/wds/orb6

"Stelle Doppie" Double Star Database. https://www.stelledoppie.it/index2.php

Astrometric Measurements of WDS 04136-2532

Vivek Vijayakumar[1] and Curran Poulsen[2], Alex Falatoun[3] Pat Boyce[4], and Grady Boyce[4]

1. San Marcos High School, San Marcos, CA
2. Justin Siena High School, Napa, CA
3. Mesa Community College, San Diego, CA
4. Boyce Research Initiatives and Education Foundation (BRIEF), San Diego, CA

Abstract: Astrometric measurements were obtained for WDS 04136-2532 (SEE 34) using the iTelescope network. A mean position angle of 63.3° ± 0.6° and a separation distance of 15.5" ± 0.1" were measured showing an increase of 0.5º and decrease of 0.7" respectively from the last observation in epoch 2003.95. Historical data, combined with our recent measurements, did not indicate signs of orbital motion, but instead supports a linear trend.

Introduction

The research conducted in this paper is part of a program through Boyce Research Initiatives and Education Foundation (BRIEF) that allows high school students, college students, and other amateur astronomers, the opportunity to conduct scientific research and learn real world applications of the scientific process. The focus of study is astrometric measurements, position angle (Theta) and separation (Rho) of double star systems listed in the Washington Double Star (WDS) Catalog where candidates were selected, imaged, and analyzed to help add to the understanding of whether the star's association is merely an optical double or a gravitationally bound star system. Determining the latter in conjunction with other measurements could provide significant insight to the stars, such as their mass, which in turn opens opportunities to find radius, density and more.

For this research, the double stars available for conducting research were reviewed in the WDS Catalog based on their visibility during the Fall semester (August - February), and filtered by a minimum separation of 6 arcseconds with a magnitude difference no greater than 6. Additionally, the double star system selected has less than 10 observations making it favorable to study because our research provides additional observations, which may assist with further analysis of this system at some future date.

The star system ultimately chosen was WDS 04136 -2532 (henceforth referred to as SEE 34), for having met the aforementioned criteria for examination, and our team's desire to prevent a large data gap, since the last measurement was over a decade ago. The observation history for SEE 34 is outlined in Table 1.

Table 1. Historical Measurements of SEE 34

WDS 04136-2532 (SEE 34)		
Epoch	*Position Angle θ (°)*	*Separation ρ (")*
1897.76	55.1	19.78
1899.26	53.5	19.00
1906.72	55.8	19.10
1945.01	60.0	18.12
1979.941	61.0	16.90
1998.91	62.0	16.22
1999.713	62.7	16.167
2003.93	62.76	16.179

Astrometric Measurements of WDS 04136-2532

Figure 1. *iTelescope Network's T32 telescope in Siding Spring, Australia*

Figure 2. iTelescope Network's T30 Telescope in Siding Spring Australia

Equipment, Observations, and Data Analysis Procedures

Equipment

iTelescope Network's T32, Figure 1, is located the Siding Spring Observatory in New South Wales, Australia. The attached charged coupled device (CCD) has an anti-blooming gate full well and uses a 17" Planewave CDK optical tube assembly (OTA) on a Planewave Ascension 200HR mount. This telescope was selected due to its geographical location and its high resolution at 0.63"/pixel.

Due to the magnitude difference in the pair, and the fact that the primary emits more light at longer wavelengths, iTelescope Network's T30, Figure 2, was selected for its UV filter to assist in separating the stars on the CCD chip. Located in the Siding Spring Observatory, T30 has a CCD with a 100,000e- Non-anti blooming gate, a 20" Planewave OTA, and a Planewave Ascension 200HR mount with a resolution of 0.81"/pixel.

Observations

The date of observation was chosen to align as closely as possible to a new moon phase in order to have the lowest luminosity from the moon as determined by the Staralt visibility tool (Sorensen, 2002)[1].

Six images were taken at epoch 2017.87 with T32.

Three of these images were with a Hydrogen-alpha filter at 60 seconds exposure, and three images were with a blue filter at 60 seconds exposure. The images with the Hydrogen-alpha filter had over saturated pixels, while the blue filters produced one image where both the primary and secondary stars could be identified. Due to the long gap between observations, the one useable image was omitted from the results in order to report on only one epoch. In order to add to our collected data, on epoch 2017.95, fifteen more images were taken with T30 using a combination of UV and blue filters, though three were discarded due to excessive atmospheric distortion. Figure 3 shows one of our images of the star system.

Analysis Procedures

All images were preprocessed (flat-fielded and dark subtracted) by the iTelescope network. The pixels that contained our double star systems were checked for counts to make sure that none of the images were oversaturated. After assessing the quality of the images, they were uploaded to astrometry.net in order to assign World Coordinate System (WCS) positions.

The image analysis software SAOImage DS9 (referred to henceforth as DS9) was used to consistently measure the position angle (θ) and separation distance (ρ) for each image. First, a 7" circle was created using the Regions feature and placed over the A star, followed by a circle of the same radius around the B star.

DS9's auto-centroiding feature was used to find the

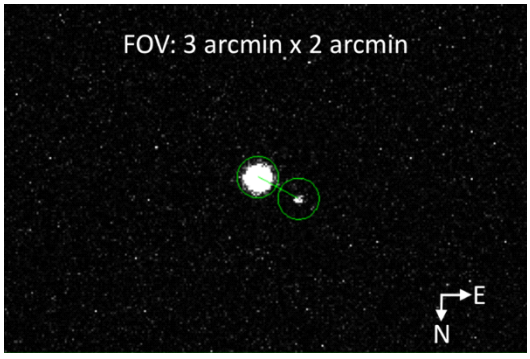

Figure 3. *One of our images of the star system, with the A component at the top left, and the B component at the bottom right*

Astrometric Measurements of WDS 04136-2532

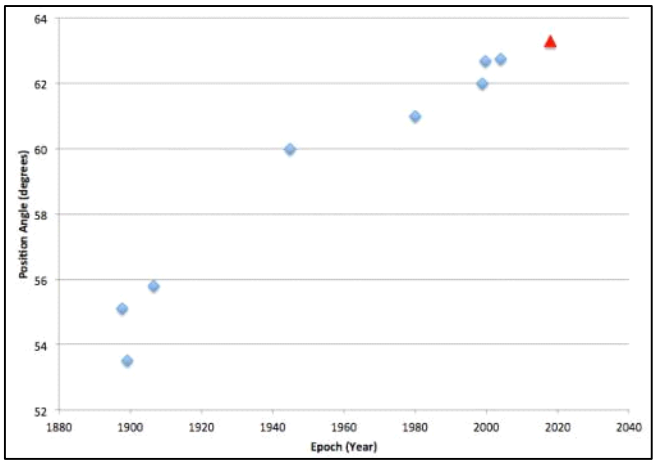

Figure 4. Position angle in degrees and epoch in years for SEE 34, including historical data and new measurement (red triangle).

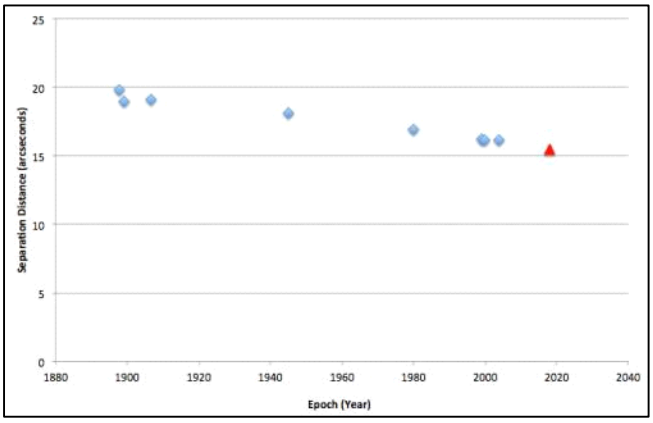

Figure 5. Graph of separation distance in arcseconds and epoch in years for SEE 34, including historical data and new measurement (red triangle).

center of each star, which effectively calculates the weighted mean position of all the counts per pixel enclosed in the circle. The coordinates for the centroid of each star were recorded and then placed as endpoints of a line segment. The length of the line segment provided the separation distance in arcseconds and its orientation relative to some reference provided the position angle.

Results

Astrometric measurements are reported in Table 2. For the epoch 2017.95 we measured a mean position angle of 63.34° ± 0.59° and separation distance of 15.49" ± 0.10". The uncertainty values are the calculated standard deviation of the mean.

Additionally, graphs of position angle vs. epoch, Figure 4, and separation distance vs. epoch, Figure 5, include our measurements in an historical context.

Discussion

We have found that our new measurement, if we omit the data point from 1899, supports a linear progression. The measurement from 1899 is an apparent outlier with respect to the other measurements, and doesn't seem to have any supporting documentation. With the position angle being 63.34° ± 0.59°, there hasn't been any change in position angle with respect to the last measurement in 2003 within the standard error of mean. With the separation distance being 15.49" ± 0.10", there has been a clear change in separation since the last measurement in 2003. When plotted in a proper motion plot (Figure 6), it is evident there is a linear progression, and the 1899 data point seems to be an outlier. This is not indicative of a physical binary, but more of an optical pair.

Conclusion

We measured the position angle and separation distance of WDS 04136-2532 (SEE 34), using observations from iTelescope Network's T30 and T32 tele- scopes. The position angle showed no significant changes since the last measurement in 2003. The separation distance has decreased by approximately one arcsecond. We conclude that SEE 34 is a linear case (if we reduce the statistical weight of the 1899 measurement).

Table 2. Position angle, separation distance and uncertainties for SEE 34[2].

WDS 04136-2532 SEE 34					
Epoch	Number of Images	Mean *Position Angle θ* (°)	σθ (°)	Mean *Separation ρ* (")	σρ (")
2017.95	12	63.3	0.6	15.5	0.1
2003.93	Last Measurement (Sinachopoulos, et al)	62.8	-	16.2	-

Astrometric Measurements of WDS 04136-2532

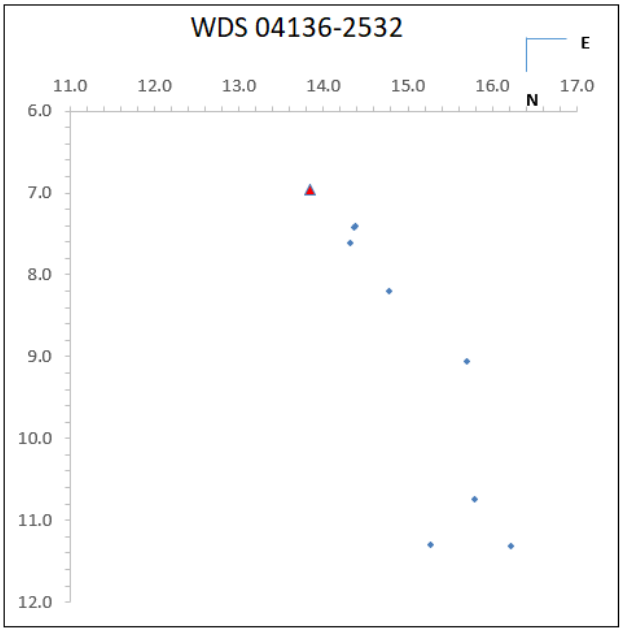

Figure 6. Relative proper motion plot of SEE 34, expressed as ΔRA vs. ΔDEC relative to the primary, placed at the origin. The blue diamonds represent previous measurements, and the red tri- angle represents measurements taken on epoch 2017.95.

Acknowledgements

The authors would like to thank the Boyce Research Initiatives and Education Foundation (B.R.I.E.F). Without their organization and guidance, none of this would have been possible. Additionally, we want to thank the United States Naval Observatory (USNO) for supplying thee historical data of our binary star system, which we used throughout the research process. We would also like to thank astronomy.net for providing the World Coordinate System (WCS) coordinates, and Matthew Salehi for additional contributions.

References

1. "Credits." *ING Banner*, 8 Aug. 2014, www.ing.iac.es/PR/credits.html.

2. Sinachopoulos, D., et al. "CCD Astrometry and Components Instrumental Magnitude Difference of 432 Hipparcos Wide Visual Double Stars." *Astronomy & Astrophysics (A&A)*, EDP Sciences, 16 July 2007, www.aanda.org/articles/aa/abs/2007/36/aa6290-06/aa6290-06.html.

Measurement of Star System 02442+4914 STF 296AB

Amanda Tran, Audrey Lee, Samuel O'Neill, Abigail Wu, and Allen Priest
The Cambridge School, San Diego, CA

Abstract: Position angle (theta) and separation (rho) measurements were obtained from multiple images of the star system WDS 02442+4914 STF 296 AB using a 17" telescope in the iTelescope network. From our 2018 measurements, STF 296 has a position angle of 304.9° degrees and separation of 20.6" arcseconds. Data recorded for STF 296 showed consistent accuracy in comparison to the current historical data.

Introduction

Double Star system WDS 02442+4914 STF 296 AB was imaged with telescopes equipped with CCD cameras to measure the position angle (theta) in degrees and separation (rho) in arcseconds. Measurements were compared with data provided by Washington Double Star Catalog (WDS).

To select double star system candidates for research, a variety of catalogs were used to find stars that fit specific criteria: the star systems had to be a minimum of six arc seconds apart, and the difference in brightness had to be no more than six orders of magnitude. The Washington Double Star Catalog, the Sixth Catalog of Orbits of Visual Binary Stars, and Stelle Doppie were all utilized to find pairs based on this criterion.

Background

From data and observations recorded in the Stelle Doppie database (Stelle Doppie Web), STF 296 is a confirmed binary star system. The US Naval Observatory has information pertaining to the data collected that was used to form a proposed orbit in their 6th Orbital Catalog (USNO Web). This star system was discovered and first measured by Friedrich Georg Wilhelm von Struve in 1782. It has been observed 79 times and was last observed in 2015. As a result of the data contained within these observations, a general orbit has been predicted, Figure 1. This paper provides a 2018 measurement to add additional data to this orbit by plotting our measurement with the historical data and comparing it to the plotted orbit provided by the US Naval Observatory.

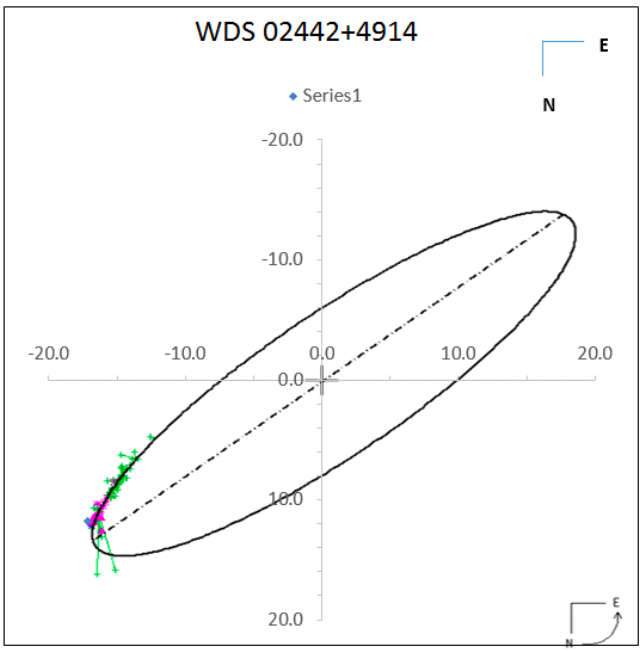

Figure 1. Proposed orbit for WDS 02442+4914 provided with historical data from Mason of the USNO

Equipment

Images were photographed using iTelescope T-21 in Mayhill, New Mexico. T-21, a deep field telescope, has a 17" platform with a FLI-PL6303E CCD camera and has a resolution of 0.96 arc-secs/pixel and an aperture of 431 mm. It operates within the iTelescope network and was selected due to its position in/visibility of

the Northern hemisphere. Dark, Flat, and Bias calibration images were provided by the iTelescope network for all images taken with T-21.

Procedures and Methods

Imaging the Stars

Images were ordered from T-21 on the iTelescope network, with exposure lengths and light filters specified for all images. Once complete, the requested images were then delivered to the Boyce Astro Research Computer (BARC) Server on a remote desktop for further processing. Additional images were acquired from a Celestron C11 SCT taken in Tierra del Sol by our mentor, Mr. Allen Priest.

Processing and Measuring the Stars

Once all the images had been taken and transferred to the BARC server, they were imported into MaxImDL to be calibrated and plate solved. The process of plate solving was conducted in order to properly orient the image in the sky with the correct Right Ascension and Declination. The PinPoint Astrometry program (included in MaximDL) was used to complete the plate-solving process by comparing stars in our images against the United States Navy UCAC-4 catalog.

The plate solved images were then imported into MiraPro to measure the position angle in degrees and the distance in arcseconds between the two stars. This was accomplished using its distance and angle function, which is able to locate the centroid of each stellar candidate. The measurements and data gathered from MiraPro were copied into Excel for statistical analyses: mean, standard deviation, standard error, and standard error percentage. Once all the data was collected from our processed images, historical data was ordered from the US Naval Observatory and is given in Table 2.

Results

The results of these image processes are outlined in Table 1. Images through a Hydrogen-alpha filter are shown in Figure 2.

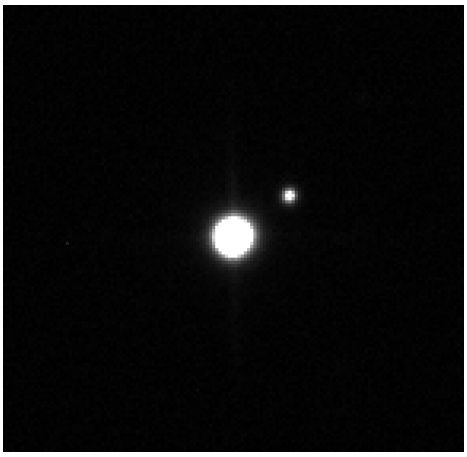

Figure 2: Hydrogen Alpha 30 Sec iTelescope)

After processing the images, the current separation between the A/B components of the system was determined to be 20.6 ± 0.6 arcseconds and the current position angle is 304.9 ± 1.4 degrees.

Discussion

The main purpose of studying this double star system was to observe any changes in data (i.e: theta or rho), if there were any, and to confirm whether or not the current proposed orbit is relatively accurate. After finding the plot for the most recent observation, the current proposed orbit seems to be the correct astronomical trajectory and is not contradicted by the newest data plot. This double star system is a confirmed physical system according to Stelle Doppie (Stelle Doppie Web), and our data did not provide any indication that it should instead be reclassified as an optical double star system.

Table 1. Theta and Rho Measurements made on 2018.923

Images	Theta (deg)	Rho (as)
1	305.3	20.9
2	302.3	19.5
3	307.0	21.4
Mean	304.9	20.6
Std. Dev.	2.8	1.0
Std. Error	1.4	0.6

Table 2. Some Historical Measurements

Date Observed	Theta (deg)	Rho (as)
1782.64	290	13.52
1845.23	295.3	15.06
1899.67	299.5	17.25
1924.898	300.8	18.43
1999.8	304.8	20.52
2018.33	304.9	20.6

Conclusion

The data collected from the star system STF 296 AB did in fact support the already proposed orbit. Our data point was consistent with the change that was to be expected in the system's movement over time. There is no current indication that this double star system is in fact an optical double.

Acknowledgements

We would like to thank the United States Naval Observatory for providing access to historical measurement data through the Washington Double Star Catalog. In addition, we thank Pat and Grady Boyce of the Boyce Research Initiatives and Education Foundation (B.R.I.E.F) for providing access to the educational materials and for providing the funding which allowed us to use the iTelescope robotic telescope system along with other software tools. We are grateful to Mr. Priest, our advisor, mentor, and teacher, for helping us to pursue all aspects of this amazing learning experience.

References

USNO Web: https://www.usno.navy.mil/USNO/astrometry/optical-IR-prod/wds/orb6

Hartkopf, W.I., Mason, B.D, 2006, "Sixth Catalog of Orbits of Visual Binary Stars", US Naval Observatory, Washington. http://www.usno.navy.mil/ USNO/astrometry/optical-IR-prod/wds/orb6

Stelle Doppie Web: https://www.stelledoppie.it/index2.php

Cross-Match of WDS KOI Objects with Gaia DR2

Wilfried R.A. Knapp
Vienna, Austria
wilfried.knapp@gmail.com

John Nanson
Star Splitters Double Star Blog
Manzanita, Oregon

Abstract: The WDS catalog contains in total 2,640 pairs with the designation KOI. So far (per end of August 2018) only 835 such objects have been confirmed by at least a second observation. Out of these 835 confirmed KOI objects 594 or ~71% were recovered as GAIA DR2 pairs. This statistic has been broken down to separation classes to check the performance of GAIA DR2 for resolving doubles in more detail. Additionally 1,043 KOI objects with so far only one observation have been confirmed by GAIA DR2 raising the percentage of confirmed KOI objects from ~32% to ~62%. Finally the matched KOI objects were checked for being potential binaries by means of common parallax.

Regarding GAIA Performance: With an update of the WDS data base in September 2018 with GAIA DR1 matches the number of confirmed KOI objects increased from 835 to 1,167 so the added value of GAIA DR2 compared to DR1 is not only the availability of proper motion and parallax data beyond TGAS but also in a significant larger number of confirmed objects.

1. Introduction

As follow up to our report "KOI objects in the WDS catalog" (Knapp&Nanson 2019) we checked this time the complete range of WDS KOI objects against the GAIA DR2 catalog.

Using the CDS TAP-VizieR tool in total 2,640 KOI objects were selected from the WDS catalog. Using the CDS X-match tool these objects were then for the primary cross-matched with DR2 with a search radius of 5" around the given WDS J2000 position. Due to the density of DR2 objects this yielded 5,237 objects. With the given GAIA DR2 J2000 positions and the WDS data for separation and position angle the J2000 position for the secondary was calculated with the caveat that GAIA DR2 provides for a few of the components of the KOI objects no proper motion values and thus the calculated positions were a mix of J2000 and J2015.5 coordinates. These calculated positions were again matched with GAIA DR2 but this time with 2" search radius for the secondaries giving 3,218 objects including the unavoidable self-matches for the primaries for objects with a separation below the 2" search radius.

As next step a drill down process was started after calculating separation and position angle for the found pairs (observation epoch J2015.5):

- Eliminating the self-matches of the primaries mentioned above
- Eliminating all pairs with a difference between calculated and WDS position angle larger than 15°
- Eliminating all pairs with a difference between calculated and WDS separation larger than 25%
- Sorting the objects by discoverer ID and checking for multiple matches made clear which objects had to be checked in detail to keep the best matches with the given WDS parameters not only for position angle and separation but also for the magnitudes
- Finally the remaining matches were checked for a corresponding magnitude delta between the components with a cut for the difference of 3 magnitudes
- As nearly all magnitudes for KOI objects are given in the red band a second check regarding the magnitudes was done to eliminate all objects with Gmags brighter than given WDS mags larger than 1.5mag – this leaves still some room for magnitude

errors in WDS as well GAIA DR2
- End result were then 1,636 remaining KOI to GAIA DR2 matches considered to be valid.

An update of the WDS catalog based on the ~80,000 GAIA DR1 matches from our report on estimating visual magnitudes (Knapp&Nanson 2018) became effective during September 2018 also for a good part of the KOI objects rendering the per end of August 2018 given number of observations for some objects as obsolete.

2. Results

The details of this cross-match and drill down process are as follows:
- 120 KOI objects are (in the WDS "precise *last* only" list) given with a separation smaller than 0.4" with 55 of them confirmed with more than 1 observation – no match is to be expected for this class of objects as this is the declared resolution limit of GAIA DR2 (Arenou et al. 2018)
- 128 KOI objects are listed with 0.4 to 1 arcsecond separation with 73 of them confirmed with more than 1 observation. 17 such objects were recovered as GAIA DR2 pairs which means a hit rate of 23%. In total 31 objects in this class were resolved in GAIA DR2 which means 14 new confirmations but also that only about 24% of the KOI pairs in this range got a hit. Taking the recovery rate for the confirmed objects as expectation for the rest of so far unconfirmed objects in this range we can estimate the number of KOI bogus objects in this class to be zero
- 305 KOI objects are listed in WDS with a separation between 1 and 2 arcseconds with 109 of them confirmed with more than 1 observation. 83 such objects were recovered as GAIA DR2 pairs means a hit rate of 76%. In total 202 objects in this class were resolved in GAIA DR2 which means 119 new confirmations. If we take the 76% ratio as expectation for this class of objects we can expect ~40 bogus KOI objects here
- 645 KOI objects are listed in WDS with a separation between 2 and 3 arcseconds with 206 of them confirmed by more than 1 observation. 165 such objects were recovered as GAIA DR2 pairs means a hit rate of 80%. In total 468 objects in this class were resolved in GAIA DR2 which means 303 new confirmations. If we take the 80% ratio as expectation for this class of objects we can expect ~60 bogus KOI objects here
- 1,442 KOI objects are listed in WDS with a separation of larger than 3 arcseconds with 392 of them confirmed by more than 1 observation. 340 such objects were recovered as GAIA DR2 pairs means a hit rate of 87%. In total 972 objects in this class were resolved in GAIA DR2 which means 632 new confirmations. If we take the 87% ratio as expectation for this class of objects we can expect ~325 bogus KOI objects here.

Some side results:
- KOI 652 AC might be a duplicate of KOI 652 AB despite listed with 3 observations
- KOI1316 AC might be a duplicate of KOI 316 AB despite listed with 3 observations
- KOI2579 AB and AC are nearly undecidable matches, AC was selected due to a better match with the given magnitudes. It seems possible that AB and AC are duplicates
- KOI6969 B and KOI 6970 B are identical
- KOI7126 B is a double itself, two measurements A;Ba and A;Bb are given as match for KOI7126 AB
- KOI2283 AB comes with a separation delta >20% for the second observation but is a perfect match with the first observation
- KOI 959 comes with an angular distance from the given J2000 position larger than 4" but this is explained by very fast proper motion. This object is also listed in GAIA DR2 with a rather bright secondary compared to the given WDS magnitude but this is still considered to be a correct match.

To counter-check our processes for being consistent we located the 30 GAIA DR2 matches from our first KOI report (Knapp&Nanson 2019) in the final list and eliminated them to avoid duplicated reporting.

In Table 1 the first 20 rows of the list of the cross-matched KOI objects are given with a subset of the data. The full list with all columns can be downloaded from the JDSO website as "KOI XX DR2":.

3. Check for Binaries

Finally the found matches were checked for being potentially binaries by calculating the distance between the components of the pairs using the parallax data provided by GAIA DR2 which was the case for at least a part of the objects. After eliminating all objects with missing or negative parallax values or Plx values smaller than 3 times the given parallax error range 564 pairs remained available for assessment according to Knapp 2018 (see Appendix A). Only 4 pairs qualified as being probable physical pairs, which is less than 1% of the

(Continued on page 245)

Table 1: Results cross-match WDS KOI objects with GAIA DR2

WDS	Disc	Comp	RA	Dec	Sep	PA	Gmag1	Gmag2	Plx1	Plx2	pmRA1	pmDec1	pmRA2	pmDec2
18410+4355	KOI3245		280.2495197	43.91506649	1.52743	184.553	12.41836	15.42990	1.9464	2.4805	8.389	-9.518	4.973	-8.831
18414+4350	KOI5457		280.3420874	43.83342728	1.33796	131.231	12.36358	12.36656	2.7475	3.5644	8.425	1.472	6.868	2.789
18426+4745	KOI 533		280.6414331	47.75205808	2.82135	255.145	14.66114	20.48529	1.6032	2.9229	8.221	25.512	5.213	23.154
18428+4355	KOI2486	AC	280.6903699	43.91905386	6.23914	84.954	12.97476	19.74163	2.0868	0.6172	6.855	-23.145	-3.963	-8.477
18437+4405	KOI1985		280.926162	44.08780364	2.78140	154.656	13.70406	18.03290	3.2413	3.0707	3.246	-24.711	2.953	-25.079
18442+4259	KOI4599		281.0436156	42.97565439	2.04427	80.883	15.30131	19.93481	0.9977	0.0320	0.283	-19.197	2.332	-14.154
18442+4319	KOI2734		281.0491988	43.32259957	2.34910	89.036	15.78024	19.17308	1.1620	0.2177	5.054	1.280	-1.670	-7.056
18445+4317	KOI4419	AB	281.1162646	43.28231994	3.96294	115.525	15.11679	20.49738	3.7793	-0.7957	-26.761	-27.821	-1.121	-1.685
18454+4340	KOI6925		281.356505	43.65860363	2.49519	126.857	15.77305	17.58996	2.9496	2.9140	-26.187	45.110	-26.093	45.903
18454+4418	KOI1820		281.3487514	44.29525246	3.70873	180.296	13.50332	20.15283	2.4682	2.1648	-7.230	3.248	5.900	1.011
18462+4414	KOI4799		281.5526276	44.22864001	3.50937	283.289	14.24587	20.22990	1.3471	-1.2733	-8.959	18.921	-1.927	-4.832
18463+4304	KOI3995		281.5757503	43.06812594	3.75982	116.810	13.31339	14.85094	0.7267	0.6290	8.050	-0.380	-5.240	-1.715
18466+4157	KOI3284	AC	281.6457236	41.95106862	3.96370	3.854	14.48515	16.80051	5.1035	1.2625	-16.762	-4.921	4.658	-5.412
18466+4335	KOI5427		281.6596045	43.58789916	3.06132	175.714	15.00100	18.72624	0.8306	0.3328	-0.117	2.447	1.854	3.081
18468+4224	KOI2914	AB	281.6915657	42.39744618	3.78573	231.351	12.13935	17.73056	1.2469	0.1011	-7.688	-15.501	1.265	-11.026
18473+4249	KOI4136		281.8231767	42.81119787	3.67657	108.592	13.95949	20.16504	0.7689	0.5617	-1.800	9.022	0.152	-1.004
18481+4338	KOI1818		282.0354942	43.63124905	2.31928	230.341	14.04304	20.07801	1.7124		0.198	-0.801		
18481+4423	KOI2385		282.0173492	44.38576419	3.54624	337.061	15.81119	20.49753	1.0424	-0.1559	-5.533	3.727	-5.275	-11.031
18485+4418	KOI4399	AB	282.1288496	44.30294392	2.11639	16.942	11.97393	17.66495	4.7145	6.7850	0.273	-39.979	0.867	-38.607
18486+4214	KOI 667		282.1544897	42.23459339	2.98301	133.005	17.25899	17.28079	0.7087	0.2418	-4.527	-3.782	-2.123	-5.837

Description of the table content:

WDS = WDS ID
Disc = Discoverer code
Comp = Components
RA = RA observation epoch 2015.5 in degrees
Dec = Dec observation epoch 2015.5 in degrees
Sep = Separation in arcseconds
PA = Position angle in degrees
Gmag1 = Gmag1
Gmag2 = Gmag2
Plx1 = Parallax 1 in mas
Plx2 = Parallax 2 in mas
pmRA1 = Proper motion RA 1 in mas
pmDec1 = Proper motion Dec 1 in mas
pmRA2 = Proper motion RA 2 in mas
pmDec2 = Proper motion Dec 2 in mas

pairs listed with usable Plx data. As the average ratio in the WDS catalog is about 15% V- or T-coded this result is quite a disappointment and raises the question why KOI objects are WDS listed as double stars at all.

In Table 2 the first 20 rows of the list of the cross-matched KOI objects are given with a subset of the data. The full list with all columns can be downloaded from the JDSO website as "KOI XX DR2 Plx".

4. Summary

To sum up the results above we get 2,520 KOI objects with a separation larger than 0.4" with 780 of them with two or more observations. 605 such objects were recovered in GAIA DR2 which means (not counting the objects with separation below 0.4") an overall hit rate of 77.5%. In total 1,673 KOI objects got resolved in GAIA DR1/2 which means close to 900 new confirmations. And overall we have to expect that ~ 425 KOI objects are most probably bogus (which means close to 17%) if we don't find other reasons for them to be not resolved in GAIA DR2 as for example extreme faintness beyond the GAIA resolution limit. Counter-checking this assumption for objects with separation >3" we found that indeed in most cases red magnitudes in the range of 20 mag or even fainter are given so the number of bogus objects to expect should be significantly smaller.

Taking a look at the GAIA DR2 recovery performance we find that pairs below 0.4" separation are generally not covered (Arenou at al. 2018). Pairs between 0.4 and 1.0" separation have a hit rate of ~23% and for objects with separation larger than 1" we find a hit rate of 76%, larger than 2" of 80% and larger than 3" of 87%. These values are slightly inferior to those of doubles with brighter secondaries (see for example Knapp 2018 on Tycho Double Stars) but obviously good enough to be of interest for getting confirmations for neglected WDS objects and especially important seems the possibility to check pairs for being potentially binaries using the GAIA DR2 parallax data.

Overall summary: While there are certainly very good reasons that KOI objects are of interest for the Kepler mission, there are with very few exceptions, certainly no reasons that KOI objects should be of interest as double stars – so any effort to get confirmation for the remaining WDS KOI objects with currently only one observation is probably of little use. But one object is certainly of special interest: KOI 959 – currently without proper motion and parallax data in GAIA but according to the LSPM catalog probably a pair with very fast common proper motion.

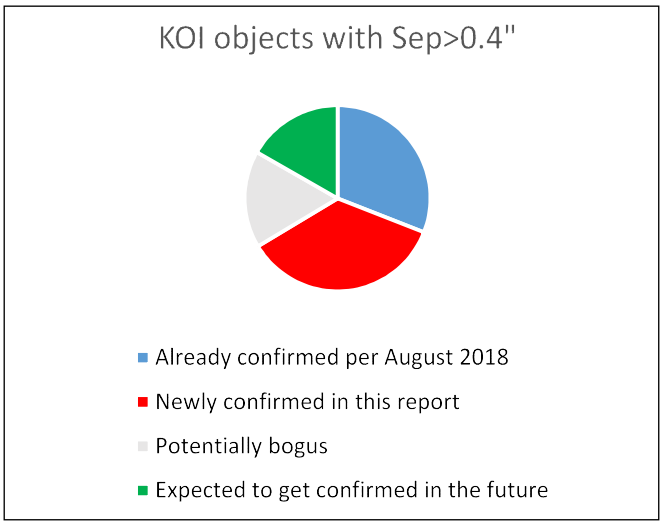

Figure 1: Confirmation status of WDS KOI objects

References

F. Arenou, X. Luri, C. Babusiaux, C. Fabricius, A. Helmi, T. Muraveva, A. C. Robin, F. Spoto, A. Vallenari, T. Antoja, T. Cantat-Gaudin, C. Jordi, N. Leclerc, C. Reylé, M. Romero-Gómez, I-C. Shih, S. Soria, C. Barache, D. Bossini, A. Bragaglia, M. A. Breddels, M. Fabrizio, S. Lambert, P.M. Marrese, D. Massari, A. Moitinho, N. Robichon, L. Ruiz-Dern, R. Sordo, J. Veljanoski, P. Di Matteo, L. Eyer, G. Jasniewicz, E. Pancino, C. Soubiran, A. Spagna, P. Tanga, C. Turon, C. Zurbach – 2018, Gaia Data Release 2: Catalogue validation, Astronomy & Astrophysics, Vol 616, A17

E. Furlan, D. R. Ciardi, M. E. Everett, M. Saylors,, J. K. Teske,, E. P. Horch,, S. B. Howell, G. T. van Belle, L. A. Hirsch, T. N. Gautier, III, E. R. Adams0, D. Barrado, K. M. S. Cartier, C. D. Dressing,, A. K. Dupree, R. L. Gilliland, J. Lillo-Box, P. W. Lucas, and J. Wang – 2017, THE KEPLER FOLLOW-UP OBSERVATION PROGRAM. I. A CATALOG OF COMPANIONS TO KEPLER STARS FROM HIGH-RESOLUTION IMAGING, The Astronomical Journal, Vol 153, Number 2, Page 71

Knapp, Wilfried R.A. and Nanson, John – 2019, KOI objects in the WDS catalog, submitted to JDSO August 10th

(Continued on page 247)

Table 2: Results of assessment for being physical based on parallax and separation

WDS	Disc	Comp	Plx1	Plx2	Sep	BCD	RCD	WCD	Plx Rat	Plx Sco	Notes
18410+4355	KOI3245		1.9464	2.4805	1.52743	15850508.017	22818415.946	29160027.344	DA	1	S
18414+4350	KOI5457		2.7475	3.5644	1.33796	2873818.599	17205963.673	36338144.104	DC	1	S
18426+4745	KOI 533		1.6032	2.9229	2.82135	25762451.788	58090858.781	76181092.372	DD	1	S
18437+4405	KOI1985		3.2413	3.0707	2.78140	660576.175	3535547.397	6623453.156	DA	1	S
18454+4340	KOI6925		2.9496	2.9140	2.49519	837.386	854342.051	4057733.658	CA	20	
18463+4304	KOI3995		0.7267	0.6290	3.75982	26568968.732	44088264.456	62200298.193	DA	1	S
18466+4157	KOI3284	AC	5.1035	1.2625	3.96370	111908741.111	122964300.287	135384296.690	DA	1	S
18485+4418	KOI4399	AB	4.7145	6.7850	2.11639	11187317.184	13351313.219	15285207.435	DA	1	S
18486+4214	KOI 667		0.7087	0.2418	2.98301	339258237.035	562003973.585	934741185.595	DC	1	S
18489+4816	KOI1287		0.6860	0.6786	2.54694	3547.337	3278900.755	53657800.601	CB	19	
18507+4135	KOI6023	AC	0.5536	0.3341	3.43035	163761613.959	244791429.943	338977656.864	DB	1	S
18516+4150	KOI6702		0.8687	0.9094	1.76030	1976.126	10626833.763	23764459.274	CA	20	
18526+4508	KOI 42	AB	6.7495	6.8521	1.66390	245.712	457600.373	974432.771	CA	20	
18533+4150	KOI 852	AC	0.7854	0.5447	5.95329	70854369.779	116054520.334	168540844.889	DB	1	S
18533+4824	KOI3564		1.6115	1.5645	4.87474	807709.538	3845265.758	6901710.092	DA	1	S
18534+4112	KOI4016	AC	4.0534	2.4449	3.33564	20880342.231	33479174.676	51250369.791	DB	1	S
18534+4112	KOI4016	AD	4.0534	3.8398	5.54167	1135102.139	2830788.847	4614794.780	DA	1	S
18534+4833	KOI 344	AB	2.1559	2.6572	4.14546	8282194.595	18050078.369	26088412.888	DB	1	S
18535+4149	KOI 510		1.1785	1.1002	2.39097	1988.705	12456464.145	35427245.260	CB	19	
18536+4131	KOI2542		3.8392	5.3342	0.76280	10853296.271	15057934.450	19647372.050	DA	1	S

Description of the table content:

WDS = WDS ID

Disc = WDS discoverer code

Comp = Components (AB if blank)

Plx1 = Parallax for primary

Plx2 = Parallax for secondary

Sep = Separation in arcseconds

BCD = Best case distance A to B in AU

RCD = Realistic case distance A to B in AU

WCD = Worst case distance A to B in AU

Plx Rat = Letter based rating for potential gravitational relationship with first letter for distance and second letter for error size

Plx Sco = Estimated probability for potential gravitational relationship

Notes = Suggested WDS code either "T" for physical or "S" for optical, else blank

(Continued from page 245)

Knapp, Wilfried R.A. and Nanson, John – 2018, Estimating Visual Magnitudes for Wide Double Stars, Journal of Double Star Observations, Vol. 14 No. 3 Pages 503-520

Knapp, Wilfried R.A. – 2018, Cross-Match of WDS TDS/TDT objects with DAIA DR2, submitted to JDSO August 25th

Knapp, Wilfried R. A. – 2018, A new concept for counter-checking of assumed Binaries, Journal of Double Star Observations, Vol. 14 No. 3 Pages 487-491

Robert W. Slawson, Andrej Prsa, William F. Welsh, Jerome A. Orosz, Michael Rucker, Natalie Batalha, Laurance R. Doyle, Scott G. Engle, Kyle Conroy, Jared Coughlin, Trevor A. Gregg, Tara Fetherolf, Donald R. Short, Gur Windmiller, Daniel C. Fabrycky, Steve B. Howell, JonM. Jenkins, Kamal Uddin, F. Mullally, Shawn E. Seader, Susan E. Thompson, Dwight T. Sanderfer, William Borucki, and David Koch – 2011, KEPLER ECLIPSING BINARY STARS. II. 2165 ECLIPSING BINARIES IN THE SECOND DATA RELEASE, The Astronomical Journal, Vol 142, Number 5, Page 160

Acknowledgements

The following tools and resources have been used for this research:

- Washington Double Star Catalog
- GAIA DR2 catalog
- Aladin Sky Atlas
- CDS TAP-VizieR TAP
- CDS X-match

Appendix A
Description of the Plx Rating Procedure

- The distance vector of the two components of a pair is calculated with the naive approach 1/Plx +/- error range and the distance between the components is then calculated using the law of cosines with the two resulting vectors and the given angular separation
- "A" for worst case distance (Plx with errors applied for largest possible result), "B" for realistic case distance (using given Plx without error) and "C" for best case distance (using Plx with errors applied for smallest possible result) less than 200,000 AU (means touching Oort clouds for two stars with Sun-like mass) and “D” for above
- "A" for Plx error less than 5% of Plx, "B" for less than 10%, "C" for less than 15% and “D” for above

The letter based scoring is then transformed into an estimated probability for being potentially gravitationally bound

Astrometry Observations of Six Uncertain Double Stars

Cooper Howlett[1], Erin Pickering[1], Joshua Breman[2], Malia Barker[3]

1. University of Hawaii Maui College, Kahului, Hawaii, USA
2. Haleakala Waldorf High School, Makawao, Hawaii, USA
3. Kihei Charter High School, Kihei, Hawaii, USA

Abstract: Double-star systems HJ3231AC, BU1341AB, STI1656, HJ1002, STI110, STF3041AB, DAM622, STF2796, and ES1865AB were observed by the Las Cumbres Telescope network at the Teide Observatory. Average separations (ρ) and position angles (θ) were determined through AstroImageJ software and compared against pre-existing data in the Stelle Doppie database. The concluded data is checked for accuracy by comparing to two reference targets and ultimately contributes to database observations for each target. Three outliers were discovered: STI1656, a possible triple star system; DAM622, where we found a nearby quintuple system; and STI110.

Introduction

In this paper, we seek to update several double-star systems with new data, while also demonstrating the accuracy of our methods by comparing our results with two well-known double-star systems acting as reference targets. This research project was a part of an Astronomy Research Seminar offered by the University of Hawaii Maui College, instructed by Hsin-Yi Shih. The team members participating in this seminar can be found above, in Figure 1.

Targets were selected from the Stelle Doppie database, and was recorded by the Washington Double Star Catalog. The database has a wide variety of attributes to sort by, including position, magnitude, and amount of stars within a system (Stelle Doppie). Preference was given to uncertain doubles: double-star systems with a low enough amount of observations to merit uncertainty regarding their binary nature. We searched for uncertain doubles, keeping in mind the low number of observations and observations made within the past 15 years. The targets were also selected with proximity to 0h Right Ascension, in order to ensure night time visibility during the fall season (Chaisson & McMillan). The reference targets were selected for their large number of observations, in order to identify and minimize procedure error. The selected targets and more information can be found in Table 1.

Figure 1. Research team for the present study. From left to right: Malia Barker, Erin Pickering, Cooper Howlett, Joshua Breman.

During analysis of the system DAM 622, a quintuple star system was unintentionally observed: ES 1865AB. We later included this system as a target. The properties of this system are described in Table 2.

Procedures

Observations were made by the Las Cumbres Telescope network, or LCO. This network consists of twenty-one robotic telescopes located in eight sites based around the world. They are all centrally connected over

Table 1. A summary of historical measurements for the double stars observed in this project. All targets are uncertain doubles, except for those marked by an asterisk (*). Asterisk indicates a reference target.

Name	Recorded ρ	Recorded Position Angle	Number of Observations	Last Recorded Observation	First Recorded Observation
HJ 3231AC	44.7″	296°	9	2012	1831
BU 1341AB	20.3″	319°	11	2015	1903
STI1656	13″	81°	4	2003	1917
HJ 1002	27.2″	26°	6	2010	1909
STI 110	7.3″	5°	7	2012	1908
DAM 622	6.9″	48°	3	2010	1999
STF3041AB*	56.4″	358°	42	2016	1891
STF 2796*	26.4″	42°	44	2010	1782

the internet and have the ability to observe an object from any time zone, using a method called time domain astronomy. Multiple analyses of factors like similar requests, weather conditions, and target locations are automatically taken into account by LCO to best determine when observations will be taken. The availability of certain telescopes to observe a specific target can also be checked using the LCO Visibility Tool. This is done by entering the RA and Declination of the target (LCO, Visibility Tool.). When best conditions have been found for each request, they are submitted to their respective telescopes and observed. The resulting data is then uploaded, and made available for download online.

Instrumentation

For each double star, fifteen to twenty observations were taken at Teide Observatory, located in the Canary Islands, Spain (LCO, Teide). The observatory rests at an elevation of 2,390 meters (AEMET.). Observations were taken using a 0.4-meter telescope supported by a C-ring Equatorial mount, as well as an SBIG STX 6303 Charge Coupled Device, or CCD camera, mounted at the Cassegrain focus (LCO, 0.4 Meter). It has a pixel scale of .59 arcseconds / pixel, and a field of view of 2K x 3K pixels. This is equivalent to a 19 x 29 arcminute field of view. The telescope was built by the Las Cumbres Observatory, similar to the equipment in Figure 2. Several different filters were used, depending on the target. Targets HJ3231AC, HJ1002, STI110, DAM622, and STF2796 were observed with the GP

Table 2. Summary of data from the quintuple system ES 1865

Name	Recorded ρ	Recorded Position Angle	Number of Observations	Last Recorded Observation	First Recorded Observation
ES 1865AB	23.7″	123°	13	2015	1913
ES 1865AD	77″	37.3°	5	2012	1971
ES 1865BC	3.7″	180°	8	2012	1913
ES 1865AE[1]	33.2″	330°	3	2013	1999
ES 1865AC[2]	N/A	N/A	0	2018	2018

Table 2 Notes

1. Also referred to as FYM204 in Stelle Doppie catalog.
2. No previous measurements.

Figure 2. An example model of the 0.4 meter telescope used, built at LCO headquarters in Santa Barbara, California.

filter, targets BU1341AB, STI1656, and STF3041AB with the RP filter. Filters were chosen for optimal signal to noise ratio with consideration for image saturation, and difference in primary versus secondary star brightness.

Methods of Data Collection

As students of the University of Hawaii, the Institute for Astronomy (IfA) has granted us a certain amount of time to access the LCO telescopes in order to obtain data for educational purposes. To request imaging from the Las Cumbres Telescopes, we needed to predetermine exposure information using the 0.4-meter telescope's exposure calculator. This included exposure time, the signal to noise ratio, and the peak photon count for the primary and secondary magnitude stars in each target (LCO, Exposure Time Calculator.). We also noted the targets' previously recorded coordinates, separations, and magnitudes from the Stelle Doppie catalog. We initially requested data on 12 targets. However, after analyzing the received data we narrowed down our selection to the eight targets - as noted in Table 3 - based on image quality and clarity of the target star system.

Before the observations were analyzed by our team, they were subject to the LCO "BANZAI" data reduction pipeline. The automatic processes used were bias and dark subtraction, bad pixel masking, flat field correction, source extraction, and astrometric solution using Astrometry.net (LCO, Data Pipeline). These processes are explained below.

Data Processing

Images were received in FITS files and previously processed by the Las Cumbres Telescope's BANZAI data processing pipeline. Our observations were created with a 2x2 binning mode, with readout times averaging less than 6 seconds. A variety of data processes were used by the pipeline to create optimal observations for analysis. An explanation of these methods can be found below.

Bad pixel masking: This flags any pixels in the detector array that are not in working observational condition; such as pixels with excessive noise or potential outliers. The bad pixels are then set to zero, removing them from the processed image and data analysis.

Bias Subtraction: This eliminates the readout signal from the CCD.

Dark subtraction: This eliminates the dark noise, created by accumulated electrons in the CCD (Nass, P).

Flat Field correction: This checks for sensitivities in different locations on the CCD (Hainaut, O.). The inaccuracies are then corrected by taking several observations of uniform light, and using the resulting average to identify locations of variable sensitivity. The sensitivity map that results can then be used to correct the light readings of observation.

Astrometric solution: Astrometry.net uses calibration meta-data and known celestial objects to calibrate the observed images to the correct coordinates in the sky. This includes the Right Ascension and Declination data for each image.

We then downloaded the processed data from the LCO web server and began to perform our own analyses.

Methods of Analysis

To analyze and view the observations, we used AstroImageJ, a FITS file reader and analysis application (AIJ). The correct view used within AstroImageJ to perform analyses can be seen in Figure 3. We first identified each uncertain double by its proximity to the center of the image and how much it visually resembled a double-star system. We then confirmed our predicted target by finding the Right Ascension and Declination of the primary star in AstroImageJ, then comparing this data to the Stelle Doppie catalog values.

To find the separation and position angles of the target system, their apertures must be plotted. This was done by setting the aperture radius to the size of the primary star and plotting it with respect to the aperture

radius of the second star. The resulting separation and position angles are generated from the plot by AstroImageJ. Record this data, and repeat the steps outlined in this paragraph with ten to fifteen more observations in the same filter, per target. If more observations are available, include them.

After the above steps, a data set of the observed separation and position angle values are created. From this data set, the average separation and position angles for each target can be found. A standard deviation can also be derived from each observed value, from which an average of standard deviation can be found per target. Our results using these analyses are stated below in Table 3 for all six chosen targets, with Table 4 stating our results for the quintuple system ES1865.

Discussion

HJ3231AC

The data collected on the double-star HJ3231AC regarding position angle and separation is the closest alignment we found when compared to previously recorded data of the system. Our method used to measure this system proved accurate, without a change in position angle, and a very slight change (less than 0.40%) in separation angle.

BU1341AB

The data collected on this binary system matched the last recorded data from 2015. There is no difference in position angle. However, a slight separation angle difference of 0.98% is presented.

STI1656

Compared to previously recorded data in Stelle Doppie, there is a slight difference in separation angle, 0.7%, and an even smaller difference in position angle, 0.14%. This is still closely consistent with the last recorded data in 2003. However, there is a dim nearby star extending from the primary magnitude star that has no previously observed data. See Figure 4. Data obtained from this star is as follows: ρ = 4.52" (arc seconds), Position Angle = 102.78° (degrees). This suggests a possible triple star system.

HJ1002

For this binary system, our data showed a decrease in both separation angle and position angle. A 0.37% decrease in separation angle and a 6.61% decrease in position angle were presented among the data for this target.

STI110

For this system, our method proved accurate in finding the separation angle. However, for the position angle, there was a percentage difference of 14.8%, which is far outside the standard deviation of percent

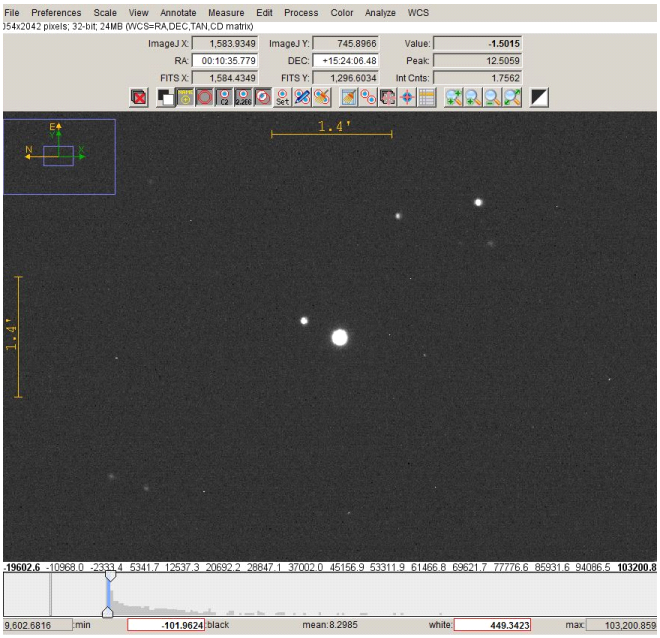

Figure 3. Example of analyzing HJ1002 image using AstroImageJ.

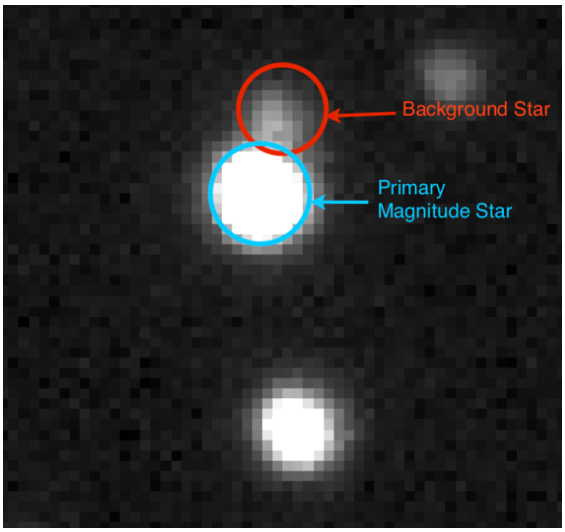

Figure 4. STI1656 FITS file shown in AstroImageJ application showing unrecorded background star.

differences across all targets (4.57%). This difference presented as a consistent difference in our measurement against the previous record, especially considering the accuracy of the target's separation measurements and that of our other targets. To check the significance of this difference, we re-measured the position angle and

Astrometry Observations of Six Uncertain Double Stars

Table 3. Summary of observation data and its comparison to previously recorded data. An asterisk (*) indicates reference targets. Uncertainies are standard deviation.

Name	Observed ρ (Average of 10 to 15 images)	Recorded ρ	ρ Percentage Difference	Observed Position Angle (Average of 10 to 15 images)	Recorded Position Angle	Position Angle Percentage Difference	Filter	Julian Date
HJ3231AC	44.87"±0.36"	44.7"	0.38%	295.99°±0.09°	296°	0%	gp	2458373
BU1341AB	20.50"±0.07"	20.3"	0.98%	319°±0.1°	319°	0%	rp	2458368
STI1656	13.09"±0.08"	13"	0.7%	80.96°±0.17°	81°	0.14%	rp	2458361
HJ1002	27.30"±0.33"	27.2"	0.37%	24.28°±0.98°	26°	6.61%	gp	2458368
STI110	7.31"±0.05"	7.3"	0.14%	5.74°±0.36°	5°	14.8%	gp	2458368
DAM622	7.04"±0.32"	6.9"	2.2%	46.90°±1.78°	48°	1.38%	gp	2458369
STF3041AB*	57.92"±1.4"	56.4"	0.23%	358.13°±0.15°	358°	0%	rp	2458368
STF2796*	26.65"±0.6″	26.4"	0.95%	41.59°±1.16°	42°	0.98%	gp	2458381

Table 4. Summary of observation data collected for quintuplet system ES1865, and its comparison to previously recorded data. ± indicates average standard deviation.

Name	Observed ρ (Average of 10 to 15 images)	Recorded ρ	ρ Percentage Difference	Observed Position Angle (Average of 10 to 15 images)	Recorded Position Angle	Position Angle Percentage Difference	Filter
ES1865AB	23.92" ± 0.5″	23.7"	0.93%	122.25° ± 0.6°	123°	0.61%	gp
ES1865AC[1]	25.37" ± 0.5″	N/A	N/A	129.73° ± 0.6°	N/A	N/A	gp
ES1865AD	37.25" ± 0.6″	37.3"	0.13%	76.52° ± 0.4°	77°	0.62%	gp
ES1865AE	33.48" ± 0.2″	33.2"	0.84%	329.75° ± 0.8°	330°	0.08%	gp

1. N/A indicates no previous measurements

separation of the system using fifteen images and calculated the average and standard deviation of each. What we calculated was 7.31"±0.05" for the separation and 5.74°±0.36° for the position angle. This result further indicates the significance of the difference between the previously recorded position angle and our observed position angle.

One possible reason for this deviation is that STI110 may be orbiting and that would present as an evolving position angle with a relatively constant separation. This hypothesis is supported by the differences in previous observations from Stelle Doppie. The first observation in 1908 recorded the position angle as 354°, but observations in 2001, 2003, and 2012 recorded 5°, 4°, and 5°, respectively, indicating a significant change, or at least inconsistent observation, in the system's position angle over the past century.

DAM622

For binary system DAM 622, we were able to contribute data to its previous record of only three observations. We found that there was quite a slight increase in separation angle, with a difference of 1.38% than its last recorded observation in 2010. Upon further observation of this double star, we came across the quintuple system, ES1865, as pictured in Figure 5. Since all the images we gathered of DAM622 provided a clear view of ES1865, we decided to go ahead and record data for that system as well, recorded in Table 4.

STF2796 (reference)

This system served as an excellent reference, as it had been observed 44 times - giving us a good platform to test the precision of our methods. The data we had collected for this system matched previously recorded data - with only a difference in ρ of 0.95%, and a difference in θ of 0.98%. This is a sufficient difference to

validate that the methods we used were accurate.

Our method of finding the separation and position angles of our targeted binary systems, in general, proved to be precise. With an overall standard deviation of ρ to be ±0.6", and standard deviation of θ to be ±1.16°, it's safe to say the data that we contributed to these double-star systems are accurate. There are, however, two that stood out in our findings, one being our unexpected observation of the quintuple system ES1865AB. Another thing that stood out in our findings was the large percentage difference found in system STI110's position angle.

STF3041AB (reference)

Binary system STF3041AB was used as our reference target, as it has been observed 42 times in the last 125 years. We were able to validate our method's accuracy with this binary system, as our results correlated closely with the data that has been previously recorded for this double star.

ES1865

This system was sort of a "bonus system" as it wasn't necessarily a hand-picked target, rather we unexpectedly came across it in images of DAM622 (a target that was originally chosen to be observed). Upon analyzing this system, we found out that it is known as a quintuple system, as there are five visible stars in this system, that we referenced as: A (primary star), B, C, D, E, as depicted in Figure 6. Although the relations between AB, AD, and AE were observed with an accumulation of 24 times, we weren't able to find any recorded data on ES1865AC (data of the primary star, "A", to star "C"), so we proceeded to record the first documented data of this relation.

Conclusion

Our initial goal was met, as we updated the data for the small number of observations on these six double-star systems with our own data sets. The method of data collection used proved successful, as we recorded an average of a 0.71% difference for separation angle and an average of 2.29% difference for position angle.

We updated information on targets STI110, HJ1002, HJ3231AC, and BU1341AB. We found unexpected results among STI1656 and DAM662.

Further research into double-star system STI1656 could reveal more information on the background star behind the primary magnitude star, possibly identifying this target as a triple star system. The magnitude of the background star would have to be determined, then observations need to be made in a filter allowing both the primary and background stars to be visible.

Because our measurements proved to be accurate, it is logical to reason that the large percent difference in position angle for target STI110 could reflect a natural change in position, like an orbit. Previous measurements support the theory, as explained in the discussion section. Further observations may or may not confirm the orbital nature of this target.

Additional research can be pursued with these targets, through photometry. It is possible to observe the ten available targets with different color filters. This could lead to updating magnitude data sets in Stelle Doppie.

Acknowledgments

We want to thank our instructor, Hsin-Yi Shih, for guiding us through the research paper process, answering all questions along the way, and reviewing the paper. Additionally, we thank the Las Cumbres Observatory for our target images, the Stelle Doppie catalogue for the recorded data, the Simbad catalogue for additional reference, and the University of Hawaii Maui College, for utilization of the computer lab and overall enriching learning opportunity. We would also like to thank Russ Genet and Vera Wallen, for contributing

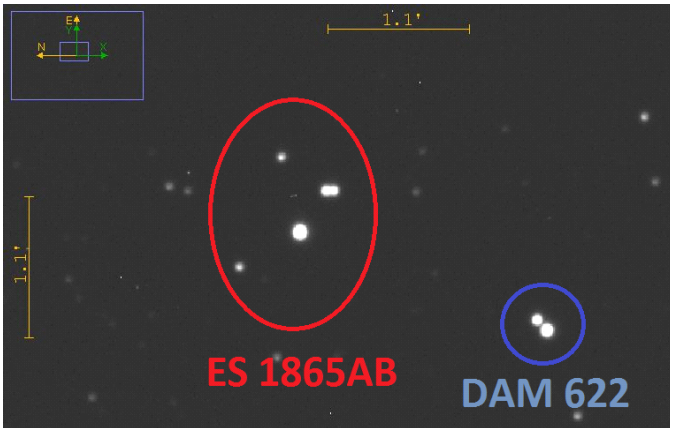

Figure 5. Observation of ES 1865AB and DAM 622, from a FITS file viewed in AstroImageJ.

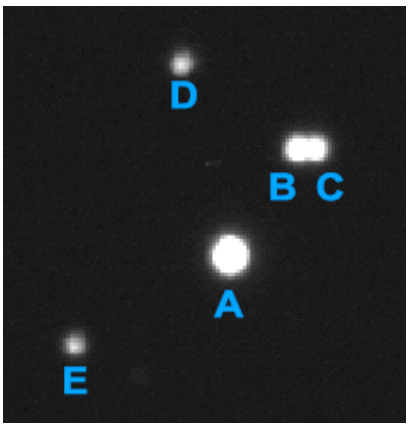

Figure 6. ES1865 and its primary star's relation to stars B, C, D, and E.

their expertise and time to review this paper. This research has made use of the Washington Double Star Catalog maintained at the U.S. Naval Observatory.

References

AEMET. (n.d.). *Standard Climate Values: Izaña El Tiempo: Madrid*. Retrieved from http://www.aemet.es/en/serviciosclimaticos/datosclimatologicos/valoresclimatologicos?l=C430E&k=coo.

AstroImageJ. (2017). Retrieved from http://www.astro.louisville.edu/software/astroimagej/

Chaisson & McMillan. (n.d.). *The Sun and Stars in the Celestial Sphere*. Retrieved from http://w.astro.berkeley.edu/~basri/astro10-03/lectures/CelestialSphere.htm

Hainaut, O. (1996, December 10). *Basic Image Processing*. Retrieved from http://www.eso.org/~ohainaut/ccd/

Las Cumbres Observatory. (2018). *0.4-meter*. Retrieved from https://lco.global/observatory/0.4m/

Las Cumbres Observatory. (n.d.). *Exposure Time Calculator*. Retrieved from https://lco.global/files/etc/exposure_time_calculator.html

Las Cumbres Observatory. (n.d.). *Data Pipeline*. Retrieved from https://lco.global/observatory/data/BANZAIpipeline/

Las Cumbres Observatory. (n.d.). *Teide*. Retrieved from https://lco.global/site/teide/

Las Cumbres Observatory. (n.d.). *Visibility Too*l. Retrieved from https://lco.global/observatory/visibility/

Nass, P. (1999, June 15). *Bias and Dark Subtraction*. Retrieved from http://www.eso.org/sci/software/esomidas/doc/user/98NOV/volb/node125.html

Stelle Doppie. (n.d.). *Stelle Doppie Double Star Database*. Retrieved from https://www.stelledoppie.it/

Astrometric Measurements of WDS 13169+1701 Binary Star System in Coma Berenices

Shannon Pangalos-Scott[1], Danielle Holden[1], Melody Fyre[1], Zach Medici[1], Jaeho Lee[2], Micaiah Doughty[1],Rebecca Chamberlain[1], Rachel Freed[5], and Russ Genet[3,4]

1. The Evergreen State College, Olympia, Washington
2. University High School, Irvine, California
3. Cuesta College, San Luis Obispo, California
4. California Polytechnic State University, San Luis Obispo, California
5. Sonoma State University, Cotati, California

Abstract: During the summer of 2018, as part of the Binary Star Research Seminar coordinated by the Institute for Student Astronomical Research (InStar), researchers took astrometric measurements of binary star system WDS 13169+1701.

Introduction

The binary system WDS 13169+1701 is located at a right ascension of 13 hrs 16 min 51.05 sec, and a declination of +17º 01' 01.9" at a distance of 36.63 light years from Earth, between the constellations Coma Berenices and Bootes (see Figure 1). This system's primary star has a magnitude of 6.66, while the secondary star has a magnitude of 9.5, with a delta magnitude (ΔM) of 2.82. The stellar classification of the primary star is K1V, with an average temperature of 3,700 - 5,200 Kelvin, and a chromaticity of pale yellow-orange. The secondary star's stellar classification is M1V, with an average temperature of 2,400 - 3,700 Kelvin, and a chromaticity of light orange-red. From a geocentric perspective, prior observations of the secondary star in this system show that it could either be traveling in a highly elongated orbital path around the primary, or it could be traveling in an observationally linear path adjacent to the primary star.

According to the Washington Double Star Catalog, the recorded observations for this system date back to 1782. Since then, there have been 214 recorded observations tracking the orbital path of the secondary star around the primary, the most recent of which was recorded in 2014. The first astrometric measurement of this system, from 1782, was made by William Herschel who wrote, "Double. About 1-3/4 degree from the 42d Comae towards Upsilon Bootis; the most south of a telescopic equilateral triangle. Excessively unequal. Larger primary star, pale color; smaller secondary star, dusky color. A third star preceding, above 1" (Herschel, 1912). The original discoverer of this star system is noted in Herschel's work as having recorded the binary pair in 800 CE with the initials BU; however, no additional evidence was recovered to reveal the full name of the discoverer or the measurements taken.

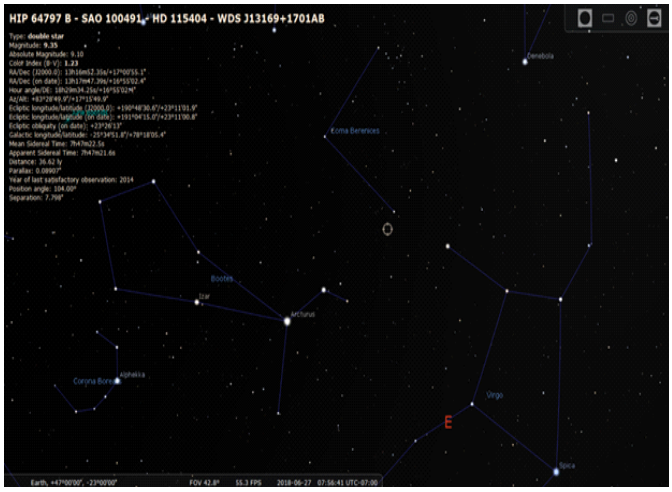

Figure 1. Night sky simulation showing the location of WDS 13169+1701 generated using Stellarium version 0.18.1.

Equipment and Procedures:

The research team compared past observational data of the stars trajectory paths from the WDS, a database maintained by the United States Naval Observatory, and current images that were requested from the Las Cumbres Observatory (LCO) portal and their global network of telescopes and observational equipment. Using LCO's network, images were taken from Haleakalā Observatory, situated 10,000 ft. above sea level on Mt. Haleakalā, a shield volcano in Hawaii. Images were

Astrometric Measurements of WDS 13169+1701 Binary Star System in Coma Berenices

Figure 2. Main telescope structure with a 2-meter and 0.4-meter telescope, Las Cumbres Observatory, Haleakalā Hawaii.

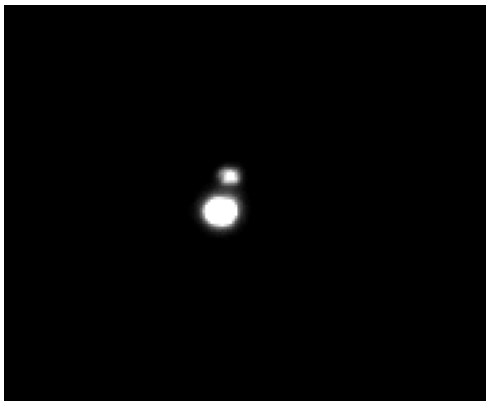

Figure 3. One-second image of WDS 13169+1701 taken from a 0.4 meter telescope at Haleakala, Hawaii and used to measure the position angle and separation.

acquired on June 26, 2018 using CCD imaging with an SBIG STL-6303 camera, with 1-sec., 5-sec., and 10-sec. exposure times using a clear, neutral filter, from the 0.4-meter Faulkes Telescope North (Figure 2).

The 5-sec and 10-sec exposure images that were requested on June 26, 2018 were discarded as they were overexposed and accurate centroiding could not be done. Using the histogram tool available in AstroImageJ to examine the overlap between the primary and secondary star, it was found that the data from the set of images with the 1-sec exposures were inconsistent and many of the images were flipped around the X axis.

A second set of ten images was requested from LCO using their 0.4-meter telescope, and they were received on August 2, 2018 with a 0.5-sec exposure time. Eight of those images had enough stars to be plate solved, and none showed the previous issue of flipping about their axis. Researchers used AstroImageJ to measure the position angle and separation between the primary and secondary stars in the system. The two smaller stars in this quadruple system were not visible in any of the requested images and were not necessary for data collection or analysis. See Figure 3.

The LCO FITS files were uploaded to astrometry.net to be plate solved; this software determines the right ascension and declination of each star. The plate solved images were then analyzed in AstroImageJ, where the brightness and contrast were adjusted to allow researchers to more accurately place the apertures on the two stars. The cursor was then dragged, using the central mouse wheel, from the primary star to the secondary star, giving the position angle, separation, and difference in magnitude of the two stars (See Figure 5).

The team used AstroImageJ to take five readings for each of the eight usable images with the 0.5-sec exposure time. All data was manually exported into a Google Sheets spreadsheet for further analysis. Researchers initially intended to calculate the averages of these five readings for each image given the variety of readings obtained from the first data set, but found that for individual image data sets, the position angle and separation measurements were identical between readings out to six significant figures. Some of this raw data can be seen in Figure 4, in both AstroImageJ and Google Sheets interfaces. The total average value, standard deviation, and standard error of the mean were calculated and are shown in Table 1.

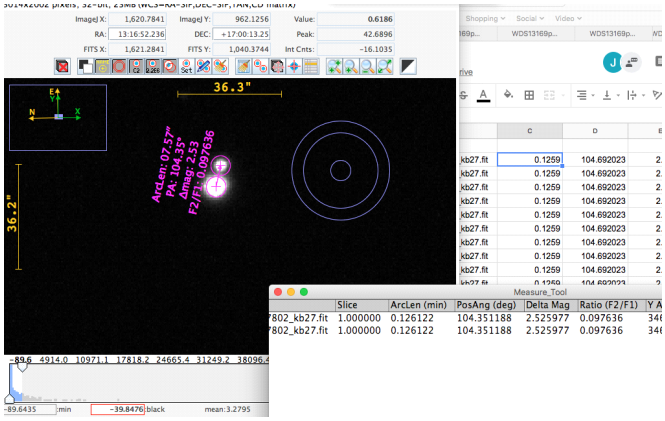

Figure 4. Screenshot of AstroImageJ interface

Results

Table 1 shows the new data, depicting the separation between the primary and secondary stars and the position angle of the secondary star in relation to the primary. Figures 5 and 6 depict past data collected and stored in the WDS, showing the change in separation

Astrometric Measurements of WDS 13169+1701 Binary Star System in Coma Berenices

Table 1: Summary of final data with standard mean, standard deviation and the standard error of the mean.

Fits images	Separation (Arc Seconds)	Position Angle (Degrees)
1	7.55	104.69
2	7.57	104.35
3	7.55	104.08
4	7.54	104.31
5	7.64	104.28
6	7.57	104.28
7	7.60	103.31
8	7.67	103.79
Mean	**7.59**	**104.14**
Standard Deviation	**0.045**	**0.419**
Standard Error of Mean	**0.016**	**0.148**

and position angle over time, with the new data point added. The new measurements were added to the orbital diagram (Figure 7) as described by Buchheim (2017).

Discussion

Throughout the research process, the team ran into a plethora of problems regarding data collection and software use. Researchers utilized AstroImageJ, an open-source software, for analysis of plate solved images, but ran into an issue with the software flipping images about their axes. There were additional issues with the software running on the personal computers of the researchers due to the requirement of a legacy Java and incompatibility with some operating systems. The original batch of images received from LCO were over exposed and difficult to plate solve. These obstacles caused delays in the collection of usable data. The research team came together and worked to improve communication and overcome these issues before the deadline by requesting a second batch of data, troubleshooting the software, and calling additional team meetings.

As shown in Table 1, only eight photographs of the ten taken from the second batch of images were able to be plate solved using nova.astrometry.net and used to take astrometrical measurements via AstroImageJ. This smaller sample size did not negatively affect results and the team did not expect it to, as the originally requested ten images was more than adequate to ensure usable and consistent data. Table 1 shows that the separation

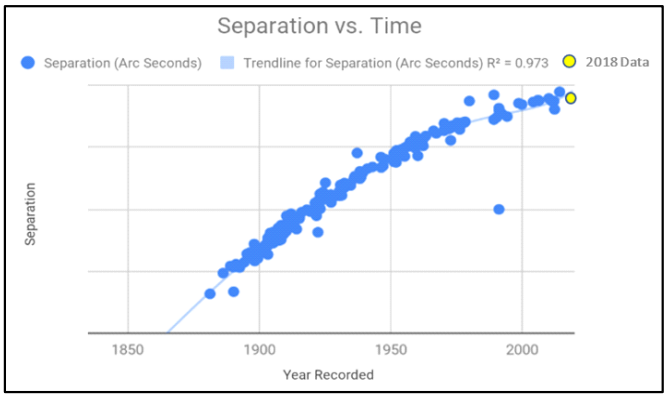

Figure 5. Historical data from the Washington Double Star Catalog of binary system 13169+1701, showing the separation of the primary relative to the secondary over time, new position shown with yellow dot.

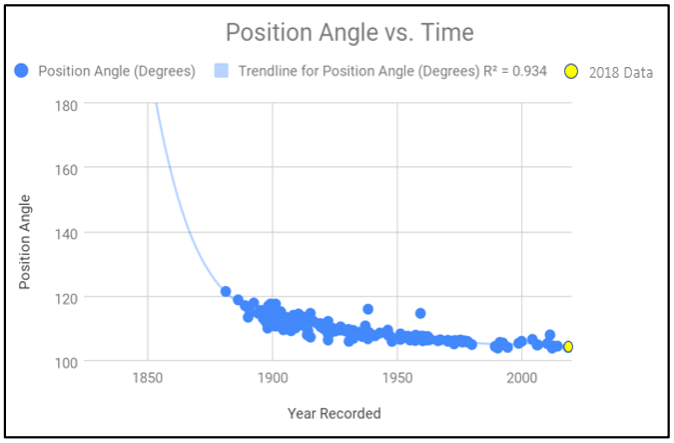

Figure 6. Historical data from the Washington Double Star Catalog of binary system 13169+1701, showing the position angle of the secondary star in relation to the primary over time. The new position is shown with a yellow dot.

angle between the primary and secondary star was determined to be 7.59 arc seconds and the position angle to be 104.14 degrees. These readings coincide with the position angle and separation values projected by Stelle Doppie with a separation of 7.775 in arc seconds and a position angle of 104.8 (Stelle Doppie, 2016). The low value of the standard deviation calculated reflects readings that are consistent and without statistical outliers. The goal of the research team was to achieve a standard deviation within one percent of our average values. The standard deviation of the separation readings is 0.045, 0.5% of the final point, and the standard deviation of the position angle is 0.419, 0.4% of the final point. Having a small error of the mean shows the same data was taken multiple times and that the standard deviation for each separate data collection was consistently small.

Astrometric Measurements of WDS 13169+1701 Binary Star System in Coma Berenices

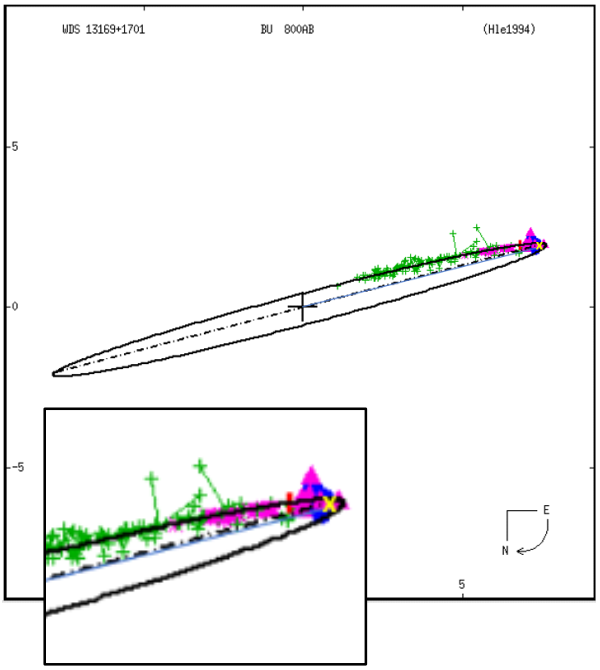

Figure 7. Orbital path of the double star WDS 13169+1701 with the newly measured position marked with a yellow "X". Inset shows the image enlarged for clarity.

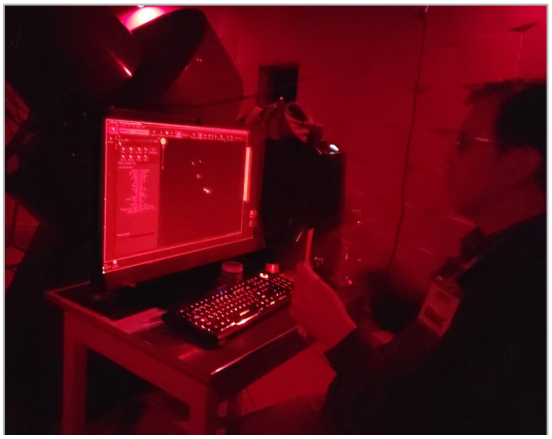

Figure 8. Eric Holcomb at University of Oregon's Pine Mountain Observatory in the Deschutes National Forest, August 6, 2018 observing 13169+1701 on the observatory's 24" Cassegrain reflector telescope. Photo by team member, Shannon Pangalos-Scott.

Figure 9. Binary system 13169+1701, taken with a 12-megapixel mobile phone camera mounted to the lens of a 24" Cassegrain reflector telescope at Pine Mountain Observatory on August 6, 2018. Photo by team member, Micaiah Dougherty.

As part of the Summer 2018 Astronomy and Cosmology program at The Evergreen State College, research team members visited the University of Oregon's Pine Mountain Observatory on August 6, 2018. Additional field observations were made at the site, using a 24-inch Cassegrain reflector telescope, although these observations were not use in the data analysis because the image quality was not optimal. (Figures 8 and 9)

Conclusion

By analyzing the new measurements from August 2, 2018, researchers were able to determine that this data is indicative of a true binary system, where the smaller secondary star is gravitationally bound to the larger primary star traveling along an estimated 770-year orbital period. The 2018 observations are values that would be expected from the current literature on this binary system, and are comparable to the position angle and separation values projected based on past orbital data and the hypothesis that the two primary stars of WDS 13169+1701 are gravitationally bound.

Acknowledgements:

From InStAR, Paul Harderson, facilitated administration. Brian Mason, of the U.S. Naval Observatory, provided past observational data. Information and data was gathered from Las Cumbres Observatory, Washington Double Star Catalogue, and Stelle Doppie. Dr. Cheryl Genet collaborated on developing educational materials, articles, publications and the Canvas website and design. Eric Holcomb operated the telescope at the University of Oregon's Pine Mountain Observatory, along with Alton Luken, the sites Operations Manager. From The Evergreen State College, George Freeman and Lee Lyttle, Academic Deans, encouraged this work, and Richard Weiss, Member of the Faculty, attended team sessions. Francisco Velez, a fellow student, supported our research and software troubleshooting.

References

Buchheim, R. K. (2017) Displaying New Measurements on WDS Orbital Plots. Journal of Double Star Observations. Vol. 13 No. 2, pp 233-236.

Genet, R., Buchheim, R.., Johnson, J., Harshaw, R., & Freed, R. (2018). *Small Telescope and Astronomical Research (STAR) Handbook*(1st ed.). Tucson, AZ: Institute for Student Astronomical Research.

Herschel, W., Dreyer, J.L, (1912) *The Scientific Papers of William Herschel,* The Royal Society, London

Las Cumbres Observatory | Many Eyes - One Vision (n.d.). Retrieved from https://lco.global/

Stellarium Astronomy Software. (n.d.). Retrieved from http://stellarium.org/

Stelle Doppie - Double Star Database, Gianluca Sordiglioni, 2016, Retrieved from http://www.stelledoppie.it/index2.php

Astrometric Measurements of Double Stars HJ 4194 and HJ 4195

Vincent Aguilar[1], Emmanuel Mercado[1], Hugh Le[1], Tianlin Zhao[1], Jae Calanog[1], Grady Boyce[2], and Pat Boyce[2]

1. San Diego Miramar College, San Diego, California USA
2. Boyce Research Initiatives and Education Foundation (BRIEF), San Diego, California, USA

Abstract: We performed astrometric measurements on the double stars WDS 08562-8341 (HJ 4194) and WDS 09135-6455 (HJ 4195) through images acquired by the Las Cumbres Observatory telescope network (LCO), using a 0.4-meter Meade telescope to image our selected double stars. The Our Solar Sibling pipeline (OSS) processed and calibrated the images, which were then analyzed using the software Mira Pro x64. From the images of HJ 4194, we calculated the mean position angle of 81.6° ±0.4°, and the separation of 18.2" ± 0.1". From the images of HJ 4195, we calculated the mean position angle of 69.6° ± 0.7°, and separation of 16.3" ± 0.2". We concluded that the data suggests that HJ 4194 is an optical double, while HJ 4195 remains undetermined.

Introduction

Position angle (θ) and separation (ρ) measurements from observing double stars can be used in combination with historical data to determine whether the double star is a gravitationally associated binary star or an optically aligned double star. If a double star is found to be a binary star, then the total system mass can be estimated using the orbit of the system. Understanding the mass of a star is the most fundamental parameter in understanding stellar astrophysics.

We aim to measure the position angle (θ) and separation (ρ) of the neglected double stars HJ 4194 and HJ 4195. Both parameters are important in determining if a secondary star is orbiting around a primary star. If a cartesian graph is made using the historical θ and ρ, and it shows that the data points of the secondary star are approximating an ellipse or part of an ellipse, then the pair is a binary star. Similarly, these same parameters can be used to determine if the secondary star is moving away from the primary star with linear motion indicating a non-gravitationally bound optical double star.

We used the Washington Double Star catalog (WDS) by Brian Mason (2012) to select the double stars in our study. The following general criteria was used to select candidate double stars:

- Right Ascension (RA) hour between 8-14 and therefore visible in the Spring.
- Declination South of -25° (Telescope is in Sutherland, South Africa)
- Difference in magnitudes (Δ Magnitude) < 1
- Separation > 6 arcseconds; distinguishes primary from secondary.
- Recognizable change in position angle.

Sir John F.W. Herschel discovered HJ 4194 and HJ 4195 in 1836. Herschel was an eminent Victorian scientist that contributed to many areas of science. Herschel discovered these double stars during an extensive telescopic survey of the southern sky from the Cape of Good Hope Observatory (The Editors of Encyclopedia Britannica, 2018). Today, the Cape of Good Hope Observatory is recognized as the headquarters of the South African Astronomical Observatory (SAAO), where our images were taken. Herschel's measurements are recorded in the WDS catalog, along with other historical measurements, and are shown in Tables 1 and 2 (Mason et al, 2012).

Astrometric Measurements of Double Stars HJ 4194 and HJ 4195

Table 1: All historical θ and ρ measurements for HJ 4194 found in the WDS. The table shows a large change in position angle and separation over the past 163 year.

HJ 4194 WDS 08562-8341		
Epoch	θ (°)	ρ (arcseconds)
1836.62	46.60°	10.00"
1882.35	52.80°	12.11"
1895.22	57.60°	15.20"
1902.24	59.40°	15.99"
1903.02	57.60°	15.81"
1919.24	62.20°	16.22"
1956.16	69.40°	16.04"
1991.70	77.30°	17.57"
1998.13	78.20°	17.73"
1999.99	79.00°	17.60"

Table 2: All historical θ and ρ measurements for HJ 4195 from the WDS. The table shows a small change in position angle, and an insignificant change in separation over the past 175 years.

HJ 4195 WDS 09135-6455		
Epoch	θ (°)	ρ (arcseconds)
1835.150	58.7°	18.000"
1879.850	62.4°	16.020"
1892.220	48.1°	19.968"
1915.320	65.8°	16.420"
1918.300	65.2°	16.370"
1928.370	63.0°	16.314"
1970.400	67.3°	16.284"
1991.630	68.3°	16.279"
1998.234	69.3°	16.040"
2000.010	68.5°	16.200"
2010.500	68.9°	16.200"

Materials and Methods

Equipment

All images were acquired from Las Cumbres Observatory (LCO). The LCO telescope used was a custom 0.4-meter Meade telescope, Figure 1, with a mounted SBIG STX-6303 high-speed camera (LCO, 2018) located at SAAO in Sutherland, South Africa. This telescope has a 1.14 arcsecond per pixel resolution with a Field of View (FOV) of 19 arcminutes x 29 arcminutes. It also features a 14-position filter wheel necessary for making observations at different bands of wavelengths.

Figure 1: An LCO custom Meade 0.4-meter telescope with SBIG STX-6303 camera used to image the selected double stars. (Source: LCO)

Observations

Images were scheduled at selected times to minimize the effect of air mass on the quality of the images. The far southern declination of HJ 4194 made the stars appear at low maximum altitude in the night sky from SAAO. HJ 4194 reached an estimated 40 degrees above the horizon, while HJ 4195 reached about 68 degrees above the horizon. HJ 4194 and HJ 4195 were imaged at their maximum altitude on the Barycentric Julian Dates (BJD) of 2458200.407541710 and 2458200.408888749.

A total of six images for each double star were taken: Luminance, R band, and Z band. Two images were taken at 1 second and 2 second exposures for both the luminance and the R band. Two images were taken with the z band filter and exposed for 9 and 18 seconds. Each image was analyzed and included in the calculation of the mean θ and ρ reported in Table 3. We created false-color-images of HJ 4194 and HJ 4195 using the software SAOImage DS9, shown in Figures 2 and 3, by merging the images taken with each filter into one image.

Afterward, the Mira Pro Distance and Angle autocentroid function was used to accurately locate the center of each star by selecting the star in the image with a crosshair. Mira automatically locates the pixel with the highest ADU within a prescribed aperture to determine the stellar centroid. The exact coordinates of that pixel was identified as the first part of a line segment, shown in Figure 4. The crosshair was dragged to the second star and the process was repeated. The software automatically calculated the θ and ρ using the coordinates from each center.

Once all images were measured, we performed a statistical analysis to determine the uncertainties associated with our results. Using the data from each image, we calculated the mean, standard deviation, and the standard error of the mean for both double stars. The results of these calculations are shown in Table 3.

Since the sample size was less than 30, we estimated the population mean using a t-distribution. We creat-

Astrometric Measurements of Double Stars HJ 4194 and HJ 4195

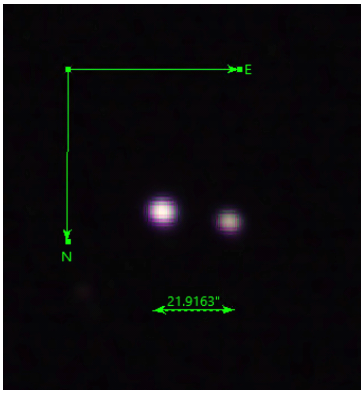

Figure 2: A false color image of HJ 4194 that we created using SAOImage DS9. The arrow represents a scale of 21.9". All six images of HJ 4194 were used to produce this image.

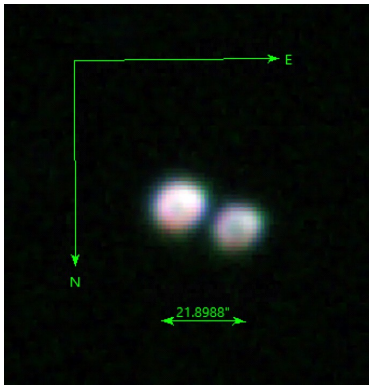

Figure 3: A false color image of HJ 4195 that we created using SAOImage DS9. The arrow represents a scale of 21.9". All six images of HJ 4195 were used to produce this image.

ed a 95% confidence interval using 5 degrees of freedom, and a t-value of 2.571. The t-value is a unit-less number which indicates the standard deviation, or the maximum or minimum deviation any possible measurement can be from the estimated population mean. The confidence interval was constructed using the formula: $x \pm t(s/\sqrt{n})$. In order to use this formula in constructing our confidence interval, and apply the central limit theorem, we used a normal probability plot to confirm that the population we were sampling from was approximately normally distributed.

Results

The astrometric measurements for epoch 2018.223 are listed in Table 4. We calculated the mean position angle of 81.6° ±0.4° for HJ 4194 with a mean separation of 18.2" ±0.1". We calculated the mean position angle 69.6° ± 0.7° for HJ 4195 with a mean separation of 16.3" ± 0.2". Each margin of error shown in Table 4 was calculated using a t-distribution with 95% confidence and 5 degrees of freedom.

Discussion

We have plotted each θ and ρ measurement of HJ 4194 using a cartesian graph tool provided by Richard Harshaw. The origin of the graph represents the primary star. Each individual data point represents the astrometric location of the secondary star in the year it was

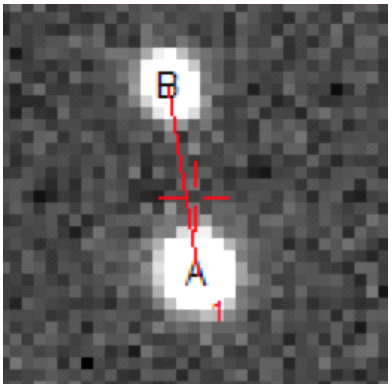

Figure 4. This is an image of the centroid function being used on Mira Pro x64. The image shows a line segment auto-centered on the primary and secondary star of HJ 4194, R-band, exposed for 1.73 sec.

measured. The position angle and separation were used to calculate X and Y-coordinates for each measurement for each pair. The position angle is represented by the angle measured from the north axis sweeping out counter-clockwise to an individual data point. The separation is the distance in arcseconds from the origin to the individual data point. Figure 5 shows the historical data plotted with and without the data points we are assuming to have significant errors.

Each measurement is shown in chronological order

Table 3: Results of our measurements.

Double Star	Measure	# of images	Mean	Standard Deviation	Standard Error of the Mean
HJ 4194	Separation	6	18.20	0.09	0.037
	Position Angle	6	81.61	0.35	0.142
HJ 4195	Separation	6	16.33	0.21	0.085
	Position Angle	6	69.55	0.67	0.275

Astrometric Measurements of Double Stars HJ 4194 and HJ 4195

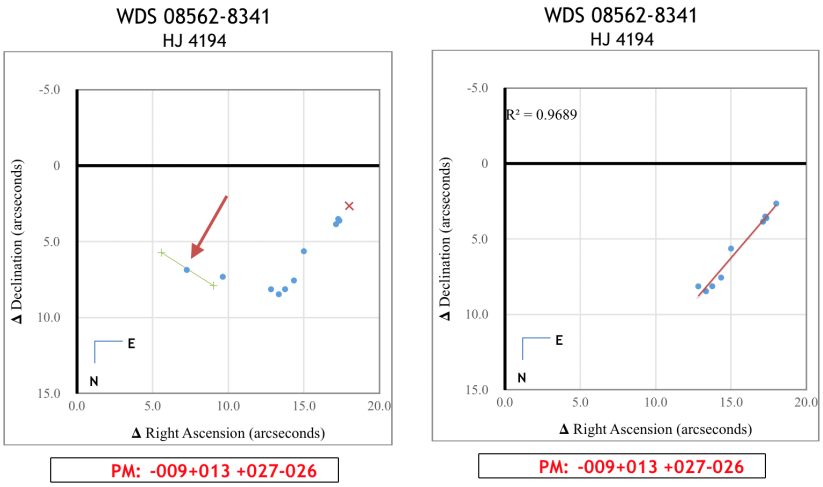

Figure 5. Plot of the historical data for HJ 4194 with errors and without.

from left to right and ends with our measurement highlighted by a red "x". The first data point was measured by Herschel and is highlighted by a red arrow. The green crosses and the line connecting them represent the two values that were averaged to produce this measurement (Herschel, 1847). Since Herschel was known for having imprecise data and his two measurements contain a very large spread in variation, we are assuming that the first data point highlighted by the arrow is also erroneous. The second data point was measured by Mr. Lawrence Hargrave with a 7 1/4 inch telescope. In the article containing the measurements by Mr. Hargrave, H.C. Russell, F.R.S., Government Astronomer, states "The positions of the other stars are approximate only" (Russell, 1892). This statement seems to suggest that the second measurement is imprecise. If we assume that these two data points are erroneous or imprecise and choose to omit them, then we can see a clear linear motion trend in the remaining data points.

Furthermore, the graph in Figure 6 shows that star B's position angle has changed by approximately 40 degrees over roughly 200 years, and appears to be increasing at a constant rate of approximately 0.2025° per year. However, if our previous assumption is correct, then the data points in Figure 6 will approach a horizontal asymptote perhaps in less than 500 years. The more distant star B becomes the position angle should appear to change less and less between 180-90 degrees.

In the cartesian graph of HJ 4195, Figure 7, the numbered data points make it difficult to discern any trend in the data. Number one was recorded by Herschel, and it is likely to have a lot of error associated with it since only one measurement was made. As we have shown with HJ 4194, Herschel had a large variation in his measurements. Number three appears to be an outlier. It was the result of a "rereduction of the Astrographic Catalogue" by the US Naval Observatory (Urban et al, 1998). In the associated article Urban states "[With respect to position] Three bands of low-precision are evident. These correspond to the Vatican, Postdam and Sydney zones" (Urban et al, 1998). The Sydney Observatory was responsible for imaging an area of the sky containing HJ 4195. Despite these issues there is a curved trend made by the remaining data points.

In addition, the pair of stars appear to be moving together in the same plane, excluding the plane in the line of sight. The pair of stars have a nearly identical proper motion. Star B also appears to show little movement in separation. This behavior suggests that star B is

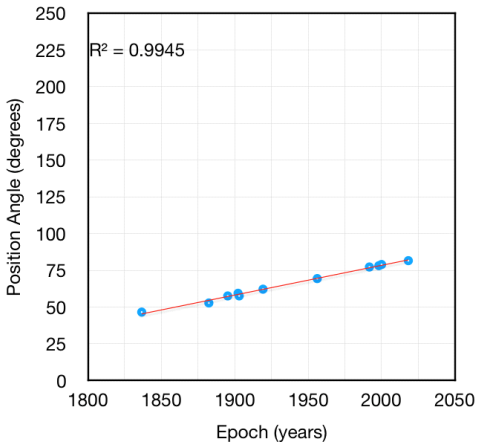

Figure 6: HJ 4194 Θ vs. Time.

Astrometric Measurements of Double Stars HJ 4194 and HJ 4195

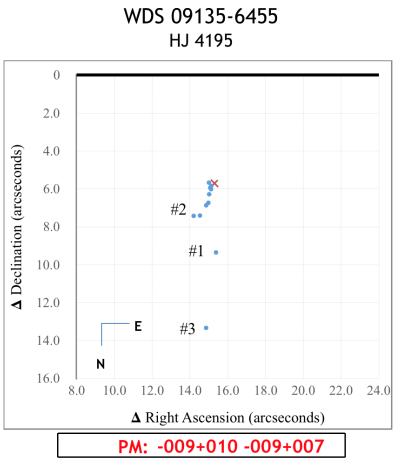

Figure 7. Plot of the historical data for HJ 4195.

possibly a common proper motion pair. However, more astrometric measurements are needed to monitor the curved trend in case this pair is a true binary star.

The distances from our Sun to each star were estimated by using parallax data and trigonometry. The European Space Agency (ESA) mission Gaia provided the parallax data for HJ 4194 and HJ 4195 (Gaia Collaboration et al, 2016). One astronomical unit (AU), or the distance from Earth to the Sun, was divided by the parallax in arcseconds providing a distance in parsecs.

Table 5 provides the parallax measurement for each component of HJ 4194 and HJ 4195, including the margin of error. Table 6 provides the minimum and maximum distance in parsecs based on the parallax data in Table 5 for each star.

The parallax data in Table 5, and the subsequent distances in Table 6, show that HJ 4194 is most likely an optical double. Star A is at a distance between 1189.63-1260.40 parsecs away and Star B is between 168.01-169.38 parsecs away from our Sun. Thus, the parallax data shows that the stars in HJ 4194 are at least 1020.25 parsecs away from each-other, and too far apart to be gravitationally bound.

The parallax and distance data for HJ 4195 also shows no overlap in distances. Although the Gaia DR1 data showed a considerable overlap in parallax, the newly released parallax data shows that these stars may not be close to each-other at all (X. Luri et al, 2018). Any conclusion drawn from the parallax data runs contrary to those drawn from the nearly identical proper motion and the short arc which suggest these stars are physically associated.

At the suggestion of Richard Harshaw, we estimated the minimum separation between the stars in HJ 4195. First we calculated a weighted parallax using Equation 1. The weighted parallax was converted to parsecs, and finally multiplied by the last ρ measurement in the WDS. The results of this calculation show that the minimum separation by far exceeds the true separations of binary systems surveyed in the 6th orbital catalog, Table 7. The highest true separation calculated was 1,707 AU, while an estimate of our double star was 23,107 AU (Harshaw, 2018).

$$PXweighted = \frac{\left[\left(1-\frac{PxAerror}{PxA}\right)PxA+\left(1-\frac{PxBerror}{PxB}\right)PxB\right]}{\left(1-\frac{PxAerror}{PxA}\right)+\left(1-\frac{PxBerror}{PxB}\right)}$$

We recommend that future research on both double stars should focus on gathering more astrometric data to confirm that Star B is moving away from Star A in HJ 4194, and to confirm that the data points observed in the cartesian graph of HJ 4195 are forming a short arc.

Conclusion

The astrometric measurements θ and ρ were successfully measured for both double star pairs. The data suggests that the secondary star in HJ 4194 is moving away from the primary, with the parallax data indicating that it is highly unlikely that the component stars are close enough to have a gravitational connection. For these reasons we have concluded that HJ 4194 is likely to be an optical double.

Table 5: Parallax data for each star (Source: Gaia DR2).

	HJ 4194		HJ 4195	
	Star A	Star B	Star A	Star B
Parallax (ams)	0.817	5.928	0.798	0.605
Margin of error	± 0.0236	± 0.0241	± 0.028	± 0.0267

Table 6: Projected distance to each star in parsecs (Source: Gaia DR2).

	HJ 4194		HJ 4195	
	Star A	Star B	Star A	Star B
Min Dist.	1189.63	168.01	1210.65	1583.03
Max Dist.	1260.40	169.38	1298.70	1729.21

Table 7: Estimated minimum separation between the stars of HJ 4195.

Weighted Parallax (mas)	Distance (Parsecs)	Minimum Separation (AU)
0.702	1,424.6	23,107

At present, we were unable to conclude the nature of HJ 4195 with the current data. The data for HJ 4195 shows that star B is showing very little change in θ and ρ. The cartesian graph in Figure 9 shows that the data points for Star B show evidence of a short arc with apparent outliers. However, the parallax data shows that there is no significant overlap in distance. The minimum separation calculated from the weighted parallax is much higher than that of known binary systems.

Acknowledgments

The Astronomy Research Seminar is an educational program which teaches students how to employ the scientific process in the field of astrometry. The seminar gives students an opportunity to collaborate, develop critical thinking, develop scientific writing skills, and present the results of their investigation to the scientific community.

We thank Dr. Jae Calanog, San Diego Miramar College for his invaluable assistance with helping us to understand the fundamentals of astrometry, mentoring us through the scientific writing process, and improving our imaging techniques. His critique of our research and supervision has greatly improved our paper.

We would also like to extend our gratitude to Judith Hante, Professor, San Diego Miramar College for sharing her statistical expertise during our analysis of the results. We are more confident in our results, thanks to her guidance with t-distributions.

Lastly, we thank and appreciate all who funded our research, Las Cumbres Observatory network for providing the equipment, and Our Solar Sibling pipeline for processing our images.

This work has made use of data from the European Space Agency (ESA) mission Gaia (https://www.cosmos.esa.int/gaia), processed by the Gaia Data Processing and Analysis Consortium (DPAC, https://www.cosmos.esa.int/web/gaia/dpac/consortium). Funding for the DPAC has been provided by national institutions, in particular the institutions participating in the Gaia Multilateral Agreement. The VizieR catalogue access tool, CDS, Strasbourg, France was also used. The original description of the VizieR service was published in A&AS 143, 23, http://vizier.u-strasbg.fr/viz-bin/VizieR

References

Fitzgerald, M.T. (2018, accepted), "The Our Solar Siblings Pipeline: Tackling the data issues of the scaling problem for robotic telescope based astronomy education projects.", Robotic Telescopes, Student Research and Education Proceedings

Mason, Brian. et al, 2012, Washington Double Star Catalog, Astronomy Department, United States Naval Observatory, http://ad.usno.navy.mil/proj/WDS/

Boyce, G. and Boyce, P., Boyce Research Initiatives and Education Foundation (BRIEF), http://www.boyce-astro.org/home.html.

Prusti, T. et al, 2016, Astronomy & Astrophysics, **595**, A1. European Space Agency (ESA) mission Gaia, https://www.cosmos.esa.int/web/gaia.

Brown, A.G.A., et al, 2018, *Gaia Data Release 2. Summary of the contents and survey properties*. European Space Agency (ESA) mission Gaia, https://www.cosmos.esa.int/web/gaia.

Luri, X., et al, 2018, *Gaia Data Release 2:Using Gaia Parallaxes*. European Space Agency (ESA) mission Gaia, https://www.cosmos.esa.int/web/gaia.

Las Cumbres Observatory (LCO), 2018, 0.4 Meter, JPEG, Las Cumbres Observatory, Global Headquarters California, accessed 22 March 2018, https://lco.global/observatory/telescopes.

Encyclopedia Britannica, 2018, Sir John Herschel, 1st Baronet, accessed 22 March 2018, https://www.britannica.com/biography/John-Herschel.

Russell, H.C., 1892, “Measures of Double Stars made at Sydney Observatory in the Years 1882-89,” Memoirs of the Royal Astronomical Society, **50**, 57, http://adsabs.harvard.edu/abs/1892MmRAS..50...57R.

Herschel, Sir John F. W., 1847, “Results of Astronomical Observations Made During the Years 1834, 5, 6, 7, 8, at the Cape of Good Hope; being the completion of a telescopic survey of the whole surface of the visible heavens, commenced in 1825”, London, Smith, Elder and Co, https://hdl.handle.net/2027/nyp.33433087544387.

Harshaw, R., 2018, “Measurements of 427 Double Stars With Speckle Interferometry: The Winter/Spring 2017 Observing Program at Brilliant Sky Observatory, Part 1,” *Journal of Double Star Observations*, **14** (2), 284.

Measurements of Neglected Double Stars: December 2018 Report

Joseph M. Carro
Cuesta College, San Luis Obispo, California

Abstract: This article presents measurements of 30 neglected double stars. The stars were selected from the Washington Double Star Catalog published by the United States Naval Observatory. The photographs were taken by remote telescopes. The measurements were done by the author.

Methodology

Photographs were taken using telescopes operated by the Open Science Observatory located in the Canary Islands near the west coast of Africa. Those telescopes are located at an elevation of 2,300 meters on the island of Tenerife. The Open Science Observatory has a corrected Dall-Kirkham telescope with an aperture of 420mm, and a focal length of 2,940mm. The methods used to calibrate the instruments of those observatories are unknown to this author.

The camera used most frequently at the Open Sciences Observatory was a ProLine KAF-16803. The photographs were analyzed by the author using the programs SKY X, a product of Software Bisque.

After accumulating the photographs, averages were calculated for the position angles and separations. All of the star patterns were compared with the data from Washington Double Star catalog to insure correctness. The results are listed in Table 1, which contain averages of measurements.

Report

The following information is reported for each star: the WDS code with constellation, the discoverer code with component, the position angle, the separation, the number of measurements, the calendar date of the last observation, and the Julian date of the last observation.

The column headings are: WDS number/Con = Washington Double Star identifier/Constellation code, DC = Discovery Code and components, PA = position angle, Sep = Separation, Mts = number of measurements, and Date = the last observation date.

Acknowledgements

This research made use of the SIMBAD database operated at CDS, Strasbourg, France, the Aladin Sky Atlas, and the Washington Double Star Catalog maintained by the United States Naval Observatory.

References

Mason, B., Washington Double Star Catalog - Northern Neglected Stars List 1

Measurements of Neglected Double Stars: December 2018 Report

Table 1. Measurements

WDS number/Con	Dis. Code	Position Ang.	Separation	Measures	Calendar Date	Julian Date
00016+3714 AND	ES 2444	249.25	9.5	3	2018 10 21	2458414
01332+3231 TRI	SEI 17	191.9	25.5	3	2018 10 02	2458394
02043+2911 TRI	CHE 34	74.24	13.2	3	2018 08 30	2458361
02053+2836 TRI	CHE 40	141.51	32.2	3	2018 08 30	2458361
02060+2806 TRI	CHE 45	43.17	41.9	3	2018 08 30	2458361
02070+2923 TRI	CHE 49	110.3	32	3	2018 08 30	2458361
02073+2829TRI	CHE 50	290.77	11.6	3	2018 10 13	2458405
02083+2933 TRI	CHE 56	55.47	28.3	3	2018 08 30	2458361
02085+2833 TRI	CHE 58	291.4	14.7	3	2018 08 30	2458361
02086+2918 TRI	CHE 59AB	216.43	27.5	3	2018 08 30	2458361
02086+2918 TRI	BTG 7AC	209.19	39.9	3	2018 08 30	2458361
02086+2918 TRI	BTG 7AD	297.02	28.5	3	2018 08 30	2458361
02086+2918 TRI	BTG 7BC	196.07	12.6	3	2018 08 30	2458361
02087+2921 TRI	CHE 60	275.05	29.3	3	2018 08 30	2458361
02109 2941 TRI	CHE 64	124.73	16.9	3	2018 08 30	2458361
02109+2846 TRI	CHE 65	126.82	28.7	3	2018 08 30	2458361
07179-0142 MON	BAL 466AB	343.07	14.9	3	2018 10 14	2458361
07179-0142 MON	BAL 466AC	329.32	20.6	3	2018 10 14	2458361
07179-0142 MON	BAL 466BC	299.16	6.9	3	2018 10 14	2458361
07453-0026 MON	HJ 767AB	163.33	21.4	3	2018 10 25	2458417
07453-0026 MON	SIN 31AD	100.36	26	3	2018 10 25	2458417
07453-0026 MON	SIN 31AE	27.99	27.9	3	2018 10 25	2458417
07453-0026 MON	SIN 31AF	160.36	28.2	3	2018 10 25	2458417
07453-0026 MON	SIN 31AG	163.92	31.67	3	2018 10 25	2458417
07453-0026 MON	SIN 31AH	323.25	42.6	3	2018 10 25	2458417
07453-0026 MON	SIN 31AJ	73.81	169.2	3	2018 10 25	2458417
07453-0026 MON	SIN 31AK	63.91	179.2	3	2018 10 25	2458417
09047-0806 HYA	J 2895	170.45	7.9	3	2018 10 20	2458412
10302+3050 LMI	SEI 520	359.78	7.9	5	2018 10 11	2458403
10375+3015 LMI	HJ 487AB	1.11	12.7	3	2018 10 13	2458405
10375+3015 LMI	OPI 17AC	283.52	52.6	3	2018 10 13	2458405
11396+3125 UMA	SEI 526	236.48	412	5	2018 10 24	2458416
12463+0847 VIR	BGH 41	271.39	119	6	2018 08 17	2458348
14505-0527 LIB	HJ 4708	165.62	23.7	5	2018 08 17	2458348
15171+2851 CRB	BGH 57	40.9	575.4	3	2018 08 04	2458335
15565+1540 SER	STT 584AB	325.64	313.9	5	2018 08 17	2458348
16152-0046 SER	HJ 1290	113.2	20.1	3	2018 08 17	2458348
17200-0801 OPH	ENG 60AB	232.55	90.8	3	2018 08 17	2458348
17219-1846 OPH	SLE 14	289.95	16.3	3	2018 08 17	2458348
17349-0044 OPH	BAL 891AB	203.97	20	4	2018 08 30	2458361
17349-0044 OPH	BAL 891AC	193.87	18.5	4	2018 08 30	2458361
17349-0044 OPH	BAL 891BC	89.8	3.8	4	2018 08 30	2458361
17577+0426 OPH	BAR 44	69	145.9	3	2018 08 17	2458348
18176+0333 OPH	BAL2487AB	334.67	11.2	4	2018 10 03	2458395
18176+0333 OPH	BAL2487BC	167.93	31.8	4	2018 10 03	2458395

Duplicity Discovery of HIP 33753 from Asteroidal Occultation by (479)Caprera

Toshio Hirose
Japan Occultation Information Network (JOIN), Tokyo, Japan
thirose@cam.hi-ho.ne.jp

Miyoshi Ida, Higashi-Ohumi, Shiga, Japan
Hideto Yamamura, Maibara, Shiga, Japan
Shigeo Uchiyama, Kashiwa, Chiba, Japan
Akie Hashimoto, Chichibu, Saitama, Japan
Reijin Aikawa, Sakado, Saitama, Japan
Kazumi Terakubo, Fuchu, Tokyo, Japan
Mikiya Sato, Fuchu, Tokyo, Japan
Kunihiro Shima, Fujimi, Nagano, Japan

Abstract: An occultation of HIP 33753 by the asteroid (479) Caprera on December 10, 2018 showed this star to be a double star. Both components of the double star were occulted as recorded by eight observers. The separation of the two components is 0.0054 ± 0.0004 arc-seconds at a position angle of 46.4 ± 3.7 degrees. The magnitude of the primary component is estimated to be 8.4 ± 0.1 V. The magnitude of the secondary component is estimated to be 8.6 ± 0.1 V.

Observation

On 2018 December 10, eleven observers occupying or operating sites across the Japan observed the asteroid (479) Caprera occult the star HIP 33753. See Figure 1 for the path map of the event [1] and observer's site. Five sites (1, 5, 6, 7, 8 in Figure 1) observed a two-step drop in brightness by recording method to video camera, and three sites (2, 3, 4 in Figure 1) observed gradual events by visual method. These observed events are indicating double star. Three sites had a miss. All recorded occultation times and data from the observers can be found in IOTA records for the event, and mentioned in the "Tenmon-Nenkan (Astronomical annual book)" that will be published from Seibundo-Shinkosya every year in Japanese [2]. The observations were made at the each site and with the equipment shown in Table 1.

The target star is magnitude 7.73V (Hipparcos - VizieR). The asteroid magnitude as predicted by S. Preston was 12.9 V [1]. The calculated combined magnitude of the star and asteroid is 7.72 V. The expected magnitude drop at occultation was 5.8 magnitudes. The star is not listed in the Fourth Interferometric Catalogue, nor is it listed in the Washington Double Star catalog.

Analysis

The observations were analyzed in the standard manner described by R. L. Millis and J. L. Elliot [3]. The result of the calculation reduction is shown in Figure 2. The light curve in site 1 is shown in Figure 3. Similarly, the light curve in site 6 and site 8 is shown in Figure 4 and Figure 5 respectively. In these light curve figures, X-axis is shown the video frame number and Y-axis is shown the brightness [4].

In visual method, "a moment to completely disappear" and "a moment to appear" are judged at "D" and "R" each. So, for visual observers, Star A was observed at "D", but Star B was observed at "R", in this event. In figure 2, letter from "a" to "p" are shown with step events in figure 3 to Figure 5 for the light curves. Then, in Figure 6, Elliptic A is applicable to the observed points for Star A, and Elliptic B is applicable to the observed points for Star B. The dimensions of each elliptic A and B were estimated by the least-squares method [5], as follows.

(Text continues on page 272)

Duplicity Discovery of HIP 33753 from Asteroidal Occultation by (479)Caprera

Table 1. Site number, Observers, equipment, methods, and results

Site No.	Observer(s)	Location	State	Telescope Type	Telescope Dia (cm)	Method	Fig. 2 Chords	Result
1	Shigeo Uchiyama	Kashiwa	Chiba	SCT	25	Video+GPS Time Inst.	1	Two-Step
2	Reijin Aikawa	Sakado	Saitama	SCT	20.3	Visual+SW Time Signal	2	Gradually
3	Akie Hashimoto	Chichibu	Saitama	SCT	40	Visual+SW GPS Signal	3	Gradually
4	Kazumi Terakubo	Fuchu	Tokyo	Refractor	7.6	Visual+Tape Time Sig.	4	Gradually
5	Mikiya Sato	Fuchu	Tokyo	Telephoto	(F2.8)	Movie+BPM Time Signal	5	Two-step
6	Toshio Hirose	Ohta-ku	Tokyo	Refractor	6.5	Video+JJY Time Inst.	6	Two-step
7	Kunihiro Shima	Fujimi	Nagano	SCT	45	Movie+NPT	7	Two-Step
8	Hideto Yamamura	Hakusan	Ishikawa	SCT	20	Video+GPS Time Inst.	8	Two-D/R
9	Toshihiro Horaguchi	Tsukuba	Ibaraki	SCT	50 6	Video+GPS Time Inst. Visual	-	Miss
10	Satoshi Watanabe	Oyama	Tochigi	SCT	30	Movie+JJY Time Signal	-	Miss
11	Hideto Watanabe	Inabe	Mie	Refractor	13	Video+GPS Time Inst.	-	Miss

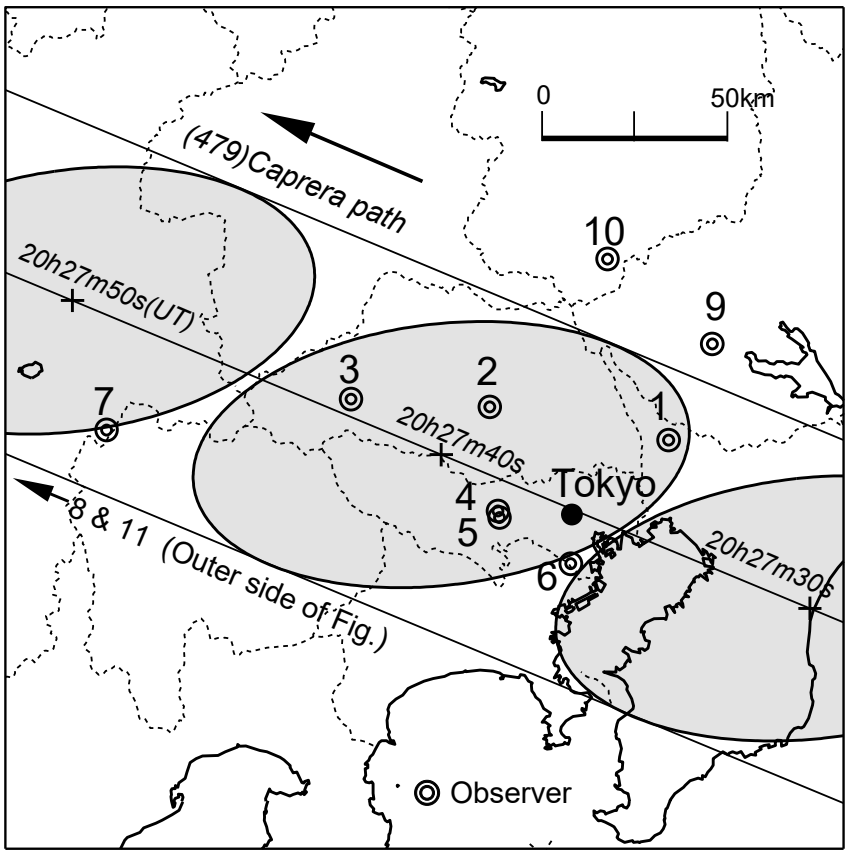

Figure 1: (479)Caprera Predicted path on 2018 December 10 (U.T.) & Observer's Site number

Duplicity Discovery of HIP 33753 from Asteroidal Occultation by (479)Caprera

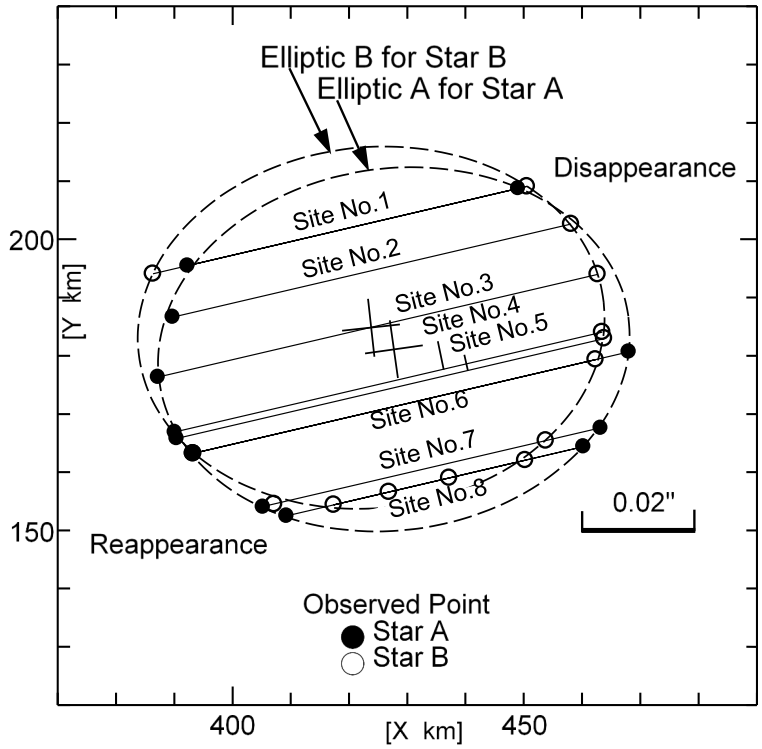

Figure 2. Occultation Reduction showing distinct step-event on D and R by Star A and B

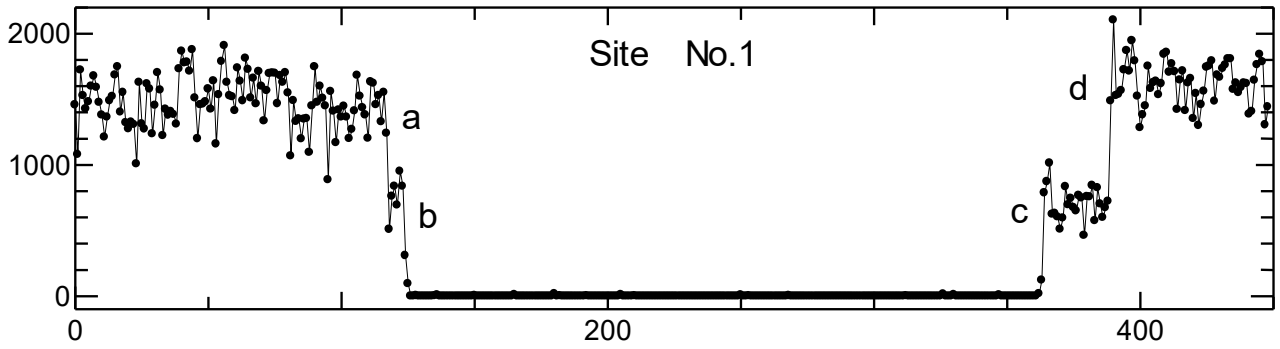

Figure 3. Site No.1 light curve showing distinct two-step event on D (a, b) and R (c, d)

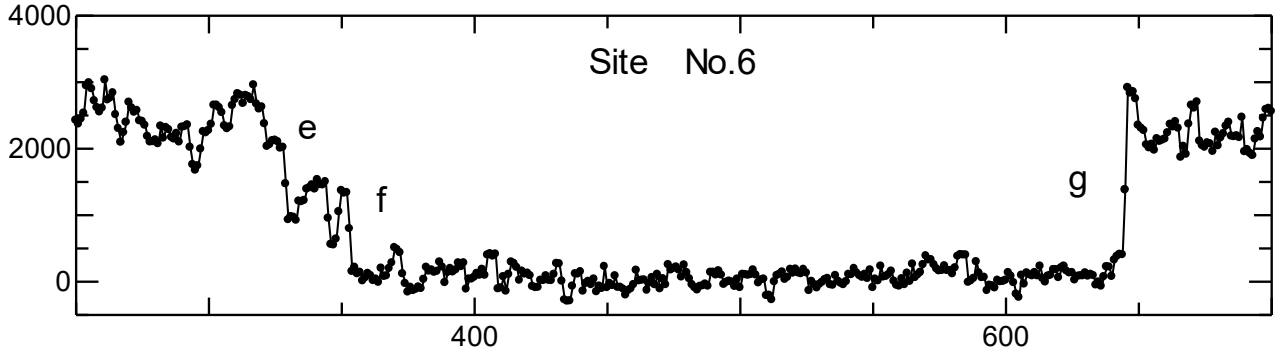

***Figure 4**: Site No.6 light curve showing two-event on D (e, f) and no step–event on R (g)*

Duplicity Discovery of HIP 33753 from Asteroidal Occultation by (479)Caprera

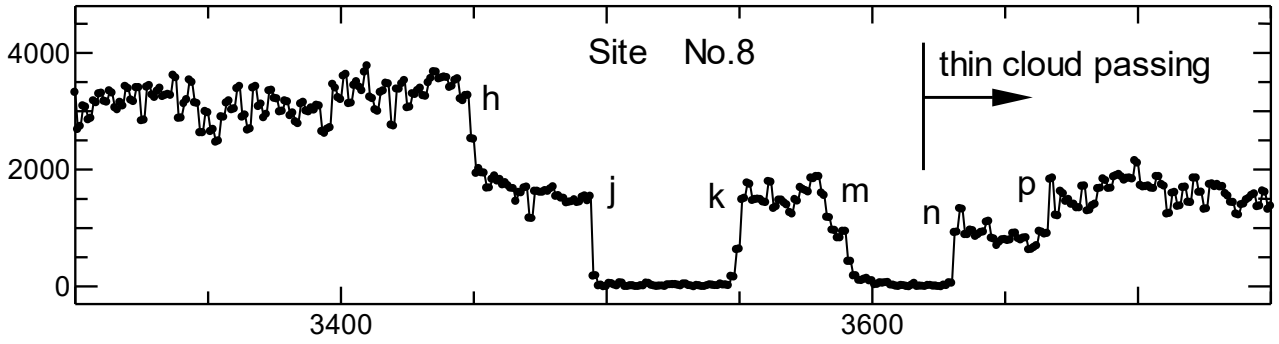

Figure 5. Site No.8 light curve showing two-event on D (j, m) & R (k, n) by Star B only

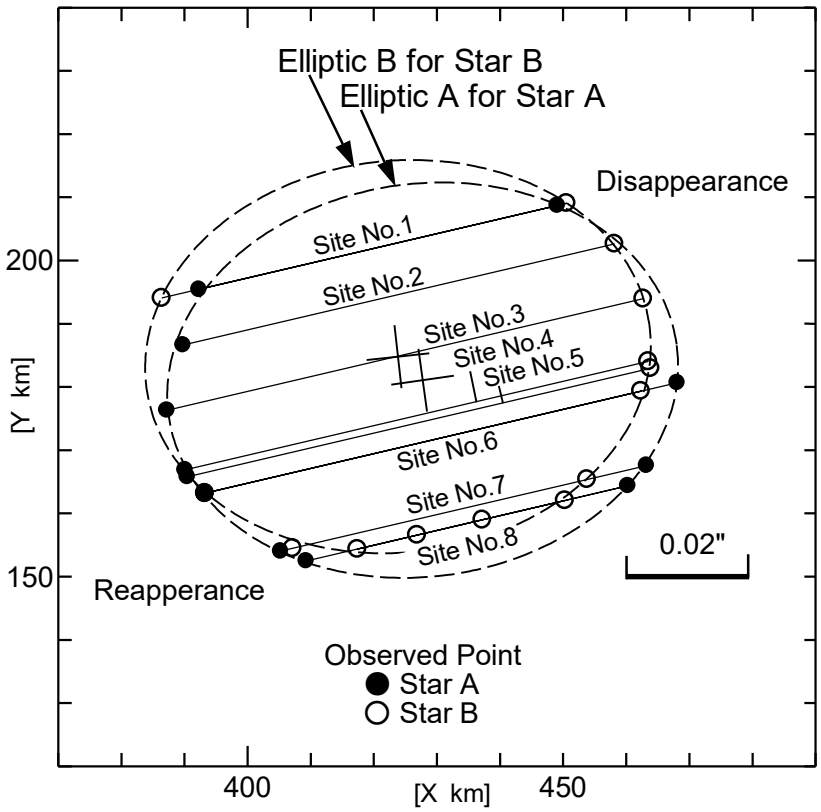

Figure 6. Elliptic A and B adapts to the observed point for Star A and Star B each

Table 2:Star A and Star B, Magnitude from the brightness level

Points on the light curve in Figs. 3-5	Brightness Level	Calculated Star Magnitude
a	1482±132	Star A= 8.44 Star B= 8.51
b	763±103	
c	706±82	Star A= 8.34 Star B= 8.63
d	1626±114	
e & g	2385±247	Star A= 8.38 Star B= 8.57
f	1094±212	
h	3223±308	Star A= 8.42 Star B= 8.53
j,k,m	1526±136	

Duplicity Discovery of HIP 33753 from Asteroidal Occultation by (479)Caprera

(Continued from page 268)

Elliptic A

Dimension (80.3 ± 0.3) km x (62.0 ± 0.6) km
Axis Angle 6.3 ± 0.8 degree
Center Coordinates
X (423.825 ± 0.132) km, **Y**(184.799 ± 0.178) km

Elliptic B

Dimension (81.3 ± 0.7) km x (62.1 ± 1.1) km
Axis Angle 8.0 ±1.5 degree
Center Coordinates
X (427.734 ± 0.270) km, **Y**(181.075 ± 0.340) km

As for these two shapes, the dimensions should accord when they suppose that the form of the asteroid has a geometric ellipse. However, the different dimensions may be caused by the irre-gularity on the rim of the asteroid, otherwise. So the difference of two central locations in the coordinate means elongation of the double star.

Based on the data presented in these values and the equatorial horizontal parallax of the asteroid (6.558 arcsecond), the separation of the two components is 0.0054 ± 0.0004 arc-seconds at a position angle of 46.4 ± 3.7 degrees.

Magnitude estimates for each component were made using the brightness measurements provided by the values on Table 2. The magnitudes of the two stars are estimated to be 8.40 V and 8.56 V [6].

The finished plot of the double Based on the data presented in this report, the double star characteristics are:

Star: HIP 33753 – magnitude 7.73
SAO 96373
TYCHO 2 0756-01375-1
PPM 123384
HD 52154
UCAC4 514-035495
Spectral type A2
Coord. (J2000) 07 00 39.3118
+12 44 24.054 (Simbad [7])
Mag A 8.4 ± 0.1 V (Estimated from HIP)
Mag B 8.6 ± 0.1 V (Estimated from HIP)
Sep. 0.0054 ± 0.0004 arc-seconds
P.A. 46.4± 3.7degrees
Epoch 2018.945

Finally, point of “m” may show another star within Star B, in figure 5.

References

1. Asteroid Occultation Updates, Steve Preston, http://www.asteroidoccultation.com/
2. Tenmon-Nenkan p226-223, Toshio Hirose et al. Seibundo-Shinkosya, 2018
3. Asteroid p98-118, Tom Gehrels, University of Arizona Press, 1979
4. Limovie software, Light curve measurement tool http://astrolimovie.info/
5. Data Analysis, Takashi Awaya, Gakkai Press Center, 1991
6. The Observer’s Guide To Astronomy Vol.1, p533 , Patrick Martinez, Cambridge University Press, 1994
7. Coordinates ICRS (equinox and epoch=J2000.0) as reported in Simbad

Speckle Interferometry with the OCA Kuhn 22" Telescope - II

Rick Wasson

Murrieta, California
ricksshobs@verizon.net

Abstract: This paper reports Speckle Interferometry measurements of double stars made during 2017, using the Kuhn 22-inch telescope of the Orange County Astronomers, a ZWO ASI 290MM CMOS camera, and four interference filters. Observations are reported for 71 systems. Targeted separations ranged from 0.3" to 3.0", but wider components of several multiple systems were also measured. Astrometric data reduction utilized the REDUC and Speckle Tool Box programs, and bispectrum analysis was also done for all stars. Equipment, data acquisition, astrometric and photometric data reduction and analyses are described. Results for several stars are discussed in detail.

Introduction

The author is a member of the Orange County Astronomers (OCA), one of the largest and most active amateur astronomy clubs in the United States. One of the many privileges of OCA membership is the use, after completing a training course, of the Kuhn 22-inch (0.56 meter) f/8 Cassegrain telescope. The observatory is located at the club's Anza observing site in the hills about 15 miles northeast of Mount Palomar Observatory, at 4300 feet elevation under a moderately dark sky.

The first article in this series (Wasson, 2018) reported on the beginning use of the Kuhn 22" for speckle interferometry of close double stars. This paper describes the continuing observational program, with two major improvements: (1) An improved camera, the ZWO ASI290MM with low read noise and improved near-IR sensitivity; (2) Adding Bispectrum Analysis (BSA) to the normal Autocorrelation (AC) method of speckle analysis. Only significant changes to methods and equipment from the previous paper are discussed here. The telescope and instrumentation ready for speckle interferometry are shown in Figure 1.

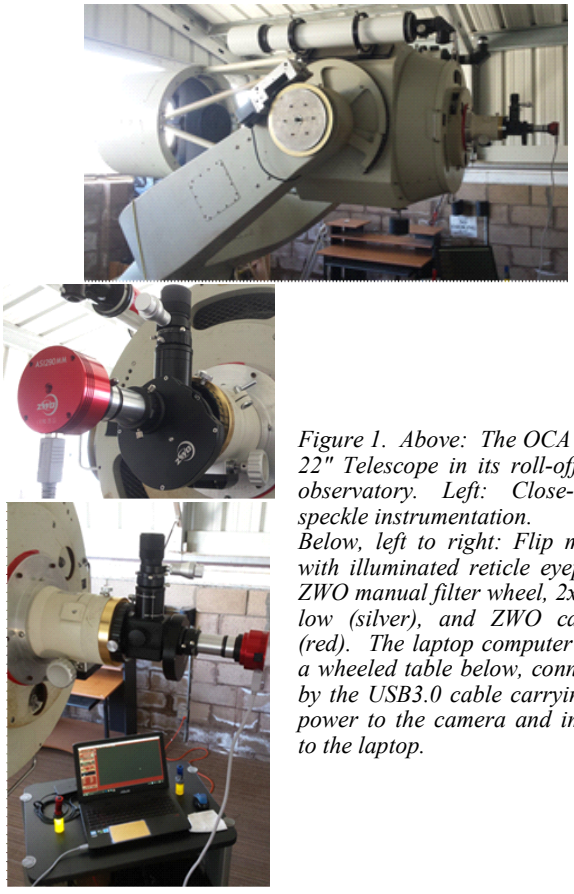

Figure 1. Above: The OCA Kuhn 22" Telescope in its roll-off roof observatory. Left: Close-up of speckle instrumentation.
Below, left to right: Flip mirror with illuminated reticle eyepiece, ZWO manual filter wheel, 2x Barlow (silver), and ZWO camera (red). The laptop computer is on a wheeled table below, connected by the USB3.0 cable carrying 5V power to the camera and images to the laptop.

Camera Upgrade

All observations in this paper used a ZWO ASI290MM high-speed monochrome camera, which has a Sony IMX290LLR back-illuminated CMOS detector with 2.90 μ square pixels in a 1936x1096 array,

and a rolling shutter. This un-cooled camera was chosen because the back-illuminated design, new technology for CMOS cameras, gives improved sensitivity in the near-IR spectral region; because the read noise is very low (~1e- rms depending on gain); and because this high-tech unit is available for only about $400US. It has a high-speed USB3.0 interface (more than 30 fps full frame), providing 12-bit images. The Quantum Efficiency (QE) is believed to be about 70% peak at 600 nm, and still 24% at 900nm.

Because of the small pixels, less magnification is required to reach the optimum speckle image scale – about 7 to 8 pixels across the Airy disk diameter (Rowe, 2016) – a good compromise between more pixel sampling and less light available per pixel. Therefore, a simple 2x Barlow is used on the Kuhn 22", providing f/16, a plate scale of about 0.066 arc-sec/pixel, and about 8.8 pixels across the Airy disk at 650nm wavelength. The speckle field is small - about 2.2'x1.2' - but is adequate for close double stars, and large enough for easy centering with an illuminated reticle eyepiece.

Filters

A ZWO manual filter wheel was used, housing the three 1¼-inch filters already in hand; a longer wavelength IR-pass filter (IR807) was added to make use of the better near-IR QE of the back-illuminated sensor, for observations of very red stars (Serot et al, 2018). Table 1 gives the characteristics of the four interference filters used for the observations reported here. These filters are not members of any photometric standard series, but they are economical, durable, and cover the detectable wavelength range of the camera well.

For the two long-pass filters in Table 1, asterisks indicate convolved characteristics: i.e., filter transmission times QE of the CMOS detector. The "50% Band Pass" column for these two filters is 50% cut-on transmission on the short side, but it is assumed to be 1 micron on the long side because detection is determined by the Silicon detector sensitivity limit (~1μ) rather than filter transmission.

Target Selection and Observation

Double star targets were chosen by searching the Washington Double Star (WDS) Catalog, primarily using the search tool WDS1.2 (Rowe, 2017). Input parameters include ranges for RA and Dec, primary star magnitude, magnitude difference and separation. This program also gives a list of possible reference stars within 3 degrees of the target; the list may be sorted by distance or magnitude. These are very important, time-saving features for the user, making it easy to select a suitable reference star, which should be as close to the target star as possible in terms of location, magnitude and color (spectral type). A reference star was usually observed immediately after every double star.

The target search parameters generally employed were:

- 0.3" < Separation < 3.0".
- Primary star brighter than magnitude 11.
- Declination between +68° and -2° (i.e.,observatory latitude ~33° +/- 35°).

Special consideration was given to binary stars which already have orbital solutions, in the hope of providing additional speckle measurements for refining the orbits. For some stars, especially those with orbits, detailed information was found at the Italian website Stelle-Doppie (Sordiglioni, 2016), including SAO number, orbital period, and current orbit ephemerides for Separation (ρ) and Position Angle (θ).

A "master" Target List was built as an EXCEL workbook, covering the entire RA range in spreadsheets of 2 hours each. The WDS orbit plots were also copied and hyper-linked into the spreadsheets for quick reference. For each observing run, a copy of the workbook was made, to serve as the observing log by entering observation date, sequence numbers, filters and notes into the spreadsheets in real time.

A sequence of 1000 frames was acquired for most

Table 1. Filter characteristics. These interference filters typically have a sharp rise and fall of about 10 nm width, and a high, nearly constant transmission plateau (95+%). The "IR742" and "IR807" filters are long-pass IR transmission filters.

Filter	Manufacturer Name	50% Band Pass (nm)	Center Wavelength (nm)	Width (nm)	Peak Transition
G	Baader G (LRGB Series)	495 - 575	534	80	96%
R	Baader R (LRGB Series)	585 - 690	636	105	98%
IR742	Astronomik ProPlanet 742	736 – *	844 *	260 *	56% *
IR807	Astronomik ProPlanet 807	800 – *	885 *	200 *	44% *

double and reference stars; more than one sequence was recorded for some doubles having a faint secondary star, with the intention to improve S/N. Stars were generally observed at zenith angles less than about 35 degrees, because an atmospheric dispersion corrector was not used; it has been found that for larger zenith angles atmospheric dispersion "smearing" becomes noticeable for the moderate-width filters of Table 1, possibly degrading separation and position angle accuracy.

Acquisition and Analysis Software

All data acquisition, processing and analysis was performed on a laptop computer with Intel i7 quad processors, running Windows 10. FireCapture 2.6 (Edelmann, 2015) software was used for all data acquisition. This very versatile program, designed primarily for planetary imaging, can be used with many types of astronomy cameras, easily handles fast USB3.0 data speeds from the camera, and can store raw data frames as FITS files, a convenient format for Speckle data processing in both REDUC (Losse, 2015) and Speckle Tool Box (STB) software (Rowe & Genet, 2015).

The Drift Calibration method (Wasson, 2018) was used to calibrate each night's data for Plate Scale and Camera Orientation on the sky. Multiple drifts were made throughout the night - typically several drifts on each of several bright reference stars; the average of all drift results was used to reduce all the speckle data for that night.

Each drift sequence was first edited in REDUC to delete frames where the star was absent from the field, not moving, or overlapped the edge. A convenient Drift Calibration tool is part of the STB data reduction program (Harshaw, Rowe and Genet, 2017). Plate scale was about 0.0662 arc-sec/pixel. Standard deviation of plate scale calibrations for the 6 nights of observation ranged from 0.00022 to 0.00044"/pixel. Standard deviation of the camera orientation on the sky ranged from 0.13 to 0.37 degree.

STB version 1.13 software (Rowe, Genet, Wasson, 2019) was employed for all speckle data analysis. It includes tools for both normal speckle AC and triple correlation BSA. The first step of processing was assembly of each sequence of double or reference star images into FITS cube format. STB has a simple-to-use tool to create the FITS cubes, which centers each frame on the star and, if desired, crops all frames to a smaller size, to speed up processing time and reduce file storage space. The original speckle frames were a 512x512 pixel region of interest (ROI) near the center of the larger camera field of view, allowing plenty of room for approximate centering and movement from seeing and telescope tracking errors. In creating the FITS cubes, the field was cropped to 128x128 pixels (or 256x256 for wide doubles), but the original frames are not altered.

Dark frames were generally not recorded or used in AC or BSA processing. Of course, if dark frames were to be used, they must be taken with exactly the same camera ROI as the speckle frames, and the master dark must be subtracted from all *original* speckle frames - before creating a FITS cube with smaller cropped frames. This is because these smaller images are randomly positioned to follow the star movements and center it, losing registry with both original and dark frames.

Normal speckle AC processing, including deconvolution with a reference star, was first performed for all the double stars; results were written to a .csv (spreadsheet) file – another convenient STB feature. The latest WDS observation or orbit ephemerides was used to select the correct θ quadrant from the two peaks given by the AC solution. The same set of double and reference star FITS cubes were then used for BSA in STB1.13, and these results were copied into the AC spreadsheet for comparison.

Bispectrum Analysis

Bispectrum analysis – also known as triple-correlation – is an extension of the AC speckle analysis technique; ρ, θ and Δmagnitude of double stars down to near the diffraction limit can be measured. BSA has been used by professional astronomers for some time (Horch, et al, 1999). STB1.13 became available to amateur speckle observers in 2017 for experimental testing (Serot, et al, 2018), and is expected to be available by request from the author in 2019.

Two inherent mathematical limitations arise from AC processing: (1) the 180° uncertainty of θ, because of the two identical secondary peaks in the AC; and (2) amplitudes of the AC peaks have no relationship with star brightness, so magnitudes of the components cannot be measured.

The goal of BSA is to overcome the limitations of AC through more advanced mathematical processing. The first step is calculation of the bispectrum from the average of the triple correlation of all individual images; this four-dimensional BSA processing takes roughly 10 times more CPU time than that for the AC power spectrum alone. The second step, using the STB "Bispectrum Phase Reconstruction" tool, is an iterative procedure under control of the user, which yields a reconstructed diffraction-limited image with atmospheric distortion removed. Processing with the bispectrum of a reference (single) star serves to reduce optical and atmospheric aberrations which are common to both double and reference images, just as it does for an autocorrelation. Mathematical filtering techniques may also

Speckle Interferometry with the OCA Kuhn 22" Telescope - II

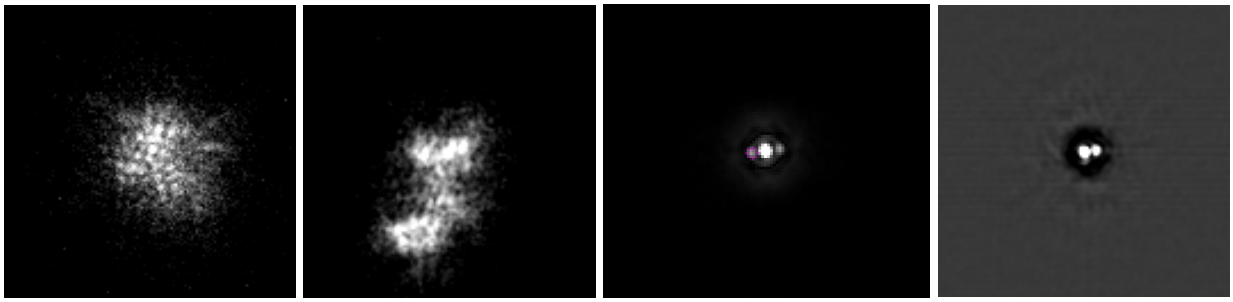

Figure 2. An example of processing results for the double star 11190+1416 STF1527, WDS magnitudes 7.01/7.99, Δmag = 0.98, spectrum F9V. 3000 frames were recorded, using 0.030 sec exposures, in the G filter. Left to Right: Two representative raw speckle frames; the autocorrelation (ρ = 0.312", θ = 277.42 deg.); the BSA reconstructed image (ρ = 0.338", θ = 277.46 deg, Δmag = 1.16).

be applied to improve the S/N and clarity of the image. Examples of the AC and BSA reconstructed image for a typical double star are shown in Figure 2.

Bispectrum ΔMagnitudes

STB 1.13 has a convenient tool for measuring ρ, θ and Δmagnitude from the BSA reconstructed image. The user chooses circular photometry apertures for the primary star, secondary star and background. Measurement of Δmagnitude must use the *same* photometry aperture for both the primary and secondary components, but not necessarily for the background. The importance of using the same star apertures is illustrated by the photometric "growth curve" in Figure 3. The measured magnitude of a star obviously depends on the aperture radius, but noise limits the maximum useful radius. Fortunately, stars of different brightness have the *same* point spread function (PSF), differing only in flux amplitude. The same aperture captures the same *proportion* of light for both stars, giving the correct Δmagnitude even though not all the light is included. The aperture should be sized for the fainter star, limited to the radius where noise begins to be added faster than starlight.

In practice, speckle photometry of close double stars is generally less accurate than conventional wide-

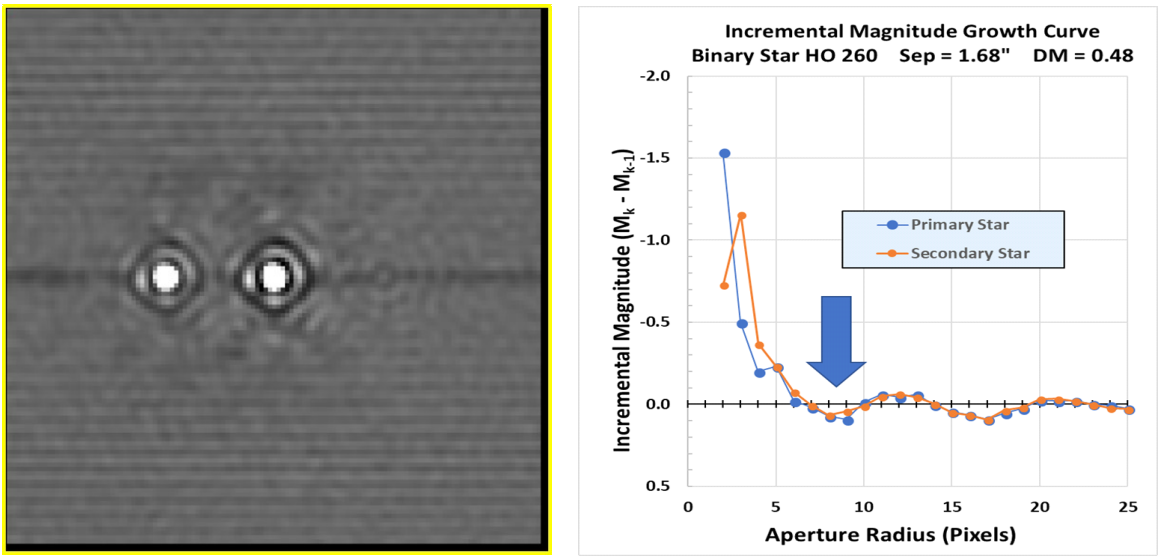

Figure 3. Left: BSA reconstructed image of the binary HO260, ρ = 1.68". The image is stretched to show low-amplitude detail; the Airy disk, 1st diffraction ring, and parts of the 2nd ring are clearly visible. Residual low-level fixed pattern noise also becomes visible as horizontal lines. Right: The magnitude vs aperture "growth curve." Brightness grows as radius of the photometric aperture increases, but the growth curve is shown here as the declining difference in magnitude for a one-pixel increase in radius (valid only for Radius>2). This format, which is analogous to the Point Spread Function, amplifies the curve sensitivity so that the shallow diffraction rings can be clearly seen. PSF of the two stars is the same in radial extent, even though their brightness is different by 0.5 magnitude. The Rayleigh criterion (blue arrow) is at the minimum of the 1st ring.

field CCD photometry. Four obvious challenges are: (1) BSA images are mathematical reconstructions (not original recordings of flux), so noise can affect every step of reconstruction processing; (2) short exposures limit the S/N of faint stars, (3) the two nearby PSFs may overlap each other, similar to crowded-field photometry; (4) diffraction rings of separated stars may still overlap and interfere with the companion PSF, adding "signal" to the wrong star.

No attempt has been made here to transform the non-standard filter Δmagnitude results to any standard photometric system, but work is underway to investigate that possibility. Further issues associated with measurement of Δmagnitudes are discussed in Serot, et al, 2018.

Speckle Measurement Quality

Quality of the speckle measurements was not statistically evaluated. Usually only one sequence was recorded, consisting of 1000 frames; for systems with large Δmagnitude, multiple sequences were sometimes taken. However, no statistical information was calculated because all the available frames were combined into one large FITS cube for AC and BSA processing, with the intention of maximizing S/N.

A *qualitative* figure of merit was assigned to each measurement, as shown in Table 2, with values rated from 1 (good) to 7 (not useable). The same criteria were used for both AC and BSA results. When measuring ρ and θ in STB, most doubles were bright and wide enough to yield very repeatable "solid" solutions - meaning that the peaks (centroids) of the AC or BSA image were accurately located and did not shift when moving the measurement aperture slightly. Observations with mild atmospheric dispersion, causing slightly "smeared" AC or BSA image peaks, were assigned quality 2. Close or faint secondary measurements were given values of 3 or 4, respectively, if the measurements were still "solid."

For very close and/or faint doubles, where measurements were marginal and difficult, higher numbers were assigned. Values of 5 are considered uncertain, because the secondary peak was not clearly separated from the central peak, making its centroid location questionable. Values of 6 are also uncertain because the faint secondary peak was distorted by, or not clearly distinguishable from, background noise or primary contamination. A value of 7 indicates that no reasonable measurement was possible. In Tables 2 and 3 below, those measurements having poor quality of 5, 6 or 7 are flagged in color.

Double Star AC and BSA Measures

Speckle measurements with the OCA Kuhn 22-inch telescope reported in Table 3 were made from March through October 2017.

Double stars with separation up to 3" were targeted, but several of these are multiple systems in which an additional component, having a wider separation (up to about 6"), was also measured. One reference star was inadvertently chosen which happened to be the wide double STF2398 (ρ ~ 8"); therefore, it was also measured by using the bright primary of the original, well-resolved double (BU385AB) in the role of "reference" star. Such wide components were certainly not within the same isoplanatic patch - therefore, speckle techniques do not strictly apply. However, the same speckle processing was used for them, and the results seem reasonable.

It must be noted that the observations of 2017 October 15 (2017.789) were taken at half the normal plate scale (0.1308 instead of 0.066) because the 2x Barlow was inadvertently left out of the optical assembly. Therefore, these observations are somewhat pixelated, compromising the accuracy of ρ, θ, and Δmagnitude measurements, which are considered approximate. An

Table 2. Qualitative Figure of Merit for ρ and θ measurements. A Figure of Merit code number is given for each measurement in Table 3.

Figure of Merit	Notes Related to Quality of the Observations
1	Bright, clear AC or BSA image. Solid measurement.
2	Some distortion of fringes or peaks, but measurement solid.
3	Close, but measurement clear, solid.
4	Companion faint, but measurement clear, solid.
5	Very close. Measurement uncertain.
6	Companion very faint. Measurement uncertain.
7	Companion too close or faint. Measurement NOT valid.

Speckle Interferometry with the OCA Kuhn 22" Telescope - II

Table 4. Statistics for the differences between AC and BSA measurements.

	θ (deg)	ρ (arc-sec)
Average (AC-BSA)	-0.05	-0.007
Standard Deviation	1.16	0.021
Error of Mean	0.13	0.002

example is given for the star 00308+4732 BU394AB below. Only stars whose separation is greater than 0.6", about twice the normally achievable resolution, are reported for that date.

The differences between AC and BSA are summarized in Table 4, for the 81 measurements of Table 3 which have results from both methods. The average values for θ and ρ differences are close to zero, as they should be since both techniques were always applied to the same original image data, validating that the differences are random. Thus, it is believed there are no significant systematic errors in the AC or BSA astrometry. The standard deviations may be a rough indication of the overall uncertainty of the measurements of Table 3: θ ~ ± 1 degree and ρ ~ ± 0.02".

Discussion of Selected Double Stars

Many of the stars observed in Table 3 are binaries with at least a preliminary orbit. Some were found to have large O-C values for ρ or θ, relative to the orbit ephemerides. In addition, a few stars had large movement from relatively few prior measures. Some of these stars are discussed below, as are observational circumstances that may affect the measurements.

In all Figures 4 through 15, where AC and BSA images are shown, the orientation is North up and East left. The corresponding WDS orbit plots, however, are shown in their customary rotated orientation.

The binary star **00308+4732 BU394AB** is shown in Figure 4. As noted above, this star was observed on

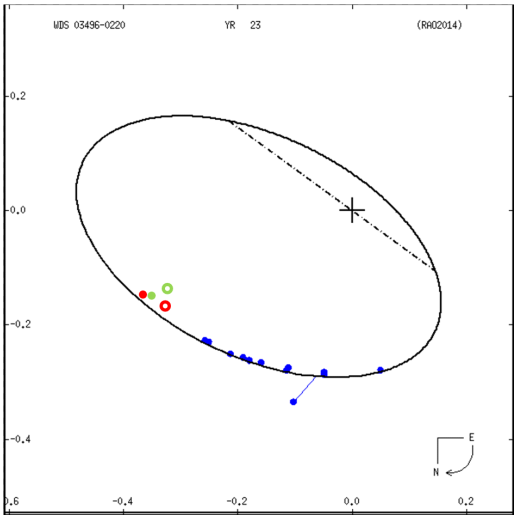

Figure 5. YR 23 orbit plot from the WDS 6th Orbit Catalog. The new AC points from Table 3 are shown as open green and red circles for the G and R filters, respectively. The new BSA points are solid green and red circles respectively, for the G and R filters.

2017 October 15, without the 2x Barlow installed; therefore, the AC and BSA images are pixelated and the measurement accuracy is degraded.

The WDS orbit of binary **03496-0220 YR23** (Riddle, et al, 2015) having a period of 54 years is shown in Figure 5. Although not resolved by Hipparcos, it was classified as "suspected non-single." Regular speckle observations were begun in 2000 with the 3.5-meter WIYN telescope at Kitt Peak (Horch, et al, 2002), and all observations to date have been made with speckle or adaptive optics techniques. YR23 is a triple system; one of the visual components is an unresolved spectroscopic binary.

The new data points from Table 3 have been added to the WDS orbit plot in Figure 5. These points, which are approaching the diffraction limit of the 22-inch telescope, obviously have considerably more scatter than

(Text continues on page 281)

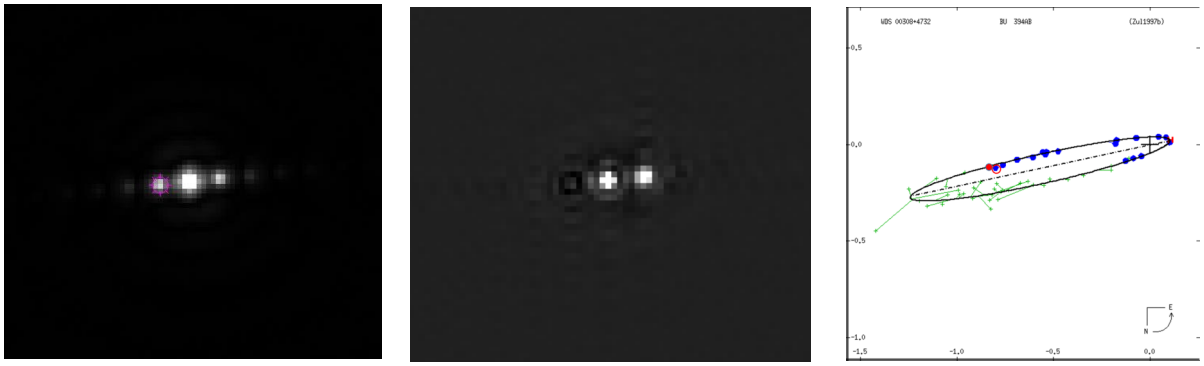

Figure 4. AC and BSA images of BU394AB in the R filter, showing the pixilation caused by observation at inadequate pixel scale (0.1308"/pixel). Left: AC. Middle: BSA reconstructed image. Right: WDS orbit plot with Table 3 measures added as red circles, AC open, and BSA solid.

Speckle Interferometry with the OCA Kuhn 22" Telescope - II

Table 3. Speckle measurements in 2017, using the OCA Kuhn 22-inch telescope, ZWO ASI290MM CMOS camera, and interference filters. The columns are: Besselian observation date, WDS RA and Dec, WDS discovery designation, WDS magnitudes of primary/ secondary, WDS magnitude difference (secondary-primary), WDS spectrum, observation filter (Table 1), AC position angle observed (deg), AC separation observed (arc-sec), BSA position angle observed (deg), BSA separation observed (arc-sec), BSA magnitude difference observed (secondary-primary), and qualitative figure of merit (Table 2) for AC/BSA.

Date	WDS	Discovery	mA / mB	DMag	Spectrum	Filter	AC θ	AC ρ	BSA θ	BSA ρ	BSA ΔMag	Qual
2017.789	00308+4732	BU 394AB	8.49 / 8.77	0.28	G0	R	278.52	0.809	278.28	0.840	0.17	1 / 1
2017.789	00504+5038	BU 232AB	8.46 / 8.79	0.33	F5	R	255.49	0.914	255.51	0.927	0.20	1 / 1
2017.170	03496-0220	YR 23	7.73 / 8.29	0.56	G0	G	292.56	0.351	296.37	0.366	0.58	2 / 2
2017.170	03496-0220					R	293.22	0.379	292.13	0.394	0.17	2 / 2
2017.170	03503+2535	STT 65	5.73 / 6.52	0.79	A2V + A5V	G	201.84	0.440	202.01	0.449	0.44	2 / 2
2017.170	04199+1631	STT 79	7.26 / 8.62	1.36	F9V	G	7.66	0.546	7.21	0.549	1.15	1 / 1
2017.170	04199+1631					R	6.79	0.524	8.05	0.555	1.11	2 / 2
2017.257	06214+0216	A 2667	6.63 / 8.02	1.39	A4.5V	G	279.70	0.319	279.37	0.324	0.95	3 / 3
2017.214	06573+5825	STT 159AB	4.45 / 5.50	1.05	G8III + F8V	IR742	234.74	0.696	235.60	0.717	1.55	1 / 1
2017.257	07401+0514	STF1126AB	6.55 / 6.96	0.41	A0III	G	175.54	0.870	175.82	0.883	0.53	1 / 1
2017.257	07401+0514					R	175.62	0.870	175.80	0.880	0.55	1 / 1
2017.170	07417+0942	STF1130	8.76 / 9.48	0.72	G0	R	61.79	0.522	62.03	0.528	0.49	1 / 1
2017.170	07573+0108	STT 185	7.3 / 7.1	0.20	F7V	R	19.78	0.384	19.96	0.391	0.11	1 / 1
2017.170	08041+3302	STT 187	6.94 / 8.50	1.56	A1.5V	G	337.12	0.419	336.69	0.436	0.21	1 / 1
2017.170	08044+1217	BU 581AB	8.46 / 8.83	0.37	K0V	R	217.63	0.392	219.60	0.395	0.13	1 / 1
2017.170	08044+1217					R	217.99	0.393	218.60	0.391	0.15	1 / 1
2017.170	08044+1217	BU 581AC	8.46 / 11.78	3.32	K0V	R	221.98	5.526	222.02	5.527	2.84	1 / 1
2017.170	08044+1217					R	221.96	5.498	221.95	5.535	2.60	1 / 1
2017.214	08050+5825	A 1073	9.24 / 9.89	0.65	F8	IR742	-	-	-	-	-	7 / 7
2017.170	08122+1739	STF1196AB	5.30 / 6.25	0.95	F8V	R	14.77	1.149	14.63	1.146	0.31	1 / 1
2017.170	08122+1739					IR742	14.79	1.146	14.36	1.149	0.34	1 / 1
2017.170	08122+1739	STF1196AC	5.30 / 5.85	0.55	F8V	R	61.18	6.263	61.17	6.263	0.38	1 / 1
2017.170	08122+1739					IR742	61.19	6.258	61.26	6.264	0.35	1 / 1
2017.170	08122+1739	HUT 1CaCb	6.2 / 7.1	0.90	M1	R	273.27	0.417	-	-	-	6 / 7
2017.170	08122+1739					IR742	270.79	0.464	-	-	-	6 / 7
2017.214	08231+2001	HO 525AB	9.83 / 9.89	0.06	F5	R	353.96	0.436	353.79	0.445	0.80	1 / 1
2017.214	08531+5457	A 1584	8.99 / 7.72	-1.27	G0	R	93.29	0.677	93.30	0.683	0.08	1 / 1
2017.331	08592+4803	HJ 2477AB	3.13 / 9.9	6.07	A7IV	IR807	89.76	2.418	-	-	-	6 / 7
2017.331	08592+4803	HU 628AC	3.13 / 10.1	6.97	A7IV	IR807	111.96	2.185	-	-	-	6 / 7
2017.331	08592+4803	HU 628BC	9.9 / 10.1	0.20	M1	IR807	206.17	0.915	-	-	-	4 / 7
2017.170	09006+4147	KUI 37AB	4.18 / 6.48	2.30	F3V + K0V	R	138.15	0.435	140.49	0.402	1.70	6 / 5
2017.170	09006+4147					IR742	143.78	0.480	143.70	0.452	1.74	6 / 3
2017.214	09036+4709	A 1585	4.16 / 4.54	0.38	A1V	G	283.66	0.274	284.95	0.263	0.31	5 / 5
2017.214	09179+2834	STF3121AB	7.9 / 8.0	0.10	K0	R	23.10	0.468	22.72	0.476	-0.02	1 / 1
2017.214	09186+2049	HO 43	9.31 / 9.46	0.15	F5	R	96.64	0.611	97.14	0.606	0.35	1 / 1
2017.257	09210+3811	STF1338AB	6.72 / 7.08	0.36	F2V + F4V	G	311.61	1.155	311.58	1.149	0.35	1 / 1
2017.257	09210+3811					R	311.39	1.150	311.30	1.150	0.32	1 / 1
2017.214	09260+2839	A 222	9.13 / 9.41	0.28	F8	R	4.25	0.384	4.81	0.372	0.32	1 / 1
2017.257	09285+0903	STF1356	5.69 / 7.28	1.59	F9IV	R	112.19	0.845	112.13	0.848	0.51	1 / 1
2017.214	09521+5404	STT 208	5.28 / 5.39	0.11	A2V	G	307.18	0.395	308.31	0.401	0.08	1 / 1
2017.257	09591+5316	A 1346	8.84 / 9.66	0.82	F8	R	178.10	0.570	178.26	0.607	0.99	2 / 2
2017.331	10163+1744	STT 215	7.25 / 7.46	0.21	A9IV	IR742	175.99	1.507	176.01	1.506	0.37	1 / 1
2017.331	10192+2034	STF1423	9.4 / 10.08	0.68	K0	IR742	310.96	0.726	310.77	0.713	0.98	1 / 1
2017.331	10269+1713	STT 217	7.85 / 8.58	0.73	F6V	IR742	149.04	0.827	149.27	0.832	0.35	1 / 2

Table 3 concludes on the next page.

Speckle Interferometry with the OCA Kuhn 22" Telescope - II

Table 3 (conclusion). Speckle measurements in 2017, using the OCA Kuhn 22-inch telescope, ZWO ASI290MM CMOS camera, and interference filters. The columns are: Besselian observation date, WDS RA and Dec, WDS discovery designation, WDS magnitudes of primary/secondary, WDS magnitude difference (secondary-primary), WDS spectrum, observation filter (Table 1), AC position angle observed (deg), AC separation observed (arc-sec), BSA position angle observed (deg), BSA separation observed (arc-sec), BSA magnitude difference observed (secondary-primary), and qualitative figure of merit (Table 2) for AC/BSA.

Date	WDS	Discovery	mA / mB	DMag	Spectrum	Filter	AC θ	AC ρ	BSA θ	BSA ρ	BSA ΔMag	Qual
2017.214	10279+3642	HU 879	4.62 / 6.04	1.42	G8III	R	228.41	0.531	227.62	0.530	1.26	1 / 1
2017.214	10426+0335	A 2768	6.92 / 8.45	1.53	F7V	R	241.98	0.625	242.83	0.626	1.30	1 / 1
2017.170	10454+3831	HO 532AC	9.42 / 11.76	2.34	M2	IR742	230.53	0.749	231.03	0.731	1.79	1 / 1
2017.257	10480+4107	STT 229	7.62 / 7.92	0.30	A5IV	R	257.26	0.677	257.43	0.682	0.29	1 / 1
2017.257	10544+3840	COU1746	10.70 / 10.91	0.21	K0	IR742	329.94	0.374	331.17	0.325	0.16	6 / 6
2017.331	10585+1711	A 2375	10.44 / 10.03	-0.41	G5	R	169.76	0.505	169.17	0.522	-0.40	1 / 1
2017.257	11037+6145	BU 1077AB	2.02 / 4.95	2.93	G9III	R	339.38	0.775	342.38	0.806	3.59	6 / 6
2017.331	11107+3110	HJ 2562	10.53 / 11.4	0.87	K5	IR742	221.56	0.992	221.05	1.009	0.79	1 / 1
2017.257	11182+3132	STF1523AB	4.33 / 4.80	0.47	F9V + G9V	R	164.52	1.904	164.58	1.908	0.41	2 / 2
2017.331	11190+1416	STF1527	7.01 / 7.99	0.98	F9V	G	277.42	0.312	277.46	0.338	1.16	3 / 3
2017.170	11239+1032	STF1536AB	4.06 / 6.71	2.65	F4IV	IR807	94.78	2.180	94.85	2.180	1.98	1 / 1
2017.331	11293+3025	L 11	7.22 / 10.35	3.13	F6V	IR742	277.93	1.072	276.64	1.066	2.77	4 / 4
2017.257	11308+4117	STT 234	7.45 / 8.13	0.68	F6V	R	181.23	0.404	181.05	0.431	0.18	2 / 2
2017.257	11323+6105	STT 235AB	5.69 / 7.55	1.86	F8V	R	42.58	0.929	42.95	0.931	1.43	1 / 1
2017.257	12060+6842	STF3123AB	8.01 / 7.9	-0.11	F6V	G	190.60	0.304	189.92	0.308	0.23	5 / 5
2017.257	12060+6842	STF3123AB,C	7.2 / 15.7	8.50	F6V	IR807	301.62	2.954	301.92	3.004	5.06	4 / 4
2017.331	12108+3953	STF1606	7.44 / 7.93	0.49	A8III	G	144.73	0.582	144.44	0.587	0.52	1 / 1
2017.214	12291+3123	STT 251	8.35 / 9.27	0.92	G0	R	59.79	0.727	59.58	0.731	1.15	1 / 1
2017.214	12572+0818	FIN 380	7.50 / 7.88	0.38	F5	G	-	-	-	-	-	7 / 7
2017.257	13007+5622	BU 1082	5.02 / 7.88	2.86	F2V	R	126.88	0.781	127.33	0.775	2.00	1 / 1
2017.331	13081+2657	STT 260	8.98 / 9.5	0.52	F9V	G	41.31	0.310	41.49	0.314	0.18	3 / 3
2017.331	13091+2127	HU 572	8.73 / 10.08	1.35	G5	G	332.27	0.529	333.39	0.524	1.37	1 / 1
2017.257	13198+4747	HU 644AB	9.11 / 9.87	0.76	K0	G	79.22	0.361	79.20	0.357	0.96	1 / 1
2017.331	13235+2914	HO 260	9.6 / 9.94	0.34	M0+M0.5	R	89.00	1.682	88.97	1.683	0.46	1 / 1
2017.331	13258+4430	A 1609AB	9.49 / 8.79	-0.70	K0	R	66.40	0.345	66.93	0.341	0.13	3 / 5
2017.331	13258+4430	—	—	—	—	IR807	65.85	0.394	63.03	0.336	0.43	5 / 5
2017.331	13258+4430	A 1609AC	8.33 / 13	4.67	K0	R	220.04	2.566	220.02	2.565	2.86	4 / 4
2017.331	13258+4430					IR807	219.86	2.541	220.09	2.552	2.29	4 / 4
2017.331	13284+1543	STT 266	7.97 / 8.42	0.45	F5	G	357.59	2.012	357.65	2.010	0.62	1 / 1
2017.331	13482+2248	COU 401	9.5 / 10.6	1.10	G0+G8	G	6.78	0.331	-	-	-	5 / 7
2017.331	13577+5200	A 1614	8.99 / 9.13	0.14	G5	R	299.34	1.447	299.40	1.449	0.37	1 / 1
2017.531	17366+4827	COU1922	7.72 / 9.64	1.92	F6V	G	83.29	0.348	79.34	0.375	1.34	1 / 1
2017.531	17366+4827					R	81.61	0.377	78.09	0.400	1.55	1 / 1
2017.789	20102+4357	STT 400	7.6 / 9.83	2.23	G3V	R	327.58	0.644	328.76	0.695	0.15	1 / 1
2017.789	20210+4437	A 725	9.46 / 10.23	0.77	K0	R	25.99	0.854	25.13	0.878	0.64	1 / 1
2017.789	21137+6424	H 1 48	7.21 / 7.33	0.12	G2IV+G2IV	R	244.10	0.695	242.55	0.740	0.08	1 / 1
2017.789	21148+3803	AGC 13AB	3.83 / 6.57	2.74	F3V+F7V	R	190.72	0.895	-	-	-	4 / 7
2017.789	21223+5734	A 764AB	8.23 / 10.69	2.46	G5	R	199.10	1.338	198.88	1.319	-1.84	1 / 1
2017.789	22202+2931	BU 1216	8.61 / 9.21	0.60	F5	R	276.52	0.961	275.81	0.968	0.47	1 / 1
2017.789	22281+1215	BU 701AB	7.34 / 9.62	2.28	K0V	R	175.82	0.993	178.91	1.073	2.27	1 / 1
2017.789	22514+2623	HO 482AB	7.34 / 8.29	0.95	A9V	R	13.06	0.528	12.70	0.561	0.11	1 / 1
2017.789	23075+3250	STF2978	6.35 / 7.46	1.11	A3V	R	144.47	8.356	144.61	8.344	1.12	1 / 1
2017.789	23103+3229	BU 385AB	7.44 / 8.23	0.79	B9V	R	83.78	0.644	83.23	0.703	0.47	1 / 1
2017.789	23189+0524	BU 80AB	8.18 / 9.39	1.21	K0	R	253.18	0.799	250.57	0.787	0.78	1 / 1
2017.789	23420+2018	STT 503AB	8.26 / 8.63	0.37	F8	R	134.03	1.051	134.34	1.047	0.26	1 / 1
2017.789	23455+2025	STT 505	6.75 / 9.61	2.86	G8III	R	59.72	2.386	60.11	2.394	2.38	1 / 1

Speckle Interferometry with the OCA Kuhn 22" Telescope - II

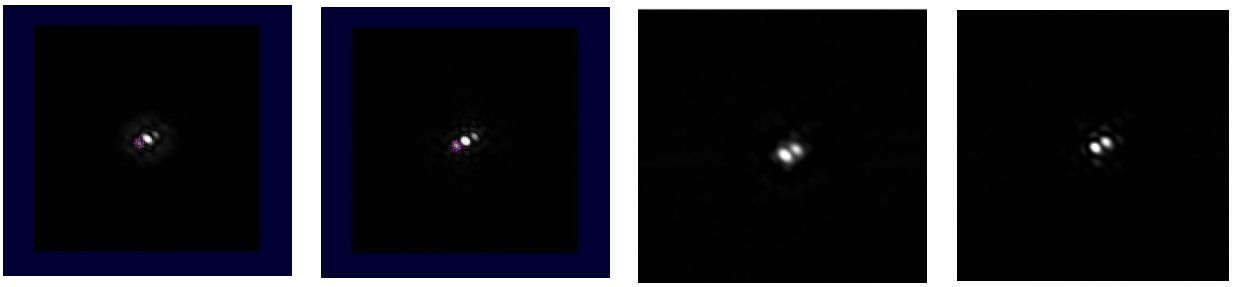

Figure 6. AC and BSA images of YR23, showing the smearing that arises from observation at too large a zenith angle. Left to right: AC in G filter, AC in R, BSA in G, BSA in R. Atmospheric dispersion appears to be greater in the G filter.

(Continued from page 278)

those from larger telescopes. It is likely that atmospheric dispersion also contributed to the scatter, because the star was observed at a zenith angle greater than 35 degrees. Both the AC and BSA measures, in both G and R filters, suffer from smearing by atmospheric dispersion, as seen in Figure 6.

The triple system **08044+1217 BU581ABC** is shown in Figure 7. In the autocorrelogram, the close AB components, which have nearly equal brightness, show multiple peaks when brightened enough to make the C component visible (~3 magnitudes fainter). In addition, the bright pair produces double peaks for C itself. The BSA image gives the proper view. The position angles of AB and AC happen to be nearly the same (Table 3). There are two entries in Table 3 for the same R filter, because this system was inadvertently observed twice in the same night. The WDS 45-year, grade 2 orbit for the AB pair has speckle observations covering nearly an entire orbit.

Figure 8 shows the binary star **09186+2049 HO43**, which has a recently-updated orbit solution (Tokovinin, 2016), with a period of 359 years. The new orbit relied heavily on recent accurate astrometry from Hipparcos, Tycho and speckle observations, which were rapidly departing from the previous (1989) orbit. The current points of Table 3 are in good agreement with the new orbit. Although Hipparcos data are generally considered more accurate than Tycho, in this case it may be that Tycho is favored because the components are slightly fainter than magnitude 9, the threshold for Hipparcos optimum accuracy.

The binary **10454+3831 HO532AC** is shown in Figure 9. It was observed in the IR742 filter because of the very red WDS spectral type (M2), and because of the large Δmagnitude (2.34). The red filter should reduce the magnitude difference if the secondary star is cooler (later type) than the primary, and indeed, the BSA Dmagnitude in Table 3 is 1.79. The WDS orbit plot is also shown in Figure 9, having a period of 161 years. However, based on inspection of historical data from the WDS Observation Catalog, together with the current observations, the orbit solution (Mante, 2000) is unlikely because some of the data points seem to be plotted in error. The WDS orbit ephemerides gives θ = 37 degrees (N-E quadrant) in 2017, but the bispectrum image shows that the secondary is currently in the opposite (S-W) quadrant, θ ~ 230 degrees (Table 3).

In Figure 9, the current AC and BSA points have

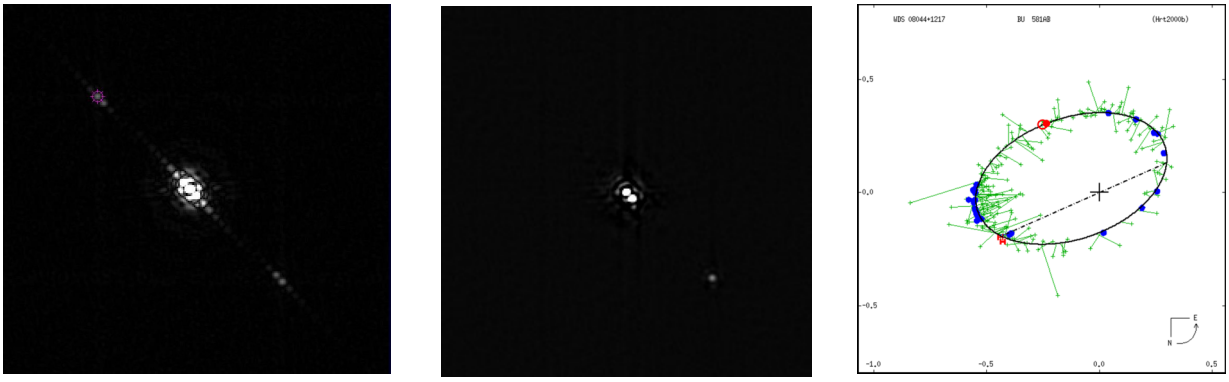

Figure 7. The triple system BU581ABC, observed in the R filter. Left and Middle: The autocorrelation and BSA reconstructed image, respectively. Right: The WDS orbit of the AB pair; Table 3 results are added as red circles - autocorrelation solid, and BSA open.

Speckle Interferometry with the OCA Kuhn 22" Telescope - II

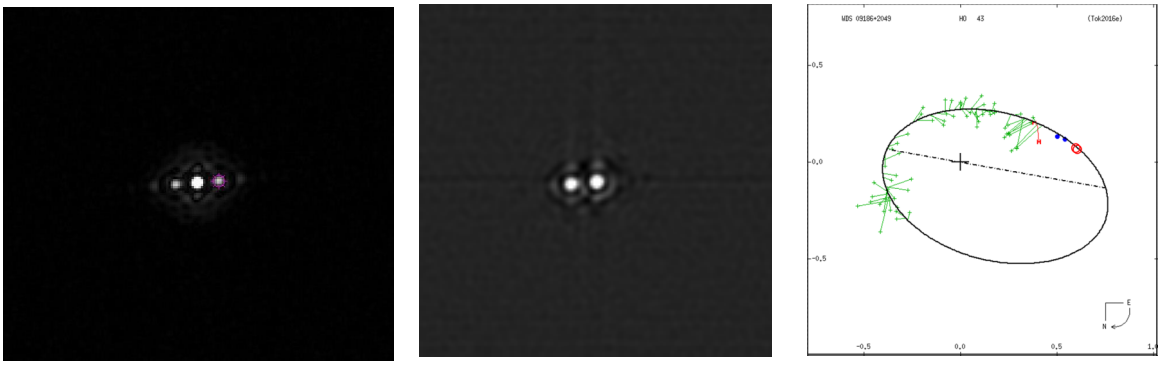

Figure 8. The binary HO43, observed in the R filter. Left: The autocorrelation. Middle: The BSA reconstructed image. Right: The WDS 2016 orbit, with Table 3 results added as red circles.

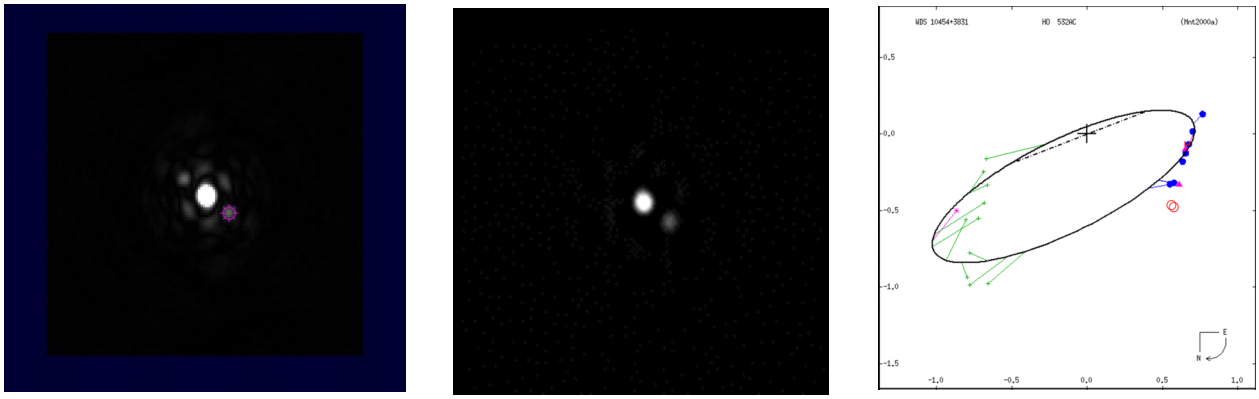

Figure 9. The HO532AC system. The AC and BSA image are at Left and Middle, respectively. Right: Orbit plot from the WDS 6th Orbit Catalog. The new AC and BSA points have been added as red circles. Note that these points (Table 3) were observed at θ ~ 230 deg, but that they are plotted in the opposite quadrant here (θ ~ 50 deg), to be consistent with the earlier plotted speckle points. The conclusion is that all the recent points in the orbit plot are in the wrong quadrant.

been added to the orbit plot, continuing the departure trend from the orbit solution; but note that they have been intentionally plotted in the opposite (N-E) quadrant (θ~50 deg), to appear consistent with the earlier plotted speckle points. The photographic, CCD and Hipparcos points, which don't show up well in the Figure because they happen to be nearly coincident with some speckle points, have also been plotted 180 degrees from their originally reported position angle; but these techniques have no θ ambiguity as AC does.

Figure 10 shows all data plotted with θ as *originally* reported in the WDS Observation Catalog, in a common North-up, East-left orientation. The visual micrometer data are all in the N-W quadrant, as in the orbit plot of Figure 9. However, the true locations of all recent data are 180 degrees from their Figure 9 locations – including the photographic and CCD points. The current AC and BSA points are plotted as given in Table 3, consistent with the bispectrum image.

In Figure 10 all the data fall together nicely, in both time sequence and position, forming a gently-curved

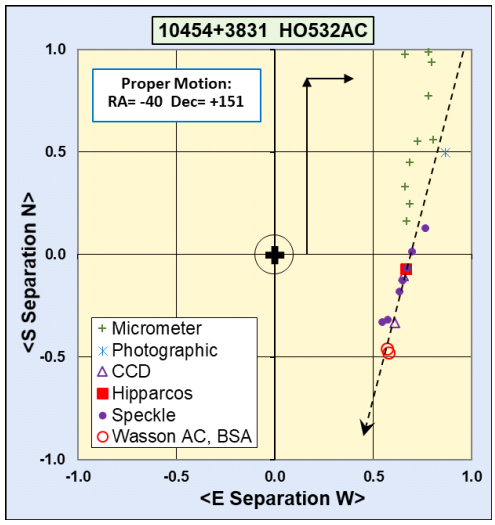

Figure 10. All observations of HO532AC from the WDS Observation Catalog. The solid arrows represent the WDS primary PM components in RA (-40) and Dec (+151), with an arbitrary scale. Their slope (dashed arrow) matches the astrometric points, however, the vectors would be much longer if scaled to the 121-year duration of the observations.

Speckle Interferometry with the OCA Kuhn 22" Telescope - II

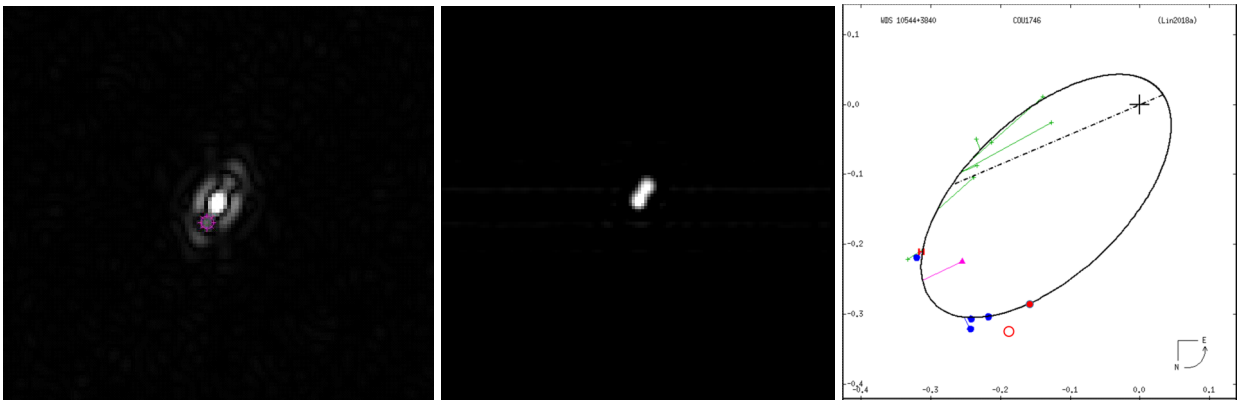

Figure 11. The COU1746 system observed with the IR742 filter. Left: AC. Middle: BSA reconstructed image. Right: WDS orbit plot, updated in 2018 based on three recent speckle points. The points from Table 3 are shown as red circles (AC open, BSA solid).

below the trend. The slope of the proper motion (PM) vectors, as shown in the Figure, happens to match the observations reasonably well. However, PM is given only for the primary star; if the faint star were far in the background, the primary PM would have carried the stars about 18" apart over the 121 years of observations, more than 10 times what has been observed. Therefore, the A and C components are probably traveling together, making HO532AC a true binary. It is recommended that a new orbit solution should be attempted, using the reported values of θ to correct the quadrant problem. However, a new orbit will evidently have a period much longer than 161 years.

10544+3840 COU1746, shown in Figure 11, was observed in the IR742 filter because it has late spectral type K0, is fairly faint, and the ephemerides from a previous orbit solution predicted ρ to be adequately wide (0.47"). However, consistent with the 2018 orbit update, it appears to be much closer (ρ < 0.4"), near or Rayleigh limit for the 844nm effective wavelength. Therefore, the AC has poor quality, and the BSA is not clearly resolved; for these reasons, the centroid peaks were uncertain, and both techniques were assessed as quality code 6 in Table 3. Even though the measurements are near the recently-updated orbit (Figure 11, right), they are not considered reliable.

The binary **11293+3025 L11** is seen in Figure 12. The IR742 IR-pass filter was used because of the large Δmagnitude of 3.13, together with adequately resolved separation. The primary spectral type is F6V (dwarf); therefore, the fainter secondary is probably a G or early K dwarf. As expected, the near IR-pass filter reduced the Dmagnitude somewhat, to 2.77. The Gaia satellite data release DR2 indicates this double is a close neighbor of the Sun, distance 67 parsecs, and the two components have similar PM.

The L11 orbit plot shows only one previous "speckle" data point, taken with the Palomar Observa-

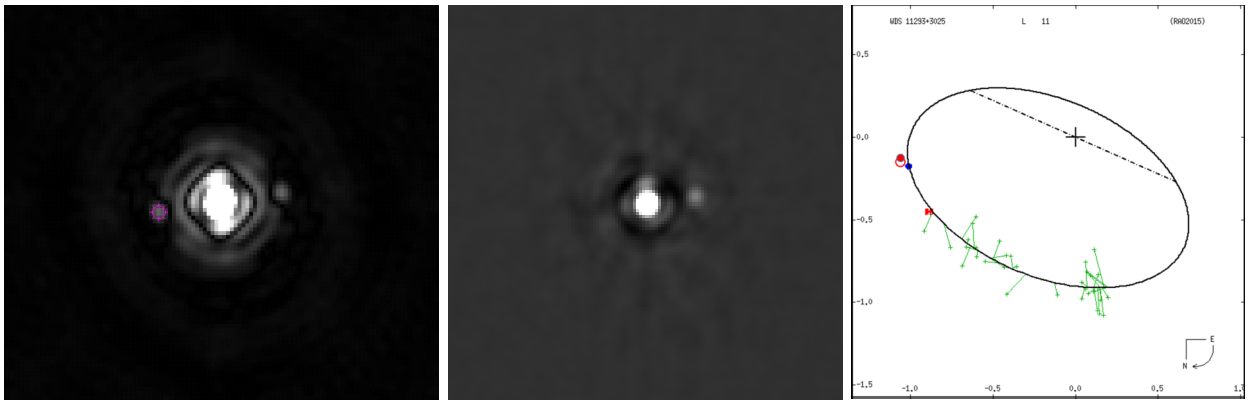

Figure 12. The binary 11293+3025 L11, observed with the IR742 filter. Left: AC, Middle: BSA reconstructed image. Right: WDS orbit plot, having only one previous speckle point. The data from Table 3 are red circles, AC open and BSA solid.

Speckle Interferometry with the OCA Kuhn 22" Telescope - II

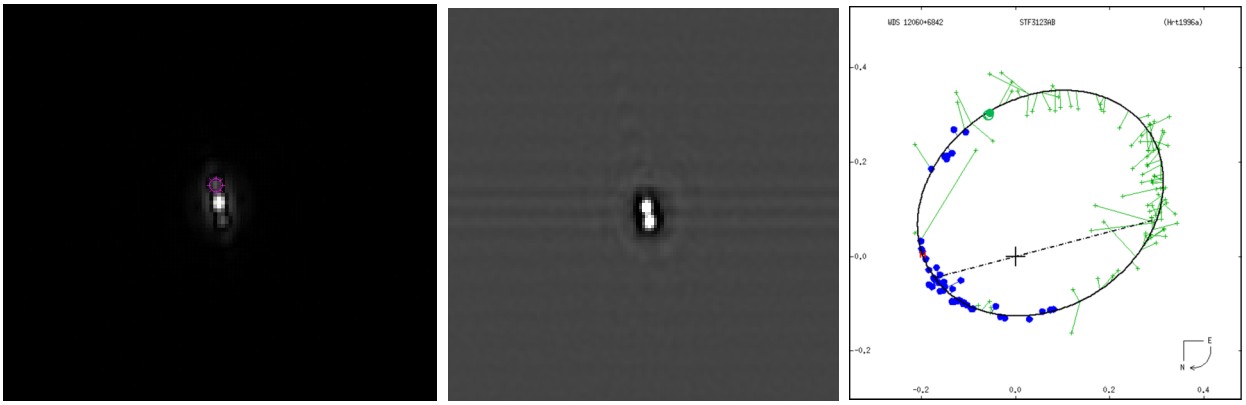

Figure 13. The binary 12060+6842 STF3123AB, observed with the G filter. Left: AC. Middle: BSA reconstructed image, highly stretched but not showing the C component. Right: WDS orbit plot for the AB pair, with data from Table 3 added as green circles, AC open and BSA solid.

tory 60-inch telescope, using the Robo-AO adaptive optics system (Riddle, et al, 2015). The new points from Table 3 are in reasonable agreement with it. This system is obviously in need of more speckle observations.

The **12060+6842 STF3123AB** binary is shown in Figure 13 in the G filter. Separation is close to the Rayleigh criterion (ρ ~ 0.24"), but the AB pair is reasonably well resolved. The BSA image (middle) is highly stretched, showing residual line pattern noise near the image floor, but still not revealing the C component. It is fortunate that the AB pair has had speckle observations throughout the periastron portion of its 122-year orbit.

The C component has only been observed six times before, beginning in 1885 with the Lick 36-inch refractor; the last observation, in 1924, used the 40-inch Yerkes refractor. In attempting to detect this star, which is extremely faint for speckle (WDS magnitude 15.7), the IR807 filter was used; it was assumed that if the C star is at the same distance as the AB pair, it could be a K or M dwarf. 4000 frames were taken with a long exposure (0.150 second), permitted because the seeing is much better at this long wavelength, but nearly saturating the AB stars.

The AC and BSA image results for the IR807 filter are seen in Figure 14. The AB pair is not fully resolved at the longer wavelength, and it is over-exposed when the images are highly stretched to reveal the faint C component. It is likely that C is much redder than the AB pair because it was detected in the near-IR but not in the visible (G) filter; in addition, the WDS Δ magnitude is 8.5 (probably V band), but it is reduced to about 5 in the IR807 filter. Although detection was successful, and it appears to be quite red, it is still not certain whether the C component is gravitationally bound to the AB binary. All observations of the C position are plotted in Figure 14, showing possible slow θ motion over more than 120 years.

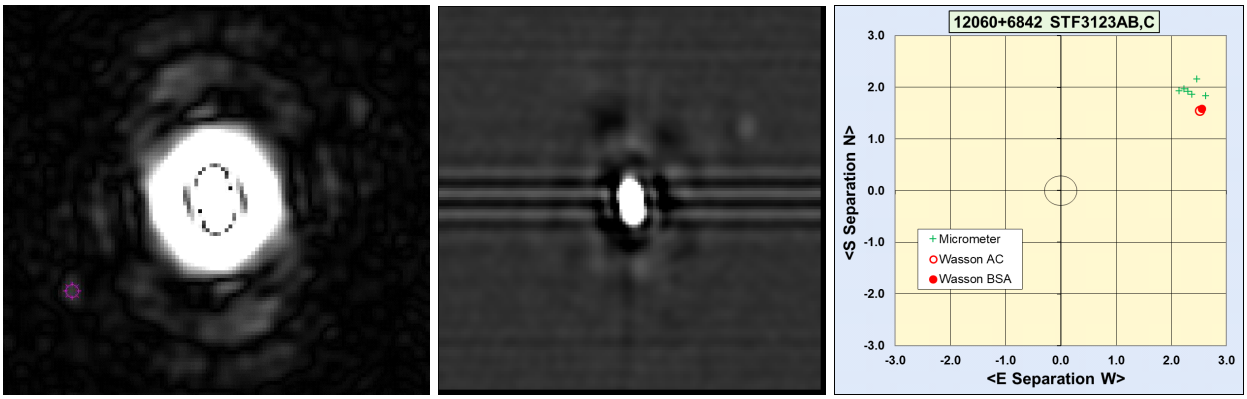

Figure 14. The binary 12060+6842 STF3123AB,C observed with the IR807 filter, and stretched to make the very faint C component visible. Left, AC. Middle: BSA reconstructed image. Right: All data plotted for the C component. The sx prior observations were made with micrometers on the world's two largest refractors.

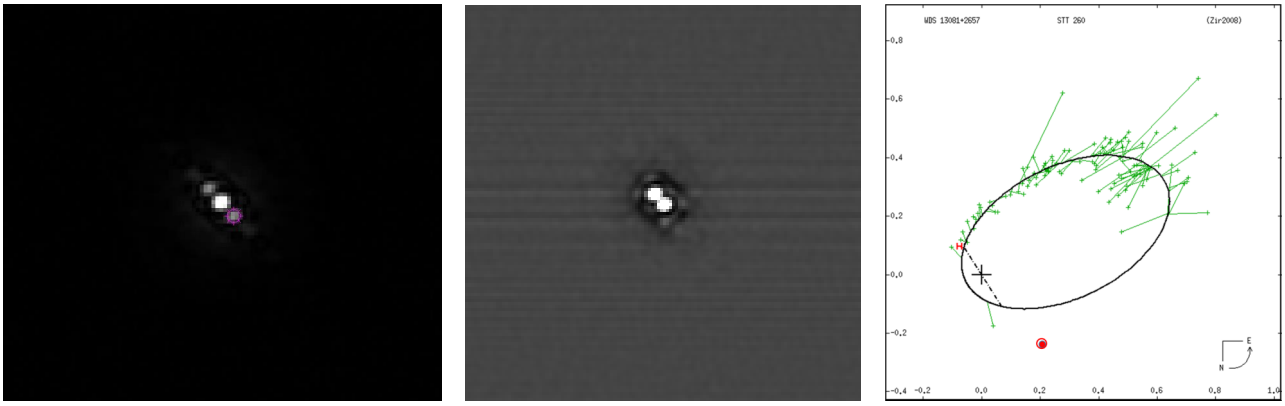

Figure 15. The binary 13081+2657 STT260 observed with the G filter. Left, AC. Middle, BSA reconstructed image. Right: WDS orbit plot with Table 3 speckle points added as red circles, AC (open) and BSA (solid).

The binary **13081+2657 STT260** was observed in the G filter, shown in Figure 15. It is unfortunate that there are no previous speckle observations, and that it was not observed with a large telescope during its recent periastron. The current AC and BSA observations are in good agreement, but they are far from the orbit ephemerides, possibly indicating a much longer period than the current 234-year orbit. Further observations are badly needed.

Acknowledgements

The author thanks Dave Rowe for his excellent Speckle Tool Box software, and particularly for the triple correlation bispectrum "tool," without which this work would not have been possible. In addition, he appreciates Rowe's WDS target-selection software, which simplifies and speeds target and reference star searches. He also thanks Russ Genet for his encouragement, correspondence, instruction and assistance along the speckle journey. The author is grateful to OCA President Barbara Toy for her dedication as custodian of the Kuhn 22-inch Telescope, and to the Orange County Astronomers for support and maintenance of the Anza site facilities. This research has made use of the Washington Double Star Catalog, the 6th Orbit Catalog, and the Observation Catalog, all maintained at the U.S. Naval Observatory, and the author particularly thanks Brian Mason for providing all previous observation data for the requested stars, and for his constructive comments.

This work has made use of data from the European Space Agency (ESA) mission Gaia (https://www.cosmos.esa.int/gaia), processed by the Gaia Data Processing and Analysis Consortium (DPAC, https://www.cosmos.esa.int/web/gaia/dpac/consortium). Funding for the DPAC has been provided by national institutions, in particular the institutions participating in the Gaia Multilateral Agreement.

References

Edelmann, Torsten, 2015. FireCapture2.4. http://firecapture.wonderplanets.de

Harshaw, Richard and Rowe, David and Genet, Russell, 2017. "The Speckle Toolbox: A Powerful Data Reduction Tool for CCD Astrometry." *Journal of Double Star Observations*, **13**, 52-67, January 1, 2017.

Horch, E., Ninkov, Z., van Altena, W. F., Meyer, R. D., Girard, T. M., and Timothy, J. G., 1999. *AJ*, **117**, 548.

Horch, E.P., Robinson, S.E., Ninkov, Z., van Altena, W.F., Meyer, R.D., Urban, S.E., Mason, B.D., 2002. *AJ,* **124**, 2245, 2002.

Losse, Florent, 2015. "REDUC 4.72." http://www.astrosurf.com/hfosaf.

Mante, R., 2000. *IAUDS Information Circulars*, **140**, 1, 2000.

Riddle et al, 2015. Riddle, R.L., Tokovinin, A., Mason, B.D., Hartkopf, W.I., Roberts, L.C., Jr., Baranec, C., Law, N.M., Bui, K., Burse, M.P., Das, H.K., Dekany, R.G., Kulkarni, S. Punnadi, S., Ramaprakash, A.N., & Tendulkar, S.P. *ApJ,* **799**, 4, 2015.

Rowe, David A. and Genet, Russell M., 2015. "User's Guide to PS3 Speckle Interferometry Reduction Program." *Journal of Double Star Observations*, **11**, 266-276.

Rowe, David A., 2016. Yahoo Group speckleinterferometry@yahoo.com.

Rowe, David A., 2017. Private communication.

Rowe, D., Genet, R., Wasson, R., 2019. In preparation for submittal to *JDSO*.

Serot, J., Wasson, R., Rowe, D., Genet, R., 2018. "Bispectrum-based Measurements of Close Large-Differential-Magnitude Visual Double Stars," *Journal of Double Star Observations*, **14-4**, 711-727, October 2018.

Sordiglioni, Gianluca, 2016. http://stelledoppie.goaction.it/index2.php?section=1.

Tokovinin, A., 2016. *ApJ,* **831**, 151, 2016.

Wasson, Rick, 2018. "Speckle Interferometry with the OCA Kuhn 22" Telescope," *Journal of Double Star Observations*, **14-2**, 223-241, April 2018.

Rick Wasson is a retired Aeronautical Engineer, who specialized in airplane aerodynamics throughout his career. He is a native of Southern California and has been an amateur astronomer since the age of 12 - about 6 decades. His astronomical interests include double stars, interferometry, photometry, asteroid occultations, and spectroscopy.

Measurements of 121 New Visual Binary Stars Suggested by the Gaia Data Release 2

J. Sérot

Clermont-Ferrand, France

Abstract: This paper reports the observation and measurement of 121 new potential visual binary stars, with magnitudes and separation ranging from 9.1 to 13.5 and 0.7 to 1.5 arcsec respectively, obtained from a mining of the data provided by the GAIA Data Release 2 in April 2018. Data mining has been carried out by a dedicated software, GDS, briefly described in this paper. Observations and measurements have been carried out between Sep 2018 and Feb 2019 by the author using a 11" reflector telescope, an ASI 290MM CMOS-based camera and bispectrum-based reduction techniques. The measurements are in very good agreement with the astrometric parameters derived from the individual positions reported in the GAIA DR2. Individual proper motions, parallaxes and radial velocities data available from the DR2 show a high probability that the discovered pairs are physical.

1. Introduction

The GAIA satellite [1], launched in late 2013, has completed a large portion of its planned observations. The second of the four planned data releases, DR2, became available to the public in April 2018. Although DR2 is a preliminary release, it contains a great deal of useful information having unprecedented accuracy [2].

In particular, the availability of very high precision astrometric solutions — with uncertainties < 0.7 mas for parallaxes and < 1.2 mas.yr^{-1} for proper motions — for more than 1.3 billion of stars up to magnitude 20 allows for the search of potentially binary systems which could have been overlooked in the existing catalogs of visual binary stars.

This was the motivation for the work described in this paper, which can be viewed as a preliminary assessment of the impact of the GAIA current and future Data Releases on the activity of visual double star observers.

2. DR2 Data Mining: the GDS Software

The work actually started when D. Rowe† wrote some code to download the GAIA DR2 database and search for potential binary stars by looking for pairs of "bright" DR2 sources whose separation — computed from their coordinates — stay under a given threshold.

Two sets of of thresholds were actually used:

- $mag_1 < 15$, $mag_2 < 18$ and 0.5" < separation < 5"
- $mag_1 < 12$, $mag_2 < 17$ and 5" < separation < 10"

The first set extracted 6,312,818 pairs, the second 507,741. The generated catalog, that was called the GDS catalog, therefore contains 6,820,559 potential pairs, for an overall size of approximately 825 MB††.

Each entry in the GDS catalog is a record giving the following information:

- The J2000 Right Ascension of the "primary" star, epoch 2015.5
- The J2000 declination of the "primary" star, epoch 2015.5
- The position angle of the pair calculated from Gaia DR2 coordinates
- The separation of the pair calculated from Gaia DR2 coordinates
- The Gaia G-magnitude of the "primary"
- The Gaia G-magnitude of the "secondary"
- The so-called Gravitationally Bound Index (see below).
- A flag indicating whether none, one or both of the two stars has Gaia 3-band photometry (Gmag, BPmag and RBmag)

† *Rowe is at Planewave Instruments, Rancho Domingez, California*

†† *The complete DR2 database is 1.3 TB.*

- A flag indicating whether a matching pair was found in the WDS catalog
- The color indices of the "primary" and the "secondary"

Of course, not all these entries will correspond to double stars, and there will be double stars that should be in the catalog but are not present. Also note that the minimum separation is 0.5 arcsec so that potential pairs with separation less than this value are not listed in the GDS catalog.

Gravitationally Bound Index

The Gravitationally Bound Index (GBI, GBIndex) is a rough measure of the likelihood that the pair is gravitationally bound†. It is based on the similarity of the proper motions (in RA and Dec), parallaxes and radial velocities, where these data are available. A lower value of GBI means that the pair is more likely to be physical. Although this indicator should be used with caution, since it can produce both false negatives and false positives, when it is less than 2.0 there is a high probability that the pair is gravitationally bound since the two stars have similar location and/or velocity.

The GB index is computed out as follows:

$$GBI = \begin{Bmatrix} MaxV & \text{if there's no available data on proper motions} \\ GBI_{PM} & \text{if data on proper motions is available} \\ GBI_{PLX} & \text{if data on parallaxes is also available} \\ GBI_{RV} & \text{if data on radial velocities is also available} \end{Bmatrix}$$

where

$$GBI_{PM} = \frac{1}{2}\left(\frac{|PMRA_0 - PMRA_1|}{PMRAErr_0 + PMRAErr_1} + \frac{|PMDec_0 - PMDec_1|}{PMDecErr_0 + PMDecErr_1} \right)$$

$$GBI_{PLX} = \frac{1}{3}\left(2GBI_{PM} + \frac{|Parallax_0 - Parallax_1|}{ParallaxErr_0 + ParallaxErr_1} \right)$$

$$GBI_{RV} = \frac{1}{4}\left(3GPI_{PLX} + \frac{|RV_0 - RV_1|}{RVErr_0 + RVErr_1} \right)$$

and

- *MaxV* is a high, arbitrary value
- $PMRA_0$ and $PMRA_1$ are the proper motions in cos(Dec)*RA of the primary star and secondary star, respectively (mas.yr^{-1}).
- $PMDec_0$ and $PMDec_1$ are the proper motions in declination of the primary star and secondary star, respectively (mas/ yr^{-1}).
- $PMRAErr_0$ and $PMRAErr_1$ are the standard errors in proper motion in cos(Dec)*RA of the primary star and secondary star, respectively (mas/ yr^{-1}).
- $PMDecErr_0$ and $PMDecErr_1$ are the standard errors in proper motion in declination of the primary star and secondary star, respectively (mas/ yr^{-1}).
- $Parallax_0$ and $Parallax_1$ are the parallaxes of the primary star and secondary star, respectively (mas).
- $ParallaxErr_0$ and $ParallaxErr_1$ are the standard errors in parallax of the primary star and secondary star, respectively (mas).
- RV_0 and RV_1 are the radial velocities of the primary star and secondary star, respectively (km.sec^{-1}).
- $RVErr_0$ and $RVErr_1$ are the standard errors in radial velocity of the primary star and secondary star, respectively (km/ sec^{-1}).

The GDS Program

The GDS catalog described in the previous section was used, in conjunction with the WDS Catalog [7], by a dedicated application, also written by D. Rowe. A preliminary†† version (1.00) of this application is illustrated in Figure 1. Selection filters used to search the catalog are set in the section marked (1). The resulting list is displayed in section (3), sorted according to the parameter specified in section (2). The first three columns give internal sequential identifiers. The other columns correspond to the catalog data described in Section 2. In particular, a "*" in column WDS indicates that a matching pair has been found in the WDS catalog. It is possible to select entries in the displayed list and save the resulting set as a CSV file for subsequent use, with the controls available in section (4).

Our targets were selected using the following criteria:

- 20h < RA < 0h and 4h < RA < 10h
- 10° < Dec < 55°
- 0.5" < Sep < 1.5"
- 8 < Cmag1 < 11.5
- 8 < Cmag2 < 13.5
- DeltaMag < 4
- GBI < 3

The maximum value for *Dec* results from physical limitations in our observatory (roof of the rolling shed), the minimum value from the ADC full correction range.

†The description of the GBIndex given in this section comes from the preliminary documentation of the GDS software written by D. Rowe. Further details should be given in a forthcoming paper.

††The GDS application will be described more in detail in a separate paper.

Measurements of 121 New Visual Binary Stars Suggested by the Gaia Data Release 2

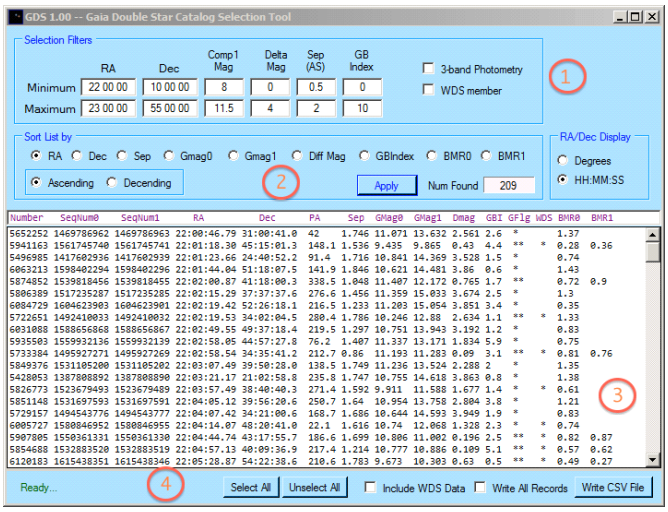

Figure 1 – Snapshot of the GDS 1.0 application

The minimum value for *Sep* results both from the GDS catalog and from our instrumentation (0.4" in theory for an 11" telescope, 0.5" in practice). The maximum value was chosen to target in priority the closest pairs, *i.e.* those for which orbital motion can be detected with the minimal span of time. The magnitude ranges have been derived from our previous experience with the used telescope and camera and the actual seeing conditions when the images where recorded. The value chosen for the GB Index is for maximizing the probability of observing physical pairs.

3. Instrumental Setup and Measurement Protocol

The instrumental setup is the same as that described in [3]. The telescope is a 280 mm Schmidt-Cassegrain reflector (Celestron C11) and the camera an ZWO ASI 290MM. With a 2x Barlow and an Atmospheric Dispersion Corrector (ADC), the resulting plate scale is 0.095 arcsec/pixel. The ADC allows us to use a broadpass L-type filter (400-700 nm), which is of critical importance for imaging faint stars (up to magnitude 13.5 in our case) with exposure times compatible with speckle analysis (typically, less than 80 ms in our average seeing conditions).

Acquisition is carried out with the Genika Astro software [4] with the camera gain setting set at 400. Exposure time for individual images range from 40 to 80 ms typically. For each target one to four sequences of 1000 images are acquired and latter converted to FITS cubes for analysis.

Calibration is carried out using the sideral drift method using the dedicated module of the Speckle-ToolBox software† as described in [5] for example.

Data reduction is performed using bispectrum analysis (BSA), also using SpeckleToolBox software as described in [5]. Although involving a significantly higher computational cost†† than lucky or simple auto-correlation based methods, BSA has the advantage of providing a non-ambiguous PA value and an estimation of the difference in magnitude between the two components.

4. Results

The reported measurements were obtained during 12 nights: six between September 10 and September 25, 2018 and six between February 13 and February 21, 2019.

Table 1 gives the list of the 121 observed stars with the associated data retrieved from the GAIA DR2. Columns 1-19 respectively gives

- the identification of the "primary" star in the UCAC4 catalog‡ [6]
- the identification of the star in the GDS catalog‡‡
- the precise coordinates of the "primary" and "secondary" stars (epoch 2015.5, equinox J2000)
- the G magnitude of the "primary" and "secondary" stars
- the proper motions of the "primary" and "secondary" stars (in mas/yr)
- the parallaxes of the "primary" and "secondary" stars (in mas)
- the radial velocities of the "primary" and "secondary" stars (in km/s)
- the computed *Gravitationally Bound Index* of the pair (as defined in Sec. 2)
- the separation (in arcsec) and position angle (in degree) of the pair, computed from their coordinates.

For the sake of readability, the magnitudes, proper motions, parallaxes and radial velocities are displayed in Table 1 with two decimals only (all computations have been carried out, of course, with the full precision values provided in DR2). When the values are not available the corresponding cell has been left blank.

The measures themselves are listed in Table 2. In

(Text continues on page 296)

†*Also developed by D. Rowe.*

†† *Which is not a real problem since most of the processing can be carried out in batch mode, without user intervention.*

‡ *We did not have access to the DR2 catalog on the computer controling the mount of the telescope, only to the UCAC4 catalog. We therefore made a previous search using the SkyChart software to correlate the coordinates given in the former to a star listed in the latter.*

‡‡ *This is the number reported in the first column in Fig. 1.*

Measurements of 121 New Visual Binary Stars Suggested by the Gaia Data Release 2

Table 1. Observed Stars

UCAC4	GDS	RA0	Dec10	RA1	Dec11	Gmag0	Gmag1	PMRA0	PMDec0	PMRA1	PMDec1	Plx0	Plx1	RV0	RV1	GBI	PA	Sep
501-037577	5154834	07:03:59.52	10:10:43.4	07:03:59.58	10:10:42.2	10.07	12.24	-4.97	-4.54	-6.37	-5.44	2.27	1.66	41.89		1.24	144	1.438
502-032372	5159755	06:52:51.28	10:19:29.1	06:52:51.35	10:19:29.1	10.90	10.95	-9.31	-5.74	-9.08	-5.89	1.70	1.75			0.38	91.17	1.114
504-047820	5167352	08:30:49.08	10:36:10.7	08:30:49.02	10:36:11.8	9.82	12.23	-44.37	3.67	-47.05	3.35	4.16	3.44	20.41		1.37	325.23	1.4
508-137021	5190019	20:30:53.79	11:26:10.2	20:30:53.82	11:26:09.6	10.02	10.54	21.77	17.84	20.50	12.06	4.61	6.83	-26.63		2.71	140.11	0.882
510-014543	5198704	05:45:09.11	11:50:30.6	05:45:09.19	11:50:31.1	11.37	12.61	3.04	-13.30	4.88	-14.98	1.55	0.95	-10.26		2.85	68.1	1.236
513-028065	5218233	06:36:54.11	12:27:57.0	06:36:54.16	12:27:58.0	10.78	11.81	-9.15	-41.42	-10.14	-41.49	5.41	5.16	-13.84		1.05	38.44	1.219
520-047616	5254941	08:33:27.27	13:48:18.1	08:33:27.24	13:48:17.4	11.28	11.99	218.52	-127.27	218.10	-123.56	14.88	15.73			2.08	211.39	0.838
520-048249	5254943	08:46:04.61	13:51:10.7	08:46:04.56	13:51:10.0	11.45	12.29	-7.16	-36.98	-5.32	-37.33	2.90	3.87			1.39	229.43	1.031
522-029027	5267398	06:39:41.32	14:19:20.7	06:39:41.25	14:19:20.2	10.42	12.55	-0.27	-2.05	1.58	-3.38	1.02	1.87			2.34	241.52	1.24
522-136397	5267041	21:13:00.77	14:12:09.2	21:13:00.87	14:12:09.7	9.12	11.01	5.40	-12.88	5.12	-12.40	2.41	2.71			1.61	71.31	1.507
525-043014	5280034	07:30:41.86	14:48:08.8	07:30:41.84	14:48:07.4	10.47	13.26	-1.20	-29.13	1.70	-33.31	3.36	3.33			2.94	195.18	1.388
528-039250	5294426	07:10:11.26	15:26:36.0	07:10:11.21	15:26:35.1	11.37	12.91	-1.89	10.62	-1.40	9.02	2.49	2.34	62.80		1.61	222.34	1.209
528-146334	5296346	21:21:49.41	15:24:19.4	21:21:49.48	15:24:19.2	11.26	12.26	5.70	0.07	8.05	3.29	1.02		-27.70		1.89	104.63	1.063
529-039966	5301950	07:21:21.06	15:44:47.6	07:21:21.08	15:44:46.6	11.35	11.51	-23.30	-7.92	-18.65	-11.32	2.65	2.66		35.00	2.15	163.76	1.091
530-034689	5304482	06:51:52.67	15:51:53.2	06:51:52.74	15:51:53.5	11.27	12.50	0.24	-4.64	-0.11	-4.72	0.67				0.63	72.49	1.127
531-012456	5309205	05:14:54.55	16:05:11.8	05:14:54.62	16:05:11.0	9.82	12.42	5.58	-5.00	1.18	-8.90	2.41	2.64			2.05	128.99	1.35
531-038132	5309542	07:09:50.19	16:02:33.9	07:09:50.27	16:02:34.3	10.86	12.60	7.54	-8.72	9.24	-9.36	2.04	3.20		-0.76	1.46	72.13	1.257
532-043579	5316942	07:54:33.98	16:20:08.8	07:54:34.07	16:20:08.8	11.40	12.38	-3.14	-5.98	-1.37	-7.65	2.74	2.28	-8.75		0.84	91.87	1.28
533-048175	5321819	08:51:26.72	16:32:47.4	08:51:26.70	16:32:46.0	10.78	12.33	-1.60	-9.43	-0.56	-9.63	3.25	3.35	3.69		2.27	188.2	1.363
536-045446	5336249	07:58:06.67	17:10:53.6	07:58:06.64	17:10:52.6	11.25	12.67	1.88	-4.79	-0.68	-2.41	1.30		8.55		1.75	202.97	0.998
540-041788	5355169	07:29:08.38	17:58:24.2	07:29:08.43	17:58:25.5	11.13	12.33	1.78	-13.01	0.80	-11.94	2.08	2.30	2.47		2.12	28.04	1.459
543-039864	5370209	07:10:32.37	18:33:30.3	07:10:32.28	18:33:30.4	11.36	13.23	-0.65	-2.43	0.32	-3.54	1.33	1.35	2.37		2.48	274.87	1.316
544-023390	5374928	06:12:10.56	18:45:03.9	06:12:10.63	18:45:05.0	10.78	11.94	-0.14	-5.20	-0.36	-4.83	1.10	0.74			0.76	39.98	1.355
545-105404	5381262	19:48:05.16	18:55:25.3	19:48:05.23	18:55:25.5	11.47	11.78	-0.04	-7.68	-1.93	-9.01	3.17	2.26		30.03	0.75	81.7	0.893
546-117797	5386333	20:06:28.00	19:08:00.2	20:06:27.94	19:08:00.4	11.45	11.61	-5.89	-9.80	-7.38	-11.07		4.26		11.43	1.97	277.15	0.954
549-009553	5398198	04:25:32.47	19:45:59.5	04:25:32.44	19:46:00.9	9.26	12.56	68.59	83.60	71.44	84.50	9.36	9.48	49.36		2.79	343.3	1.475
550-037553	5400803	07:06:30.30	19:49:53.0	07:06:30.40	19:49:53.1	11.27	12.47	18.90	-17.52	18.34	-15.19	3.99	3.93	-49.49	-50.99	1.04	87.82	1.422
553-018908	5413773	05:47:23.53	20:24:48.8	05:47:23.56	20:24:50.2	11.33	12.01	-1.55	-3.45	-1.42	-3.51	0.96	0.93			0.39	20.82	1.43
554-037934	5418022	07:24:42.71	20:36:08.3	07:24:42.76	20:36:07.4	11.04	11.74	0.82	-11.77	0.44	-13.19	1.52	3.82			1.23	145.06	1.099
554-041847	5418050	08:13:46.46	20:40:56.0	08:13:46.36	20:40:55.7	11.42	12.30	-22.61	15.55	-22.30	14.32	2.97	3.34	17.95		1.58	260.11	1.463
554-043925	5418070	08:56:18.94	20:41:40.0	08:56:18.99	20:41:39.2	11.50	11.58	4.28	-4.72	2.11	-5.71	3.47	2.61		40.25	2.21	136.25	1.147
555-023110	5422091	06:04:19.78	20:53:41.6	06:04:19.87	20:53:41.7	11.40	12.07	-2.11	-3.99	-1.28	-4.97	1.34	2.05			0.9	81.26	1.164
558-046251	5434767	08:28:19.69	21:29:45.4	08:28:19.76	21:29:45.4	11.46	11.88	-13.11	-31.75	-13.01	-32.56	4.07	4.19			1.82	47.25	1.345
559-025453	5440547	06:16:25.95	21:45:38.3	06:16:25.90	21:45:39.3	11.23	11.35	-9.09	-10.87	-6.94	-10.11			8.10		1.69	326.97	1.208
560-043758	5444618	07:49:09.64	21:57:11.6	07:49:09.59	21:57:10.8	11.26	12.48	-1.04	-5.37	0.94	-6.86	1.60	1.33			1.64	225.8	1.081
560-109791	5445609	20:06:20.28	21:59:30.7	20:06:20.25	21:59:29.4	11.10	11.46	16.02	-4.78	15.12	-4.87	3	2.75			1.59	197.92	1.378
563-110395	5456849	20:15:55.47	22:32:10.3	20:15:55.47	22:32:11.1	11.18	11.81	-5.90	-18.53	-15.01	-19.47	2.74				2.73	0.52	0.869
563-118326	5455149	20:35:29.00	22:24:42.9	20:35:28.91	22:24:42.4	11.13	12.35	12.05	8.16	13.65	7.19	3.57	3.47	-14.28		1.78	246.95	1.228
565-034117	5461201	06:55:09.65	22:48:27.0	06:55:09.74	22:48:27.7	10.46	12.24	-89.43	-43.17	-87.11	-48.82	5.34	4.99			2.8	56.62	1.354
566-022985	5466876	06:07:47.75	23:11:59.5	06:07:47.81	23:11:58.7	11.20	12.73	-5.33	-6.50	-3.00	-4.98	3.50	0.37			2.53	128.33	1.188
566-130865	5468496	23:18:45.36	23:08:37.8	23:18:45.37	23:08:38.5	11.36	11.48	-6.00	-15.43	-1.49	-14.27	3.5	1.06			1.32	13.44	0.734
569-019923	5478281	05:48:29.03	23:42:14.8	05:48:29.12	23:42:15.5	10.75	13.32	3.35	-10.93	-0.06	-9.14	2.90	2.97			2.71	62.85	1.484
572-024874	5487735	06:09:14.16	24:14:38.3	06:09:14.19	24:14:39.3	11.23	11.37	2.49	-3.94	2.43	-2.90	0.80	1.63			0.89	22.06	1.078
572-024930	5489562	06:09:20.56	24:23:35.8	06:09:20.65	24:23:35.6	11.39	12.43	2.60	-2.72	6.01	-11.30	1.26	0.94			2.89	100.55	1.222
572-025528	5489579	06:10:58.13	24:20:16.3	06:10:58.15	24:20:17.6	10.83	11.36	9.29	-1.38	10.40	-1.41	2.38	2.58			2.23	13.04	1.243
578-023649	5511272	06:05:44.51	25:28:59.6	06:05:44.45	25:29:00.4	11.36	12.17	-0.21	-1.48	3.08	1.46	2.30				2.69	315.06	1.124
578-023649	5511272	06:05:44.51	25:28:59.6	06:05:44.45	25:29:00.4	11.36	12.17	-0.21	-1.48	3.08	1.46	2.30				2.69	315.06	1.124

Table 1 continues on the next page.

Measurements of 121 New Visual Binary Stars Suggested by the Gaia Data Release 2

Table 1 (continued). Observed Stars

UCAC4	GDS	RA0	Decl0	RA1	Decl1	Gmag0	Gmag1	PMRA0	PMDec0	PMRA1	PMDec1	Plx0	Plx1	RV0	RV1	GBI	PA	Sep
579-098024	5516342	20:22:00.85	25:36:09.2	20:22:00.78	25:36:08.3	9.20	12.94	-5.13	-6.06	-3.94	-8.30	0.81	1.56			1.82	223.88	1.295
581-043221	5522841	08:58:22.20	26:01:47.4	08:58:22.27	26:01:48.2	11.41	12.05	-43.71	5.82	-42.07	4.40	3.35	3.44	-5.19		2.79	47.94	1.228
581-043221	5522841	08:58:22.20	26:01:47.4	08:58:22.27	26:01:48.2	11.41	12.05	-43.71	5.82	-42.07	4.40	3.35	3.44	-5.19		2.79	47.94	1.228
581-104282	5524095	20:23:04.73	26:05:32.2	20:23:04.82	26:05:32.5	9.70	13.03	1.29	2.76	-0.39	-3.66	1.76	1.69			1.68	76.81	1.234
581-115336	5526328	20:58:16.99	26:09:10.2	20:58:16.93	26:09:11.1	11.47	12.75	-3.47	3.77	-2.96	3.47	1.84	2.12		-19.42	0.77	314.28	1.231
583-011127	5532698	04:12:29.94	26:34:18.6	04:12:30.01	26:34:19.6	11.29	13.21	72.86	-120.04	68.35	-119.99	6.63	6.79	-56.20		2.83	43.04	1.445
583-040010	5532990	07:40:20.81	26:32:16.0	07:40:20.82	26:32:17.1	11.41	12.21	-11.98	2.01	-12.39	0.46	2.46	5.86	1.23	-0.30	2.34	4.67	1.156
584-040353	5535022	07:51:21.47	26:36:58.6	07:51:21.46	26:37:00.0	10.88	13.12	-0.11	-105.83	-0.17	-105.20	7.34	7.21	-5.76		1.82	350.87	1.365
584-076038	5535451	19:14:22.46	26:37:47.2	19:14:22.41	26:37:47.6	11.40	12.15	0.39	-16.76	2.01	-8.77	2.37	8.57	-12.30		2.74	296.97	0.785
584-110924	5536496	20:44:54.37	26:39:45.7	20:44:54.31	26:39:45.4	11.37	11.45	17.21	7.90	22.45	-1.13	8.6	8.92	2.19		1.68	250.85	0.772
592-043498	5573658	08:22:11.88	28:21:47.0	08:22:11.78	28:21:47.1	11.26	12.93	-26.27	-11.61	-27.27	-10.75	3.04	2.64	29.79		2.03	272.49	1.324
598-132616	5611324	21:47:20.55	29:32:04.9	21:47:20.52	29:32:03.1	10.95	12.57	5.60	6.94	5.67	6.45	1.67	1.71			0.55	192.8	1.838
603-114143	5636572	20:30:02.20	30:28:49.6	20:30:02.15	30:28:48.6	11.05	12.98	3.16	0.19	2.69	0.04	1.52	1.4			1.54	216.54	1.273
610-033903	5671783	06:33:58.70	31:54:57.4	06:33:58.65	31:54:58.4	10.71	11.74	6.50	-20.18	5.59	-20.82	2.70	2.60			1	325.86	1.17
610-043660	5671862	08:23:46.80	31:59:20.0	08:23:46.82	31:59:21.3	11.26	13.42	-5.10	-8.29	-4.45	-8.72	0.83	0.89	51.76		2.4	11.98	1.277
610-117005	5673506	21:00:57.90	31:55:42.4	21:00:57.98	31:55:41.4	9.92	12.57	-3.64	-8.91	-4.04	-10.38	1.97	2.7			1.15	135.74	1.495
610-129295	5671379	22:07:27.74	31:53:05.2	22:07:27.74	31:53:06.5	11.25	12.46	-1.60	-9.00	3.98	-4.67	2.53	3.63	13.08	10.33	2.62	0.31	1.319
617-039371	5701231	07:05:19.75	33:14:43.0	07:05:19.82	33:14:43.7	11.49	11.79	-16.39	-3.13	-16.61	-6.51	6.74	6.14			1.13	49.87	1.089
622-024222	5725149	05:31:40.23	34:14:26.1	05:31:40.32	34:14:26.8	11.23	12.98	1.49	-4.18	-2.45	-1.80	0.35	0.32			2.7	57.03	1.227
624-038643	5735987	07:25:07.00	34:46:26.2	07:25:06.97	34:46:25.1	11.19	11.64	8.80	-15.88	8.07	-15.74	3.36	3.22		5.35	1.51	195.62	1.201
624-118752	5735500	21:49:35.84	34:39:25.8	21:49:35.73	34:39:26.1	9.92	12.33	-13.92	-25.99	-13.54	-27.86	1.86	1.85	-22.20		1.86	282.65	1.394
626-034798	5742103	06:30:22.01	35:00:30.9	06:30:21.94	35:00:32.0	11.42	12.76	-15.68	-20.25	-17.34	-21.21	1.95				2.83	320.56	1.434
627-037471	5748409	06:58:08.98	35:23:28.3	06:58:09.08	35:23:28.1	11.33	11.92	-0.68	-0.89	-0.29	-3.16	1.38	4.64			2.3	99.59	1.208
628-021808	5752586	05:10:19.56	35:31:47.6	05:10:19.56	35:31:49.1	11.16	13.21	-0.41	-4.47	0.67	-4.81	0.79	0.53			2.86	359.01	1.441
628-033482	5750539	06:25:04.98	35:27:57.2	06:25:05.01	35:27:58.6	11.31	13.50	-0.85	-5.44	-0.71	-5.05	1.02	1.28			2.18	15.13	1.425
632-095200	5772481	20:12:13.88	36:20:50.4	20:12:13.97	36:20:50.0	11.41	12.69	0.08	-1.84	-0.29	-0.80	1.07	0.36			1.73	107.47	1.168
633-030637	5773527	05:58:54.88	36:28:03.7	05:58:54.81	36:28:03.1	11.30	11.31	-19.71	1.52	-14.92	3.70	12.97	15.46			1.71	233.41	0.99
634-098847	5785754	20:46:46.23	36:47:44.3	20:46:46.17	36:47:43.7	11.35	12.00	-6.00	-2.05	-3.99	-1.85	1.17				1.07	231.24	0.925
635-130935	5788610	23:54:41.03	36:52:40.6	23:54:41.04	36:52:41.6	11.36	13.09	-4.51	-3.28	-4.87	-3.68	1.34	1.28			0.42	8.69	0.97
636-027723	5791179	05:37:27.77	37:05:11.7	05:37:27.84	37:05:12.7	11.03	12.92	12.69	-13.03	14.29	-14.07	2.06	1.81	-14.47		1.41	40.4	1.274
637-043218	5798225	08:25:04.21	37:22:34.2	08:25:04.25	37:22:33.1	10.45	11.47	-4.98	5.70	-10.34	2.64	2.44	1.36			2.61	153.63	1.222
639-039377	5804825	07:22:15.12	37:38:03.6	07:22:15.20	37:38:04.3	11.29	12.55	-14.00	-43.85	-16.53	-43.79	3.36	2.84			1.2	55.06	1.204
641-026536	5815036	05:26:41.20	38:10:24.7	05:26:41.16	38:10:23.8	11.40	11.60	-0.41	-0.31	0.24	-1.65	0.51	0.14	-29.84		1.32	203.69	1
643-126683	5824811	23:54:43.62	38:33:43.3	23:54:43.60	38:33:43.9	11.42	13.07	-7.80	-2.39	-9.15	-4.15	2.4	3.27	1.51		1.82	340.09	0.691
646-022868	5835035	04:56:28.91	39:06:58.9	04:56:28.93	39:07:00.2	10.64	13.30	1.87	-4.00	4.12	-4.48	1.24	1.07	18.54		2.95	8.15	1.371
647-110853	5840261	22:35:55.67	39:19:09.2	22:35:55.67	39:19:08.8	10.23	12.58	-3.83	-10.53	-3.95	-11.28	1.81	1.58	-23.41		1.2	110.07	1.233
650-078863	5850432	19:52:21.48	39:59:16.3	19:52:21.41	39:59:15.9	11.13	11.56	-2.79	16.63	0.59	13.14	3.86	3.56			1.42	238.03	0.864
650-086057	5848946	20:07:55.14	39:48:33.3	20:07:55.08	39:48:33.8	11.28	11.39	-0.44	-3.06	1.10	1.33	1.74	3.1		0.16	0.97	306.85	0.887
652-091009	5856055	20:30:33.13	40:14:47.7	20:30:33.19	40:14:48.7	11.36	12.32	-2.61	0.57	1.66	1.99	1.54	1.86	5.37	11.79	1.13	34.49	1.188
653-051856	5858785	09:20:03.40	40:29:56.0	09:20:03.34	40:29:54.9	11.30	11.96	-4.84	2.00	-4.63	1.83	2.79	2.68	-12.84	-10.45	1.13	209.14	1.261
654-049141	5862330	08:10:42.03	40:41:41.5	08:10:42.10	40:41:42.6	10.60	13.16	-25.37	-13.90	-24.51	-15.69	3.15	3.17	63.57		1.26	36.16	1.315
657-103242	5874852	22:02:00.87	41:18:00.3	22:02:00.84	41:18:01.3	11.41	12.17	-14.05	-13.07	-10.15	-16.74	1.88		-10.61	-11.10	1.74	338.54	1.048
659-112855	5881290	23:27:43.35	41:46:18.8	23:27:43.33	41:46:17.9	11.44	13.15	9.59	3.14	9.80	3.53	2.45	2.52	-12.20		0.97	192.71	0.99
661-116828	5887522	23:29:20.50	42:11:17.8	23:29:20.58	42:11:17.5	11.34	11.82	7.68	-5.08	9.98	-9.94	3.9				3.18	111.66	0.953
663-024366	5892398	04:22:37.43	42:32:09.9	04:22:37.52	42:32:10.7	11.20	12.06	30.01	-23.62	27.30	-22.03	2.78	2.84			2.13	52.63	1.254
665-095928	5899734	21:11:50.92	42:59:18.1	21:11:50.82	42:59:18.1	11.45	11.88	-4.00	-9.34	-4.41	-10.65	1.18	0.48			1.01	271.12	1.038
666-044431	5902252	06:07:46.78	43:09:37.3	06:07:46.79	43:09:36.3	11.49	11.71	0.27	-19.71	-0.19	-19.85	2.67	1.91	22.34		1.29	174.33	1.02
667-106319	5907811	22:06:24.32	43:14:58.1	22:06:24.41	43:14:58.0	11.31	13.29	-4.05	2.12	-3.97	2.13	3.42	3.19	-42.51		0.31	93.72	0.955

Table 1 concludes on the next page.

Measurements of 121 New Visual Binary Stars Suggested by the Gaia Data Release 2

Table 1 (continued). Observed Stars

UCAC4	GDS	RA0	Decl0	RA1	Decl1	Gmag0	Gmag1	PMRA0	PMDec0	PMRA1	PMDec1	Plx0	Plx1	RV0	RV1	GBI	PA	Sep
668-086512	5912009	20:07:56.47	43:30:17.1	20:07:56.50	43:30:16.0	11.14	12.76	6.58	2.61	6.54	2.88	1.79	1.54			0.89	163.7	1.163
669-028818	5914553	04:43:36.70	43:43:50.2	04:43:36.70	43:43:51.4	10.98	12.62	2.67	-1.94	2.94	-1.39	2.83	2.66	-47.21		1.64	359.42	1.232
669-036212	5914672	05:18:28.90	43:46:30.5	05:18:28.79	43:46:29.8	10.64	12.72	-4.81	-3.55	-6.64	-2.09	1.55				2.66	239.36	1.4
669-052025	5914848	08:02:34.36	43:42:29.4	08:02:34.43	43:42:28.8	11.33	11.66	-1.30	3.61	3.82	-4.58	3.53	2.58	-3.79	-7.24	1.93	127.36	0.991
672-050081	5922759	07:37:41.55	44:17:20.0	07:37:41.57	44:17:18.8	10.42	11.50	-3.77	-18.78	-4.25	-17.91	2.65	1.12			2.36	166.62	1.22
673-115114	5928553	22:29:09.26	44:30:55.0	22:29:09.32	44:30:55.8	11.14	12.90	0.24	-3.64	0.00	-3.36	1.27	1.43	-1.32	2.38	0.68	38.55	1.086
675-042663	5932549	05:57:04.30	44:52:44.4	05:57:04.40	44:52:45.3	10.82	12.94	8.00	-17.54	6.65	-16.74	2.48	2.50	2.58		1.75	49.17	1.498
678-033045	5945648	05:00:53.96	45:31:42.6	05:00:53.91	45:31:41.6	11.19	11.31	28.48	-28.74	26.80	-31.30	6.15	5.84			2.19	208.42	1.123
679-034536	5949722	05:13:35.38	45:43:49.4	05:13:35.52	45:43:49.7	11.44	12.30	10.04	15.65	10.70	14.00	3.08	2.66	-26.83	-25.99	2.67	75.27	1.447
680-085239	5954567	20:35:57.26	45:55:25.9	20:35:57.21	45:55:27.1	11.38	11.99	-16.87	-17.81	-16.94	-16.36	2.27	1.94	13.44		1.18	337.38	1.272
681-079773	5956497	20:16:04.62	46:04:38.2	20:16:04.53	46:04:39.2	11.23	12.87	0.28	13.84	1.55	13.74	3.02	2.92	-23.28		1.09	316.99	1.384
686-028195	5977782	04:09:36.30	47:01:27.1	04:09:36.20	47:01:27.9	11.24	12.29	1.56	-8.95	2.83	-6.60	1.26	1.08	0.25		2.75	309.1	1.36
686-028794	5977788	04:14:12.66	47:04:00.2	04:14:12.66	47:03:58.9	11.31	13.36	0.81	-1.97	0.84	-1.81	0.43	0.71			1.15	180.99	1.249
688-081285	5989362	20:24:36.10	47:31:41.7	20:24:36.20	47:31:42.2	11.27	12.95	-15.07	-19.65	-16.37	-20.48	2.15	2.36			1.74	64.81	1.07
688-107997	5990014	21:54:41.77	47:30:03.9	21:54:41.65	47:30:03.0	10.48	12.35	10.86	-1.53	10.83	-1.57	2.72	2.78			0.32	236.37	1.506
693-050538	6006656	09:24:32.16	48:26:37.3	09:24:32.07	48:26:36.3	10.66	12.88	5.55	-5.02	6.37	-4.25	4.04	4.09	-8.75		2.23	221.13	1.297
693-113124	6009644	22:17:24.52	48:32:01.0	22:17:24.41	48:32:01.1	11.48	12.29	-7.81	-5.88	-5.89	-5.61	1.51	1.77	-0.29		2.25	271.68	1.145
694-088583	6012986	21:11:53.50	48:44:47.4	21:11:53.62	48:44:46.8	10.83	12.34	1.46	-4.76	2.15	-5.75	3.11	3.15	13.21		0.93	114.24	1.283
697-080825	6024539	20:43:24.91	49:23:21.3	20:43:24.98	49:23:21.7	11.06	11.45	-1.06	-0.13	1.58	-1.97					0.56	63.39	0.826
700-051491	6033972	09:26:52.08	49:53:11.3	09:26:52.07	49:53:12.4	11.09	11.30	-29.53	1.31	-28.08	4.46	2.87	6.19			1.47	358.03	1.067
703-048330	6047347	08:30:09.01	50:33:38.8	08:30:08.96	50:33:37.7	11.36	11.62	-29.23	-12.93	-29.47	-12.89	3.69	3.40	24.99		1.13	203.45	1.212
705-087810	6055524	21:37:52.39	50:56:16.1	21:37:52.35	50:56:15.2	11.47	11.56	0.35	2.35	6.05	-4.16	3.52	2.33			3.38	206.78	0.953
709-045021	6068142	07:04:37.44	51:40:35.8	07:04:37.38	51:40:37.0	9.77	12.45	-11.33	-16.01	-12.48	-17.11	4.21	4.63	-65.43		1.46	332.17	1.324
710-082633	6072602	21:19:53.63	51:49:47.1	21:19:53.75	51:49:47.9	11.38	12.71	4.58	1.04	4.38	1.02	1.57	1.81			1.19	53.49	1.396
714-033708	6089781	04:40:33.94	52:45:45.6	04:40:34.04	52:45:45.1	11.24	12.24	1.93	-13.99	11.31	-6.45	3.43	1.27			2.62	119.61	0.995
716-048820	6097532	09:24:06.56	53:06:56.1	09:24:06.64	53:06:57.3	11.37	12.63	-0.07	-0.86	-0.34	-0.55	2.34	2.61			1.73	29.63	1.429

Measurements of 121 New Visual Binary Stars Suggested by the Gaia Data Release 2

Table 2. Measurements

UCAC4	DATE	N	PA	SEP	DM	δPA	δSEP
501-037577	2019.133	1	143.9	1.446	2.7	0.11	-0.008
502-032372	2019.122	1	90.7	1.115		0.45	-0.001
504-047820	2019.119	1	326	1.427		-0.77	-0.027
508-137021	2018.694	3	140.2 (0.1)	0.881 (0.003)	0.8 (0.02)	0.06	-0.001
510-014543	2019.119	1	66.9	1.273		1.23	-0.037
513-028065	2019.122	1	38.4	1.228		0.04	-0.009
520-047616	2019.128	1	210	0.884		1.35	-0.046
520-048249	2019.133	1	230.1	1.048		-0.66	-0.017
522-029027	2019.122	1	242.1	1.253	2.5	-0.6	-0.013
522-136397	2018.692	4	70.9 (0.1)	1.509 (0.005)	2.2 (0.05)	-0.39	0.002
525-043014	2019.139	1	195.5	1.451		-0.28	-0.063
528-039250	2019.139	1	219.6	1.28		2.79	-0.071
528-146334	2018.719	3	104.7 (1.4)	1.064 (0.016)		0.12	0.001
529-039966	2019.119	1	163.2	1.091		0.54	0
530-034689	2019.133	1	72.4	1.142	1.5	0.13	-0.015
531-012456	2019.122	1	129	1.378	3	-0.05	-0.028
531-038132	2019.139	1	73.2	1.278	2.2	-1.04	-0.021
532-043579	2019.117	1	91.6	1.27		0.29	0.01
533-048175	2019.128	1	188.3	1.372		-0.1	-0.009
536-045446	2019.117	1	203	0.995		0	0.003
540-041788	2019.139	1	29	1.478		-0.97	-0.019
543-039864	2019.139	1	276.2	1.416		-1.36	-0.1
544-023390	2019.133	1	39.7	1.394		0.25	-0.039
545-105404	2018.694	4	78 (1.2)	0.866 (0.017)		-3.67	-0.027
546-117797	2018.692	4	276.3 (0.2)	0.959 (0.006)		-0.87	0.005
549-009553	2019.128	1	343.8	1.477	4	-0.45	-0.002
550-037553	2019.139	1	87.7	1.447		0.13	-0.025
553-018908	2019.122	1	21	1.453		-0.17	-0.023
554-037934	2019.119	1	145.1	1.073		0.01	0.026
554-041847	2019.119	1	258.9	1.498		1.24	-0.035
554-043925	2019.122	1	136.1	1.158		0.12	-0.011
555-023110	2019.122	1	80.3	1.157		1.01	0.007
558-046251	2019.122	1	46.5	1.354		0.79	-0.009
559-025453	2019.133	1	327.3	1.22		-0.31	-0.012
560-043758	2019.117	1	226.6	1.082		-0.8	-0.001
560-109791	2018.719	3	197.8 (0)	1.392 (0.014)		-0.15	0.014
563-110395	2018.694	4	1.5 (0.5)	0.878 (0.009)		1.02	0.009
563-118326	2018.733	3	246.3 (0.6)	1.206 (0.001)		-0.61	-0.022
565-034117	2019.119	1	56.6	1.38	2.3	0.07	-0.026
566-022985	2019.122	1	126.8	1.207		1.53	-0.019
566-130865	2018.717	3	14 (0.2)	0.753 (0.008)		0.51	0.019
569-019923	2019.128	1	61.1	1.469	3.5	1.74	0.015
572-024874	2019.122	1	22.1	1.085		-0.08	-0.007
572-024930	2019.122	1	99.1	1.18		1.48	0.042
572-025528	2019.133	1	13.3	1.238		-0.29	0.005
578-023649	2019.119	1	313.2	1.104		1.88	0.02
578-023649	2019.133	1	313.9	1.11		1.18	0.014
579-098024	2018.731	2	222.5 (2.6)	1.39 (0.006)		-1.39	0.095
581-043221	2019.119	1	48.1	1.235		-0.14	-0.007
581-043221	2019.122	1	47.5	1.243		0.44	-0.015
581-104282	2018.731	3	73.4 (1.1)	1.275 (0.013)	4 (0.17)	-3.42	0.041
581-115336	2018.733	3	314.5 (0.1)	1.239 (0.022)		0.18	0.008
583-011127	2019.133	1	43.2	1.498		-0.18	-0.053
583-040010	2019.117	1	5.1	1.169		-0.44	-0.013
584-040353	2019.117	1	351.7	1.377	3	-0.86	-0.012
584-076038	2018.694	4	296.6 (0.8)	0.817 (0.006)		-0.35	0.032
584-110924	2018.692	4	250.7 (0.9)	0.79 (0.003)		-0.19	0.018
592-043498	2019.122	1	273	1.349		-0.51	-0.025
598-132616	2018.692	4	192.9 (0.3)	1.847 (0.012)		0.10	0.009
603-114143	2018.719	3	219.2 (1.7)	1.393 (0.067)		2.69	0.120

Table 2 concludes on the next page.

Measurements of 121 New Visual Binary Stars Suggested by the Gaia Data Release 2

Table 2 (conclusion). Measurements

UCAC4	DATE	N	PA	SEP	DM	δPA	δSEP
610-033903	2019.133	1	326.9	1.165		-1.02	0.005
610-043660	2019.128	1	10.3	1.257		1.66	0.02
610-117005	2018.719	3	135.7 (0.5)	1.516 (0.008)	3.3 (0.03)	-0.07	0.021
610-129295	2018.733	3	-0.2 (0.8)	1.339 (0.009)	1.8 (0.02)	-0.47	0.020
617-039371	2019.119	1	49.8	1.092		0.05	-0.003
622-024222	2019.122	1	56.9	1.245	2.1	0.11	-0.018
624-038643	2019.117	1	196	1.192		-0.33	0.009
624-118752	2018.717	3	282.5 (0.2)	1.418 (0.016)	2.8 (0.07)	-0.17	0.024
626-034798	2019.133	1	320.8	1.432		-0.24	0.002
627-037471	2019.139	1	100.2	1.215		-0.58	-0.007
628-021808	2019.128	1	0.1	1.474		-1.09	-0.033
628-033482	2019.133	1	17.7	1.407		-2.55	0.018
632-095200	2018.731	3	105 (1.7)	1.092 (0.021)		-2.43	-0.076
633-030637	2019.119	1	233.6	0.977		-0.16	0.013
634-098847	2018.692	3	231.1 (0.2)	0.938 (0.003)		-0.14	0.013
635-130935	2018.717	3	11.6 (1.2)	0.943 (0.003)		2.91	-0.027
636-027723	2019.119	1	38.6	1.305		1.78	-0.031
637-043218	2019.119	1	153.7	1.231		-0.02	-0.009
639-039377	2019.139	1	54.6	1.177		0.5	0.027
641-026536	2019.119	1	203.3	0.984		0.39	0.016
643-126683	2018.717	2	336.9 (0.4)	0.716 (0.009)	2.1 (0.11)	-3.19	0.025
646-022868	2019.133	1	7.6	1.419	3.1	0.53	-0.048
647-110853	2018.733	3	109.6 (0.1)	1.245 (0.012)	2.9 (0.13)	-0.47	0.012
650-078863	2018.694	4	237.1 (0.8)	0.877 (0.012)		-0.91	0.013
650-086057	2018.694	4	307 (1.1)	0.916 (0.02)		0.19	0.029
652-091009	2018.733	3	34.1 (0.6)	1.201 (0.003)		-0.42	0.013
653-051856	2019.122	1	209.1	1.271		0.07	-0.01
654-049141	2019.122	1	37.1	1.314		-0.97	0.001
657-103242	2018.733	3	337.3 (0.9)	1.067 (0.013)		-1.28	0.019
659-112855	2018.717	3	193.2 (0.5)	0.976 (0.013)		0.45	-0.014
661-116828	2018.717	3	111.4 (0.2)	0.961 (0.008)		-0.28	0.008
663-024366	2019.122	1	53.3	1.264		-0.67	-0.01
665-095928	2018.733	3	271.1 (0.4)	1.039 (0.006)		0.00	0.001
666-044431	2019.128	1	174.8	1.009		-0.48	0.011
667-106319	2018.717	3	94.9 (1)	0.945 (0.001)	2.5 (0.06)	1.14	-0.010
668-086512	2018.719	2	162.3 (0.3)	1.152 (0.009)		-1.36	-0.012
669-028818	2019.122	1	0	1.252	2	-0.58	-0.02
669-036212	2019.119	1	238.8	1.401	2.5	0.61	-0.001
669-052025	2019.119	1	127.2	1.002		0.2	-0.011
672-050081	2019.117	1	167.3	1.231		-0.67	-0.011
673-115114	2018.733	3	38.3 (0.2)	1.064 (0.021)		-0.24	-0.022
675-042663	2019.122	1	50.1	1.511	2.5	-0.97	-0.013
678-033045	2019.119	1	208.4	1.131		0.05	-0.008
679-034536	2019.119	1	75.4	1.473		-0.1	-0.026
680-085239	2018.719	3	337.5 (0.9)	1.258 (0.024)		0.07	-0.014
681-079773	2018.733	3	315.7 (0.6)	1.418 (0.013)		-1.31	0.034
686-028195	2019.128	1	311	1.355		-1.91	0.005
686-028794	2019.133	1	181.1	1.274		-0.07	-0.025
688-081285	2018.733	3	66.8 (1.2)	1.074 (0.03)		1.99	0.004
688-107997	2018.692	3	235.6 (0.1)	1.49 (0.002)	2.2 (0.02)	-0.75	-0.016
693-050538	2019.122	1	220.1	1.349	2.7	0.99	-0.052
693-113124	2018.733	3	270.9 (0.8)	1.119 (0.004)		-0.74	-0.026
694-088583	2018.733	3	113.5 (0.2)	1.307 (0.004)		-0.72	0.024
697-080825	2018.692	4	63.7 (0.3)	0.852 (0.006)		0.34	0.026
700-051491	2019.122	1	358.3	1.08		-0.28	-0.013
703-048330	2019.119	1	203.4	1.204		0.06	0.008
705-087810	2018.694	3	206.2 (0.2)	0.943 (0.004)		-0.55	-0.010
709-045021	2019.139	1	332.6	1.35	3	-0.47	-0.026
710-082633	2018.733	3	52.6 (0.2)	1.425 (0.011)	2 (0.08)	-0.90	0.029
714-033708	2019.122	1	117.5	0.99		2.09	0.005
716-048820	2019.122	1	29.9	1.457		-0.25	-0.028

Table 2 continues on the next page.

Measurements of 121 New Visual Binary Stars Suggested by the Gaia Data Release 2

Plate 1 – Examples of bispectrum-reconstructed images (N up, E left)

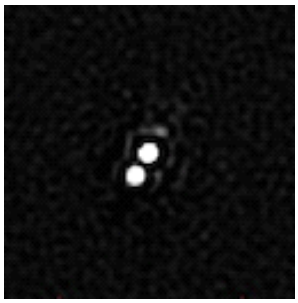	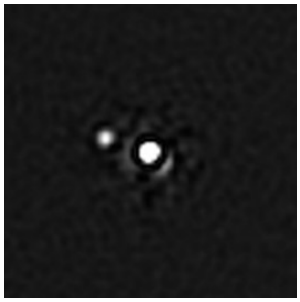	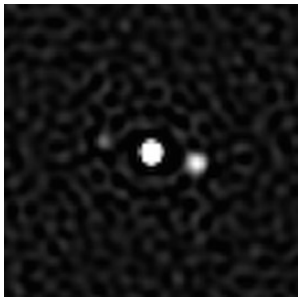	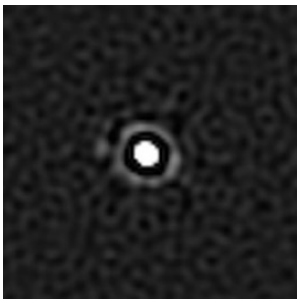
ucac4-508-137021	**ucac4-522-136397**	**ucac4-563-118326**	**ucac4-581-104282**
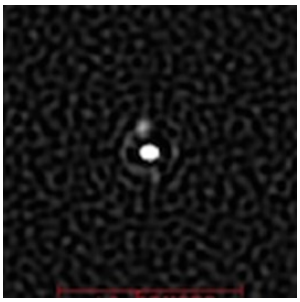	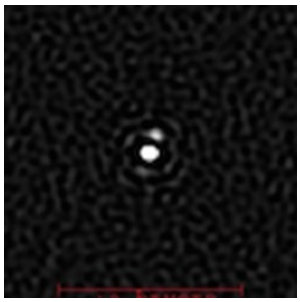	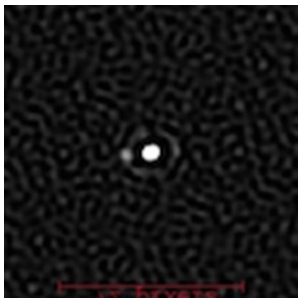	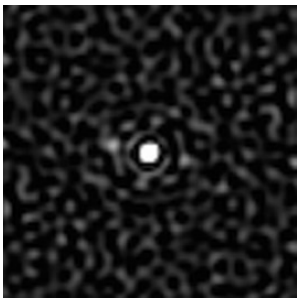
ucac4-635-130935	**ucac4-643-126683**	**ucac4-667-106319**	**ucac4-688-081285**

(Continued from page 289)

this table, columns 1-8 respectively give

- the UCAC4 identifier for the primary
- the date of the measurement (Julian epoch)
- the number N of individual measurements
- the final PA and SEP measurement (in degree and arcsec, resp.) with estimated standard error (when when N > 1)
- the estimated difference of magnitude, when this value could be reliably measured† (also with the attached standard error)
- the differences between the reported PA and SEP values and those computed from the GAIA coordinates (and listed in Table 1)

The last two columns show a very good agreement between our measurements and the astrometric values deduced from GAIA DR2 with an average and standard deviation of the difference of -0.009° / 1.08° and 4 mas / 28 mas for the position angle (δPA) and separation (δSEP) respectively

A selection of reduced images from which the measures were obtained in given in Plate 1.

5. Conclusion

The results presented in this paper seems to indicate that the GAIA mission has opened a new era for double star observers. The discovering, by a an amateur with a modest equipment, of more than 120 new potential visual binary stars – with a high probability for them of being physical – in a dozen nights of observation would simply not have been possible without the availability of the very high accuracy astrometric data produced by this mission. Processed by smart data mining systems, such as the GDS software introduced in this paper, this data will allow to focus on targets with the highest observational interest. Recently published results, also obtained from GAIA DR2 [8] indicate that a large part (> 58 %) of the pairs listed in the WDS catalog are not physical and hence do not deserve further measurements as long as orbit computation is concerned. Observing time should probably and rather be devoted to pairs with a high probability of being physical, this probability being inferred from indicators such as the GB index used by the GDS software. For such pairs – including of course those which were *not* listed in the WDS, such as those described in this paper –, subsequent measurements will of course still be of interest for orbit (re)calculation since the GAIA mission will end in late 2019. Last, but not least, availability of photometric and astrophysical data (effective temperature for example) for a large subset of the DR2 database should allow specific observation programs based on the nature of system components (for example, systems with late M-type secondaries, such as those targeted in [9]).

† *Sometimes, and for reasons that remain to be investigated, the bispectrum reconstruction process does not fully eliminate the secondary peak, precluding any reliable estimation of the difference in flux between the two components. See for example images of ucac4-563-118326 or ucac4-688-081285 on Plate 1.*

6. Acknowledgments

This work has made use of data from the European Space Agency (ESA) mission Gaia (www.cosmos.esa.int/gaia), processed by the Gaia Data Processing and Analysis Consortium (www.cosmos.esa.int/web/gaia/dpac/consortium), and of the Washington Double Star and UCAC4 catalogs, both maintained by the U.S. Naval Observatory. It also relies on the availability of the invaluable SpeckleToolBox and GDS software, kindly developed and maintained by D. Rowe. Pre-processing of images has been carried out using the Reduc software (v 5.3) developed and maintained by F. Losse

This paper is dedicated to the memory of the great double star observer René Gili (2018).

7. References

[1] http://sci.esa.int/gaia/

[2] https://www.cosmos.esa.int/web/gaia/dr2

[3] Sérot, J. Measurements of 208 Aitken Visual Binary Stars with a 280 mm Reflector. JDSO, 13(3), pp 433-443, 2017.

[4] http://genicapture.com

[5] Sérot, J., Communal J.E. Measurements of close visual double stars at the Observatory of Saint-Véran. Submitted to JDSO, 14(3), pp 476-486.

[6] http://ad.usno.navy.mil/ucac.

[7] Mason, D.B., Wycoff G.L., Hartkopf, W.I. Washington Double Stars Catalog, USNO, 2015. http://www.usno.navy.mil/USNO/astrometry/optical-IR-prod/wds/WDS

[8] Harshaw, R. Gaia DR2 and the Washington Double Star Catalog: A Tale of Two Database. JDSO, 14 (4), pp 734-740, 2018.

[9] Sérot J., Wasson N., Rowe D. and Genet R. Bispectrum-based Measurements of Close Large-Differential-Magnitude Visual Double Stars. JDSO, 14(4), pp 711-727, 2018.

Measurements of the Position Angles and Separations of the Double Stars WDS 16579+4722 AB and AC Components

Nathan Sharon[1], Renae Bishop[1], Cole Rodgers[1], Sophia Baer[2], Rachel Freed[3], Cheryl Genet[1], and Russell Genet[1,4]

1. Cuesta College, San Luis Obispo, California
2. Paso Robles High School, Paso Robles, California
3. Institute for Student Astronomical Research, California
4. California Polytechnic State University, San Luis Obispo, California

Abstract: Researchers at Cuesta College measured the position angle and separation of the multiple star system WDS 16579+4722, AB and AC components, using images requested from the Las Cumbres Observatory. The images were captured using a SBIG STX6303 CCD camera mounted to a robotic 0.4-m telescope at the Las Cumbres Observatory in Tenerife, Spain. Data collected will assist in determining if this is a binary or optical double star system. Thirty observations were analyzed using AstroImageJ software. The measured position angle of the AB components was 63.87 degrees and the separation was 5.65 arcseconds. The measured position angle of the AC components was 261.53 degrees and the separation was 112.37 arcseconds. The AB measurements differed from the expected values based on past observations; this difference could be due to the CCD images being out of focus or may be accurate within the range of recently collected data.

Introduction

Double stars are pairs of stars that, as viewed from earth, appear close to each other in the night sky. Double stars may be a binary star system, in which two stars orbit a common point, or may simply be optical doubles. Optical doubles are near one another as they appear in the sky, but in reality, these stars are vastly distant from each other. Numerous observations and measurements over a long period of time can reveal a relationship (or lack thereof) between the two stars and solidify classification. If the stars are binary, they will have a curved trajectory over time their orbits can be calculated. If their true distance from the earth is determined, the system mass (combined mass of both stars) can be calculated. Both system and stellar mass are key to understanding the properties and life cycle of a binary star system (Genet, et al. 2016).

The AC components of the double star WDS 16579+4722 were first observed in 1823 by James South and John Frederick William Herschel published in the journal "Philosophical Transactions of the Royal Society" (Herschel & South 1824). In 1908, components B and D were first observed by Robert G. Aitken at the Lick Observatory just outside of San Jose, CA (Aitken 1945). The most recent observation of both the AB and AC components were completed in 2017 by Jocelyn Sérot (Sérot 2018).

To create a list of readily measurable stars to choose from, the Washington Double Star Catalog (WDS) was filtered with the following properties in mind: a primary star dim enough that the secondary star is easily observable, a secondary star bright enough to be clearly seen, a separation great enough that stars are clearly defined from one another, and lastly, the double star's coordinates are viewable from the Las Cumbres Observatory telescopes. From this pared list, WDS 16579+4722 was selected based on its limited number of observations, existence of many outlying measurements, and relatively undefined orbital solution (see Figure 1). This star was selected as past data does not conclude beyond a doubt that the stars are binary. If new observations follow the elliptical orbit and bend to the left it may confirm that it is a binary relationship,

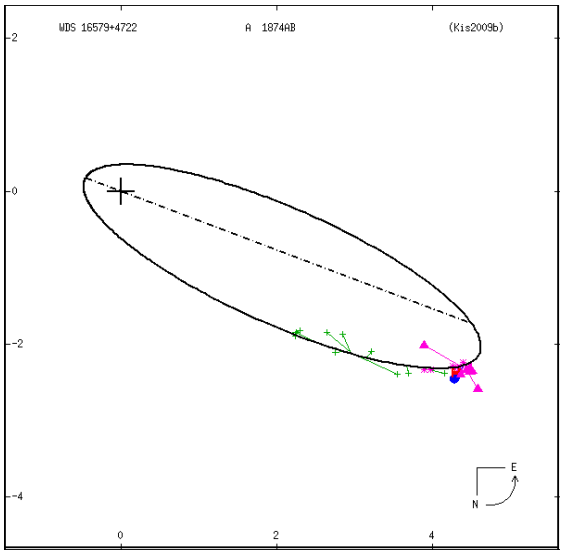

Figure 1. Orbital Diagram of WDS 16579+4722AB

whereas if the new point continues straight on, it may suggest the stars are not in a binary relationship.

Equipment and Procedures

CCD images were requested via robotic telescopes at the Las Cumbres Observatory (LCO, see Figure 2). Wholly modified Meade 0.4-m telescopes using custom equatorial mounts and SBIG STX6303 CCD imagers captured 30 images on November 1st, 2018: 10 each of 1 second, 0.75 second, and 0.5 second exposures from the Las Cumbres Observatory in Tenerife, Spain. Additionally, on this day, data from all published observations of WDS 16579+4722 was requested from Dr. Brian D. Mason of the United States Naval Observatory (USNO) to use in comparison with new data.

LCO images were converted to .fits files and analyzed using the AstroImageJ 3.2.1 software. Before measuring the position angle and separation of WDS 16579+4722, each of the 30 images had to be "plate-solved"; their precise orientation and scale determined using reference data from surrounding stars. Plate-solving was completed using Astrometry.net. Once plate-solved, two measurements of the PA and SEP of the primary and secondary (AB) and primary and tertiary (AC) components of WDS 16579+4722 were recorded in a separate table for each image in Google Sheets. An aperture setting of 4 pixels was used for the AB measurements and an aperture setting of 8 pixels was used for the AC measurements. Early measurements were made using aperture settings that were too small or too large for their respective components and yielded flawed data; these images were re-evaluated with appropriate aperture settings. The raw data was then used to create Tables 1 and 2.

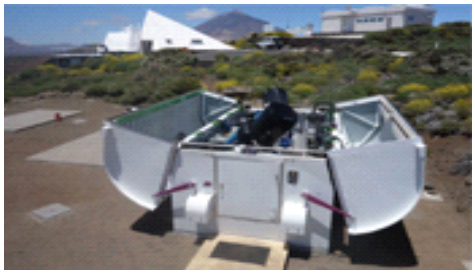

Figure 2. Telescope at Los Cumbres Observatory, Tenerife, Spain

Results

Table 1 shows the average PA and SEP of 2 measurements for each of the 30 images of WDS 16579+4722AB analyzed. The average SEP was 5.65 arcseconds and the average PA was 63.87 degrees.

Table 2 shows the average PA and SEP of 2 measurements for each of the 30 images of WDS 16579+4722AC analyzed. The average SEP was 112.37 arcseconds and the average PA was 261.54 degrees.

Figures 3 and 6 show the AB and AC components as viewed and measured in AstroImageJ. Note the

(Text continues on page 300)

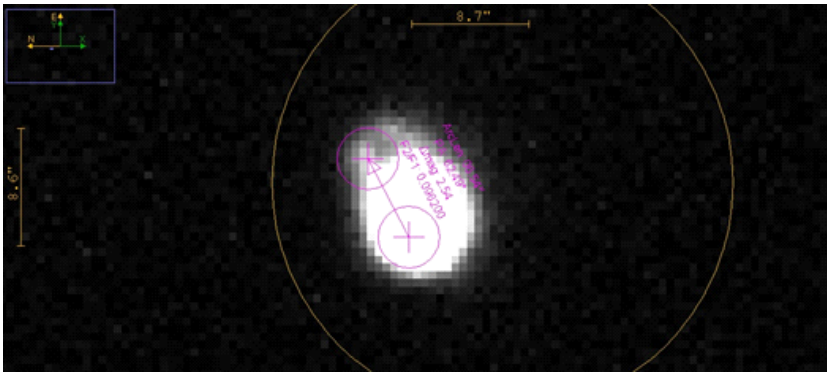

Figure 3. *WDS 16579+4722AB as viewed and measured in AstroImageJ. Note the lack of distinction of components A and B and the skew of the centroid apertures.*

Measurements of the Position Angles and Separations of the Double Stars WDS 16579+4722 ...

Table 1. Exposure (seconds), position angle (degrees) and separation (arcseconds) measurements of WDS 16579+4722AB from LCO images acquired on JD 2458425 (1 November 2018).

Time	Exposure	SEP	PA		Time	Exposure	SEP	PA
19:13:43	0.85	5.81	63.71		19:17:28.513	1.34	5.2	64.13
19:13:57	0.84	6.84	63.29		19:17:42.771	1.35	5.45	64.13
19:14:11	0.85	5.76	64.66		19:17:59.059	1.34	5.8	63.73
19:14:26	0.85	5.8	62.23		19:18:13.914	1.35	5.68	63.3
19:14:39.856	0.85	6.62	62.22		19:18:28.036	1.35	5.74	65.32
19:14:55	0.84	5.12	63.25		19:19:02.711	1.1	5.32	63.99
19:15:08.512	0.84	5.62	64.4		19:19:16.780	1.09	5.33	63.51
19:15:22	0.85	5.46	63.78		19:19:30.959	1.1	5.55	62.92
19:15:35.934	0.85	5.54	63.58		19:19:45.160	1.1	5.53	63.08
19:15:50.564	0.84	5.76	64.6		19:19:59.072	1.1	5.62	65.33
19:16:15.201	1.35	5.64	63.78		19:20:13.885	1.1	5.42	64.82
19:16:29.191	1.34	5.73	64.51		19:20:28	1.1	5.75	62.48
19:16:44.228	1.35	5.82	63.56		19:20:41.939	1.1	5.47	64.57
19:16:58.733	1.34	5.55	64.14		19:20:58.620	1.09	5.47	64.94
19:17:13.362	1.34	5.74	64.04		19:21:12.530	1.09	5.49	64.1
Avg. SEP	5.65				**Av. PA**	63.87		
SEP Std. Dev.	0.37				**PA Std. Dev.**	1.28		
SEP SEM	0.063				**PA SEM**	0.15		

Table 2. Exposure (seconds), position angle (degrees) and separation (arcseconds) measurements of the AC components of WDS 16579+4722 from LCO images acquired on 1 November 2018.

Time	Exposure	SEP	PA		Time	Exposure	SEP	PA
19:13:43	0.85	112.47	261.47		19:17:28.513	1.34	112.43	261.54
19:13:57	0.84	112.23	261.62		19:17:42.771	1.35	112.32	261.49
19:14:11	0.85	112.38	261.6		19:17:59.059	1.34	112.44	261.57
19:14:26	0.85	112.59	261.52		19:18:13.914	1.35	112.23	261.56
19:14:39.856	0.85	112.37	261.55		19:18:28.036	1.35	112.3	261.49
19:14:55	0.84	112.43	261.56		19:19:02.711	1.1	111.97	261.57
19:15:08.512	0.84	112.39	261.64		19:19:16.780	1.09	112.36	261.53
19:15:22	0.85	112.38	261.47		19:19:30.959	1.1	112.46	261.52
19:15:35.934	0.85	112.41	261.56		19:19:45.160	1.1	112.26	261.44
19:15:50.564	0.84	112.26	261.57		19:19:59.072	1.1	112.36	261.52
19:16:15.201	1.35	112.21	261.56		19:20:13.885	1.1	112.55	261.54
19:16:29.191	1.34	112.31	261.52		19:20:28	1.1	112.52	261.55
19:16:44.228	1.35	112.28	261.59		19:20:41.939	1.1	112.38	261.46
19:16:58.733	1.34	112.66	261.6		19:20:58.620	1.09	112.33	261.57
19:17:13.362	1.34	112.49	261.44		19:21:12.530	1.09	112.35	261.53
Avg. SEP	112.37				**Av. PA**	261.54		
SEP Std. Dev.	0.13				**PA Std. Dev.**	0.05		
SEP SEM	0.024				**PA SEM**	0.009		

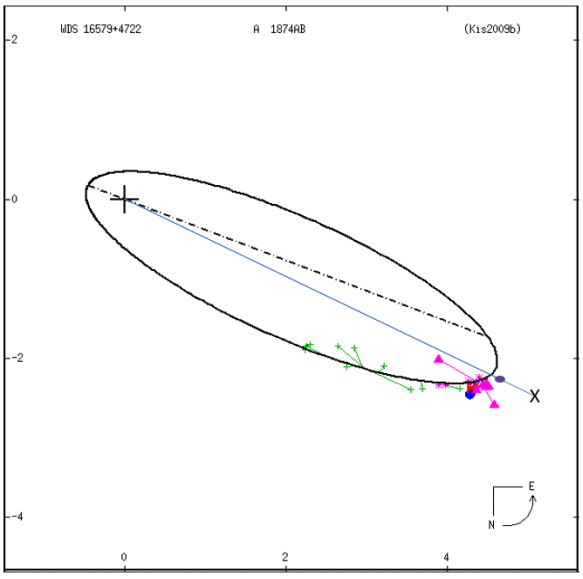

Figure 4. Orbital Diagram of WDS 16579+4722AB with newly recorded data. Data from this observation is represented by the black X; data from last recorded observation (Sérot 2018) is represented by the purple oval.

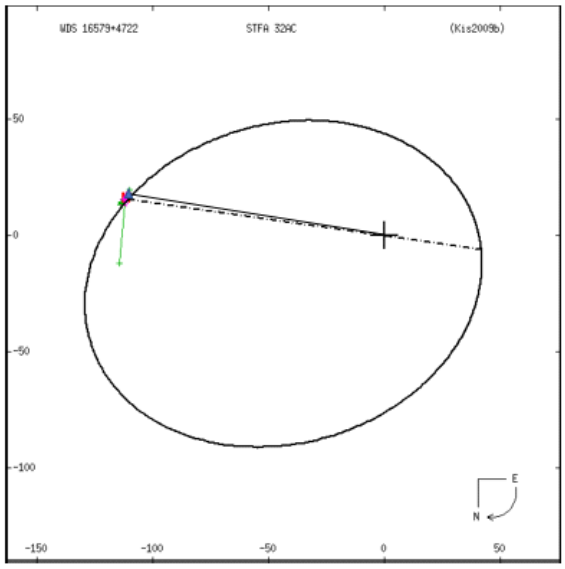

Figure 5. Orbital Diagram of WDS 16579+4722AC with newly recorded data. Data from this observation is represented by the blue triangle.

(Continued from page 298)

blurred distinction of the AB components and the consistent skew of the centroid apertures to the bottom left. Figure 4 shows the orbital diagram of the AB components of WDS 16579+4722A, while Figure 5 shows the orbital diagram of the AC components.

In Figures 7, 8, 9, and 10 the newly gathered SEP and PA of the AB and AC components are shown in comparison with data from past observations provided by the USNO. The orange points correspond to the data collected in this observation.

Discussion

Issues arose when gathering PA and SEP data from the primary component (A) and secondary component (B). The first was due to the proximity and difference in magnitudes of A and B and the second was due to a slight distortion in the images. When two stars with differing magnitudes are near one another the brighter star's light appears to saturate the area around it which makes seeing the secondary star difficult. Additionally, our images showed a consistent skewing of light to the top-right direction for all stars assessed; we concluded that the images may have been slightly out of focus. Both of these factors contributed to the inability of the AstroImageJ program to automatically find the center of B (there was no difficulty locating the center of A or C). This centroid feature is key to producing consistent results in CCD double star astrometry. As such, the center of B had to be estimated by hand for each measurement, yielding data with a large standard error. The standard error of the mean of the PA and SEP of the AB components (without use of the centroid feature) were 0.063 degrees and 0.149 arcseconds respectively, compared to the AC PA and SEP measurements' standard errors of 0.024 degrees and 0.009 arcseconds.

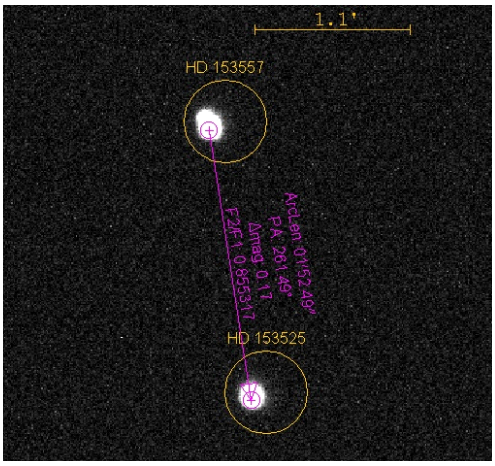

Figure 6. WDS 16579+4722Ac as viewed and measured in AstroImageJ. Note the skew of both centroid apertures to the bottom left of the image.

Conclusion

The new data seems reasonable when referenced to past data. The SEP measurement of WDS 16579+4722A was greater than projected; this may be due to the inability of AstroImageJ to centroid on the B

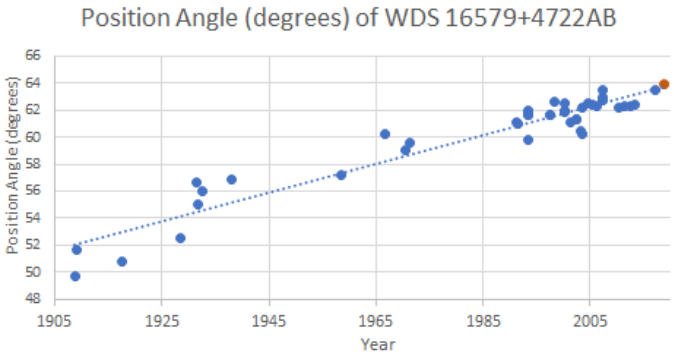

Figure 7. Position Angle of WDS 15679+4722AB over time. New data represented by orange point.

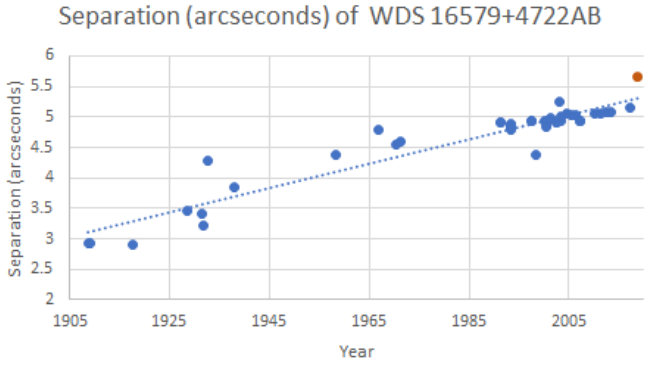

Figure 8. Separation of WDS 16579+4722AB over time. New data represented by orange point.

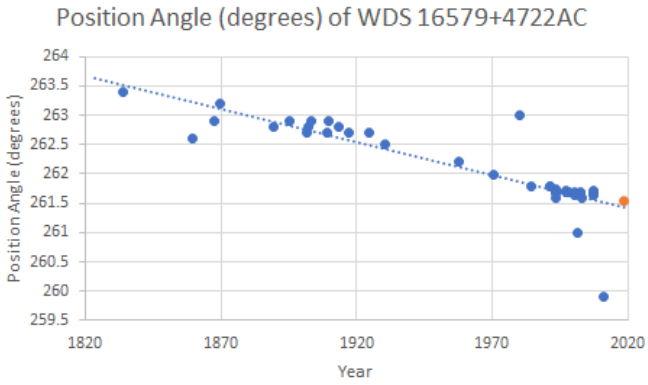

Figure 9. Position Angle of WDS 16579+4722AC over time. Two far outlying points have been omitted to remove bias. New data represented by orange point.

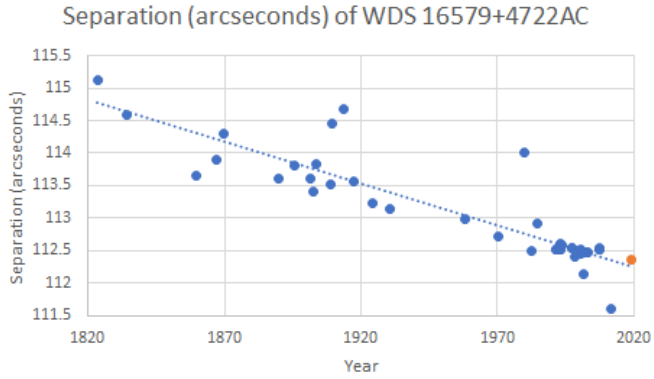

Figure 10. of WDS 16579+4722AC over time. New data represented by orange point.

component given its closeness and dimness in regard to star A and or the skewed focus of the images. The PA of WDS 16579+4722AC was exactly as projected and the SEP nearly was as well. Further observation is needed to confirm AB's relative position more accurately.

Based solely on past PA and SEP data, these new measurements of the AB components may suggest the stars are not binary and in an elliptical orbit but, conversely, are an optical double with linear relation to each other. However, the classification as a binary star is not based solely on PA and SEP measurements, but using radial velocity measurements and the apparent motion technique collected and calculated by Kiselev, A. A., et al. at the Main Astronomical Observatory of the Institute of Astronomy at the Russian Academy of Sciences. This method also enabled their team to derive the stars' masses and takes into account more factors than just observed coordinates (Kiselev, et al. 2009).

Acknowledgements

This research would not have been possible without the assistance of Dr. Brian D. Mason at the United States Naval Observatory. Our team would also like to thank Las Cumbres Observatory for generously allowing us to use their robotic telescope equipment free of charge. Lastly, we would like to thank Dr. Vera Wallen for proofreading and helping edit this paper.

References

Aitken, Robert G. "Early Work on Double Stars at the Lick Observatory." *Publications of the Astronomical Society of the Pacific*, vol. 57, 1945, p. 138., doi:10.1086/125705.

Genet, R., Johnson, J., Buchheim, R., & Harshaw, R. (2016). *Small Telescope Astronomical Research Handbook*. Santa Margarita, CA: Collins Foundation Press.

Herschel, John Frederick William, and James South. "Observations of the Apparent Distances and Positions of 380 Double and Triple Stars." *Philosophical Transactions of the Royal Society of London*, vol. 114, 1824, pp. 1–412., doi:10.1098/rstl.1824.0001.

Kiselev, A. A., et al. "A Dynamical Study of the Wide Hierarchic Triple Star ADS 10288." *Astronomy Reports*, vol. 53, no. 12, 25 June 2009, pp. 1136–1145., doi:10.1134/s1063772909120063. "16579+4722 A 1874AB (STFA 32AC)."

Sérot, Jocelyn. "Measurements of Aitken Visual Binary Stars: 2017 Report." *Journal of Double Star Observations*, vol. 14, no. 3, 1 July 2018, pp. 527–537.

Journal of Double Star Observations

April 1, 2019
Volume 15, Number 2

The Journal of Double Star Observations (ISSN 2572-4436) is an electronic journal published quarterly. Copies can be freely downloaded from http://www.jdso.org.

Questions, comments, or submissions may be directed to rclark@southalabama.edu or to rmollise@bellsouth.net

The *Journal of Double Star Observations* (*JDSO*) publishes articles on any and all aspects of astronomy involving double and binary stars. The *JDSO* is especially interested in observations made by amateur astronomers. Submitted articles announcing measurements, discoveries, or conclusions about double or binary stars may undergo a peer review. This means that a paper submitted by an amateur astronomer will be reviewed by other amateur astronomers doing similar work.

Submitted manuscripts must be original, unpublished material and written in English. They should contain an abstract and a short description or biography (2 or 3 sentences) of the author(s). For more information about format of submitted articles, please see our web site at http://www.jdso.org

Submissions should be made electronically via e-mail to rclark@southalabama.edu or to rmolise@bellsouth.net. Articles should be attached to the email in Microsoft Word, Word Perfect, Open Office, or text format. All images should be in jpg or fits format.